



CHAPTER 4

Temperature and Precipitation Across Canada

CANADA'S CHANGING CLIMATE REPORT



Government
of Canada

Gouvernement
du Canada

Canada



Authors

Xuebin Zhang, Environment and Climate Change Canada

Greg Flato, Environment and Climate Change Canada

Megan Kirchmeier-Young, Environment and Climate Change Canada

Lucie Vincent, Environment and Climate Change Canada

Hui Wan, Environment and Climate Change Canada

Xiaolan Wang, Environment and Climate Change Canada

Robin Rong, Environment and Climate Change Canada

John Fyfe, Environment and Climate Change Canada

Guilong Li, Environment and Climate Change Canada

Viatchelsav V. Kharin, Environment and Climate Change Canada

Recommended citation: Zhang, X., Flato, G., Kirchmeier-Young, M., Vincent, L., Wan, H., Wang, X., Rong, R., Fyfe, J., Li, G., Kharin, V.V. (2019): Changes in Temperature and Precipitation Across Canada; Chapter 4 *in* Bush, E. and Lemmen, D.S. (Eds.) Canada's Changing Climate Report. Government of Canada, Ottawa, Ontario, pp 112-193.



Chapter Table Of Contents

CHAPTER KEY FINDINGS (BY SECTION)

SUMMARY

4.1 Introduction

4.2: Temperature

Box 4.1: An example of climate data inhomogeneity

4.2.1: Mean temperature

4.2.1.1: Observed changes

4.2.1.2: Causes of observed changes

4.2.1.3: Projected changes and uncertainties

4.2.2: Temperature extremes and other indices

4.2.2.1 Observed changes

4.2.2.2 Causes of observed changes

4.2.2.3 Projected changes and uncertainties

4.3: Precipitation

4.3.1: Mean precipitation

4.3.1.1: Observed changes

4.3.1.2: Causes of observed changes

4.3.1.3: Projected changes and uncertainties

4.3.2: Extreme precipitation

4.3.2.1: Observed changes

4.3.2.2: Projected changes and uncertainties

Box 4.2: The impact of combined changes in temperature and precipitation on observed and projected changes in fire weather

4.4: Attribution of extreme events


Box 4.3: Methods for event attribution

4.4.1: Attribution of two recent events

4.4.1.1: 2013 Southern Alberta flood

4.4.1.2: 2016 Fort McMurray wildfire

REFERENCES

A dramatic landscape photograph featuring a lightning storm over a field of tall, golden-brown grass. The sky is dark and filled with heavy, grey clouds, with several bright, jagged lightning bolts striking down. The foreground is dominated by the dense, textured grass, which is illuminated by a low sun, creating a warm, golden glow. A dirt path or road winds through the grass towards the background. The overall mood is intense and powerful, suggesting a significant weather event.

This chapter assesses observed and projected changes in temperature and precipitation for Canada, and it presents analyses of some recent extreme events and their causes.

Chapter Key Findings

4.2: Temperature

It is *virtually certain* that Canada's climate has warmed and that it will warm further in the future. Both the observed and projected increases in mean temperature in Canada are about twice the corresponding increases in the global mean temperature, regardless of emission scenario.

Annual and seasonal mean temperatures across Canada have increased, with the greatest warming occurring in winter. Between 1948 and 2016, the best estimate of mean annual temperature increase is 1.7°C for Canada as a whole and 2.3°C for northern Canada.

While both human activities and natural variations in the climate have contributed to the observed warming in Canada, the human factor is dominant. It is *likely*¹³ that more than half of the observed warming in Canada is due to the influence of human activities.

Annual and seasonal mean temperature is projected to increase everywhere, with much larger changes in northern Canada in winter. Averaged over the country, warming projected in a low emission scenario is about 2°C higher than the 1986–2005 reference period, remaining relatively steady after 2050, whereas in a high emission scenario, temperature increases will continue, reaching more than 6°C by the late 21st century.

Future warming will be accompanied by a longer growing season, fewer heating degree days, and more cooling degree days.

Extreme temperature changes, both in observations and future projections, are consistent with warming. Extreme warm temperatures have become hotter, while extreme cold temperatures have become less cold. Such changes are projected to continue in the future, with the magnitude of change proportional to the magnitude of mean temperature change.

13 This report uses the same calibrated uncertainty language as in the IPCC's Fifth Assessment Report. The following five terms are used to express assessed levels of confidence in findings based on the availability, quality and level of agreement of the evidence: very low, low, medium, high, very high. The following terms are used to express assessed likelihoods of results: virtually certain (99%–100% probability), extremely likely (95%–100% probability), very likely (90%–100% probability), likely (66%–100% probability), about as likely as not (33%–66% probability), unlikely (0%–33% probability), very unlikely (0%–10% probability), extremely unlikely (0%–5% probability), exceptionally unlikely (0%–1% probability). These terms are typeset in italics in the text. See chapter 1 for additional explanation.

4.3: Precipitation

There is *medium confidence* that annual mean precipitation has increased, on average, in Canada, with larger percentage increases in northern Canada. Such increases are consistent with model simulations of anthropogenic climate change.

Annual and winter precipitation is projected to increase everywhere in Canada over the 21st century, with larger percentage changes in northern Canada. Summer precipitation is projected to decrease over southern Canada under a high emission scenario toward the end of the 21st century, but only small changes are projected under a low emission scenario.

For Canada as a whole, observational evidence of changes in extreme precipitation amounts, accumulated over periods of a day or less, is lacking. However, in the future, daily extreme precipitation is projected to increase (*high confidence*).

4.4: Attribution Of Extreme Events

Anthropogenic climate change has increased the likelihood of some types of extreme events, such as the 2016 Fort McMurray wildfire (*medium confidence*) and the extreme precipitation that produced the 2013 southern Alberta flood (*low confidence*).

Summary

Temperature and precipitation are fundamental climate quantities that directly affect human and natural systems. They are routinely measured as part of the meteorological observing system that provides current and historical data on changes across Canada. Changes in the observing system, such as changes in instruments or changes in location of the measurement site, must be accounted for in the analysis of the long-term historical record. The observing system is also unevenly distributed across Canada, with much of northern Canada having a very sparse network that has been in place for only about 70 years. There is **very high confidence**¹ that temperature datasets are sufficiently reliable for computing regional averages of temperature for southern Canada¹⁴ from 1900 to present and for northern Canada² from 1948 to present. There is **medium confidence** that precipitation datasets are sufficiently reliable for computing regional averages of normalized precipitation anomalies (departure from a baseline mean divided by the baseline mean) for southern Canada from 1900 to present but only **low confidence** for northern Canada from 1948 to present.

These datasets show that temperature in Canada has increased at roughly double the global mean rate, with Canada's mean annual temperature having risen about 1.7°C (**likely** range 1.1°C – 2.3°C) over the 1948–2016 period. Temperatures have increased more in northern Canada than in southern Canada, and more in winter than in summer. Annual mean temperature over northern Canada increased by 2.3°C (**likely** range 1.7°C–3.0°C) from 1948 to 2016, or roughly three times the global mean warming rate. More than half of the warming can be attributed to human-caused emissions of greenhouse gases. Climate models project similar patterns of change in the future, with the amount of warming dependent on future greenhouse gas emissions. A low emission scenario (RCP2.6), generally compatible with the global temperature goal in the Paris Agreement, will increase annual mean temperature in Canada by a further 1.8°C¹⁵ by mid-century, remaining roughly constant thereafter. A high emission scenario (RCP8.5), under which only limited emission reductions are realized, would see Canada's annual mean temperature increase by more than 6°C¹⁵ by the late 21st century. In all cases, northern Canada is projected to warm more than southern Canada, and winter temperatures are projected to increase more than summer temperatures. There will be progressively more growing degree days (a measure of the growing season, which is important for agriculture) and fewer freezing degree days (a measure of winter severity), in lock-step with the change in mean temperature.

There is **medium confidence**, given the available observing network across Canada, that annual mean precipitation has increased, on average, in Canada, with larger relative increases over northern Canada. Climate models project further precipitation increases, with annual mean precipitation projected to increase by about 7%¹⁵ under the low emission scenario (RCP2.6) and 24%¹⁵ under the high emission scenario (RCP8.5) by the late 21st century. As temperatures increase, there will continue to be a shift from snow to rain in the spring and fall seasons.

14 For simplicity, southern and northern Canada are defined according to geographical location in this report: southern Canada is defined as the region south of 60° north latitude, while the region north of this latitude is defined as northern Canada. The phrase “the North,” is used to refer to the three northern territories, based on their political boundaries (see Chapter 1, Figure 1.1).

15 The values presented in this Summary are median projections based on multiple climate models. Some models project larger increases, while others project smaller increases.

While, in general, precipitation is projected to increase in the future, summer precipitation in parts of southern Canada is projected to decrease by the late 21st century under a high emission scenario. However, there is lower confidence in this projected summer decrease than in the projected increase in annual precipitation. There is *high confidence* in the latter because different generations of models produce consistent projections, and because increased atmospheric water vapour in this part of the world should translate into more precipitation, according to our understanding of physical processes. The lower confidence for summer decreases in southern Canada is because this region is at the northern tip of the region in the continental interior of North America where precipitation is projected to decrease, and at the transition to a region where precipitation is projected to increase. The atmospheric circulation-controlled pattern is uncertain at its edge, and different models do not agree on the location of the northern boundary of this pattern.

The most serious impacts of climate change are often related to changes in climate extremes. There have been more extreme hot days and fewer extreme cold days — a trend that is projected to continue in the future. Higher temperatures in the future will contribute to increased fire potential (“fire weather”). Extreme precipitation is also projected to increase in the future, although the observational record has not yet shown evidence of consistent changes in short-duration precipitation extremes across the country.

The changing frequency of temperature and precipitation extremes can be expected to lead to a change in the likelihood of events such as wildfires, droughts, and floods. The emerging field of “event attribution” provides insights about how climate change may have affected the likelihood of events such as the 2013 flood in southern Alberta or the 2016 Fort McMurray wildfire. In both cases, human-caused greenhouse gas emissions may have increased the risk of such extreme events relative to their risk in a pre-industrial climate.

4.1: Introduction

Temperature and precipitation have a critical influence on both human society and natural systems. They influence decisions about the most suitable crops to grow in a region, building heating and cooling requirements, and the size of a street storm drain. Temperature and precipitation are also the best monitored and most heavily studied climate variables. This chapter focuses on changes in mean and extreme temperature and precipitation across Canada. It assesses past changes, our understanding of the causes of these changes, as well as future projections. In addition, we evaluate climate indices derived from temperature and precipitation data that are relevant to impacts or planning, such as heating, cooling, and growing degree days. This report also assesses changes to the physical environment that are driven mainly by the combination of temperature and precipitation, such as fire weather (see Box 4.2); snow and ice conditions (see Chapter 5); and river runoff, flood, and drought (see Chapter 6). Other climate variables, such as mean and extreme wind speeds, are not assessed in this report owing to limited analyses of available observations and limited research on the mechanisms and causes of observed and projected changes in Canada, although they are highly relevant to issues such as wind-energy production and building codes.

Extreme climate events frequently result in costly climate impacts. A single event, such as the 2013 flood in southern Alberta, can result in damage valued at billions of dollars. To better understand whether climate change has contributed to the occurrence of a particular extreme event, we assess the extent to which human influence on the climate may have played a role in such catastrophic events. As the science of event attribution is still emerging, we provide a general description of event attribution, along with two examples: the 2013 flood in southern Alberta and the 2016 Fort McMurray wildfire.

Canadian climate is wide ranging, varying from one region to another. It also naturally fluctuates from one year to another and from one decade to another, on the backdrop of human-induced changes in the climate. As we will see, natural internal climate variability¹⁶ is an important contributor to some of the observed changes discussed in this chapter. Natural internal climate variability refers to the short-term fluctuations around the mean climate at a location or over a region. Some aspects of natural variability are associated with large-scale “modes of variability,” which are robust features in the climate system with identifiable spatial and temporal characteristics (see Chapter 2, Box 2.5). For example, the positive (warm) phase of El Niño–Southern Oscillation (ENSO), known as El Niño, tends to be associated in winter with warmer air temperatures and drier conditions across much of Canada. The opposite is true during the negative (cold) phase of ENSO, known as La Niña. Other common modes of variability are also characterized by positive (warm) or negative (cold) phases that tend to be associated with warmer or cooler seasonal temperatures for all or parts of Canada (see Chapter 2, Box 2.5).

16 There are two types of variability in the climate not caused by human activities. One is a result of the chaotic nature of the climate system, referred to as natural internal climate variability. The other is a response to natural forcing external to the climate system, such as those caused by solar or volcanic activities (see Chapter 2).



4.2: Temperature

Key Message

It is *virtually certain* that Canada's climate has warmed and that it will warm further in the future. Both the observed and projected increases in mean temperature in Canada are about twice the corresponding increases in the global mean temperature, regardless of emission scenario.

Key Message

Annual and seasonal mean temperatures across Canada have increased, with the greatest warming occurring in winter. Between 1948 and 2016, the best estimate of mean annual temperature increase is 1.7°C for Canada as a whole and 2.3°C for northern Canada.

Key Message

While both human activities and natural variations in the climate have contributed to the observed warming in Canada, the human factor is dominant. It is *likely* that more than half of the observed warming in Canada is due to the influence of human activities.

Key Message

Annual and seasonal mean temperature is projected to increase everywhere, with much larger changes in northern Canada in winter. Averaged over the country, warming projected in a low emission scenario is about 2°C higher than the 1986–2005 reference period, remaining relatively steady after 2050, whereas in a high emission scenario, temperature increases will continue, reaching more than 6°C by late the 21st century.

Key Message

Future warming will be accompanied by a longer growing season, fewer heating degree days, and more cooling degree days.

Key Message

Extreme temperature changes, both in observations and future projections, are consistent with warming. Extreme warm temperatures have become hotter while extreme cold temperatures have become less cold. Such changes are projected to continue in the future, with the magnitude of change proportional to the magnitude of mean temperature change.

Temperatures referred to in this chapter are surface air temperatures, typically measured 2 m above the ground, which have an immediate effect on human comfort and health, play an important role in determining the types of crops a farmer can grow, and influence the functioning of local ecosystems. Temperatures in Canada vary widely across the country. The lowest temperature on record is -63°C , observed at Snag, Yukon, on February 3, 1947. The highest temperature on record is 45°C , observed at Midale and Yellow Grass, Saskatchewan, on July 5, 1937. Annual mean temperature provides a simple measure of the overall warmth of a region: it varies from about 10°C in some southern regions to about -20°C in the far north. Seasonally, this variability is even more pronounced. Winter averages range from -5°C in the south to about -35°C in the far north, while summer averages vary from about 22°C in the south to 2°C in the far north (Gullett and Skinner, 1992).

In some locations in Canada, temperatures have been observed for a long time. For example, an observing site in Toronto has provided continuous daily temperature records since 1840. Multiple sites have temperature records that date back a century or longer. However, the availability of temperature data is unevenly distributed across the country or over different time periods. Observation sites are relatively densely distributed in the populated portion of southern Canada, while, for much of Canada, especially northern Canada, observations are sparse (see Figure 4.1), and very few observation sites predate 1948. As a result, the analysis of past changes in temperature for Canada as a whole is limited to the period since 1948, while 1900 can be used as a starting point for records in southern Canada (Vincent et al., 2015; DeBeer et al., 2016).

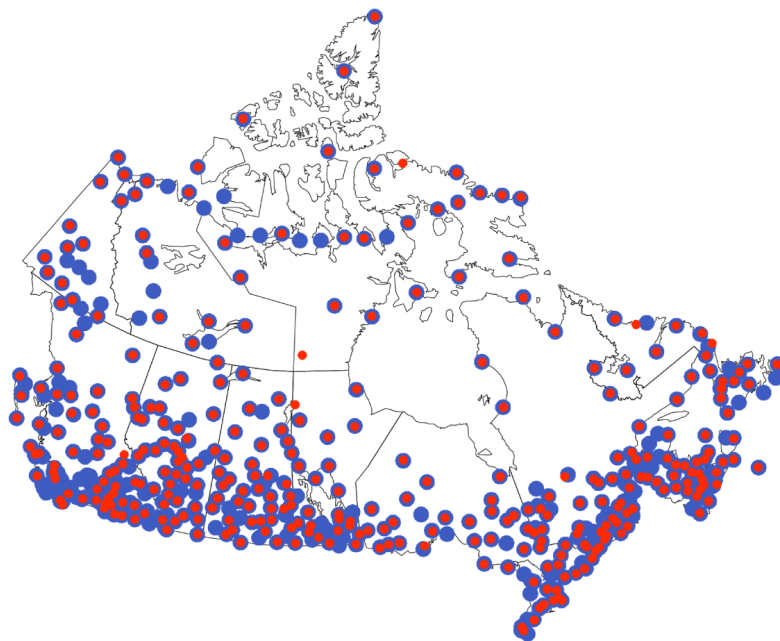


Figure 4.1: Observing stations for precipitation and temperature in Canada

Figure caption: Location of stations for which long-term precipitation (blue) and temperature (red) observations exist and for which the data have been homogenized (for temperature) and adjusted (for changes in the instruments for precipitation). Over the past two decades, monitoring technology has evolved and the climate observing network has transitioned from manual to automated observations. Procedures are currently under develop-

ment for joining and adjusting past manual and current automated climate observations in order to preserve continuity for climate monitoring and trend analysis (Milewska et al. 2018; Vincent et al. 2018).

FIGURE SOURCE: CLIMATE RESEARCH DIVISION, ENVIRONMENT AND CLIMATE CHANGE CANADA.

Temperature is also a key indicator of the climate response to human emissions of greenhouse gases (GHGs), as increasing GHG concentrations result in warming of the lower atmosphere (see Chapter 2, Section 2.3). While the original purpose of historical observations was to monitor daily to seasonal climate variability and support weather prediction, today these observations also support climate change impact studies and climate services. Monitoring instruments, observational sites, and their surrounding environment, as well as observation procedures, have undergone changes over the past century to meet new needs and to introduce new technology. These changes also introduce non-climatic changes, referred to as “data inhomogeneities,” in data records. Inhomogeneities affect the reliability of long-term trend assessment if not accounted for (Milewska and Vincent, 2016; Vincent et al., 2012, see Box 4.1). In particular, the reduction in the number of manned observational sites, with many being converted to automatic stations, has necessitated the integration of data from these different sources, which has proven challenging. Changes identified in the historical data archive reflect changes in both climate and data inhomogeneity (Vincent et al., 2012). Techniques for removing climate data inhomogeneity (“climate data homogenization”) have been developed to identify such artifacts in climate records and remove them (see Box 4.1; Vincent et al., 2002, 2012, 2017; Wang et al., 2007, 2010).

Box 4.1: An example of climate data inhomogeneity

The record of observed temperature at Amos, Quebec, shows how changes in sites and their surrounding environment can affect the estimation of long-term changes in the climate. Between 1927 and 1963, the Stevenson screen at the Amos station was located at the bottom of a hill (see Figure 4.2a) and was moved after 1963 (see Figure 4.2b) to level ground several metres away from its original place. The site was sheltered by trees and a building between 1927 and 1963, which could have prevented the cold air from draining freely during nighttime. The current site has an open exposure and is more representative of its surrounding region. Careful comparison of the temperature data at this site with those at a nearby station revealed two step-changes, one of -0.8°C in 1927 and another of 1.3°C in 1963 (see Figure 4.2c). The station history files do not provide information on the cause of the first step, but it is possible that the screen was also relocated at that time. These differences resulted in the original temperature data showing an increasing trend of 2.4°C for 1951–1995 (see Figure 4.2d), whereas, after the artifact in temperature reading was removed, a warming of only 0.8°C was shown.

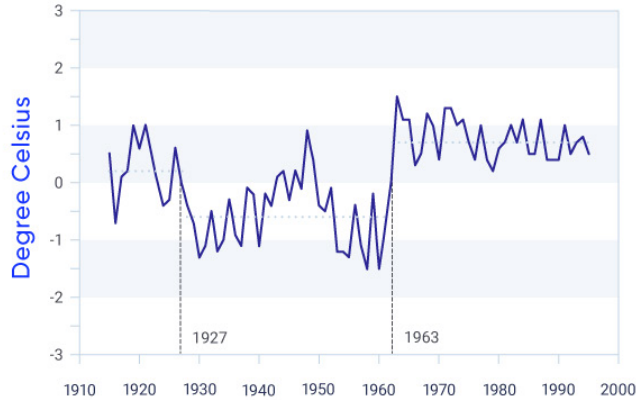
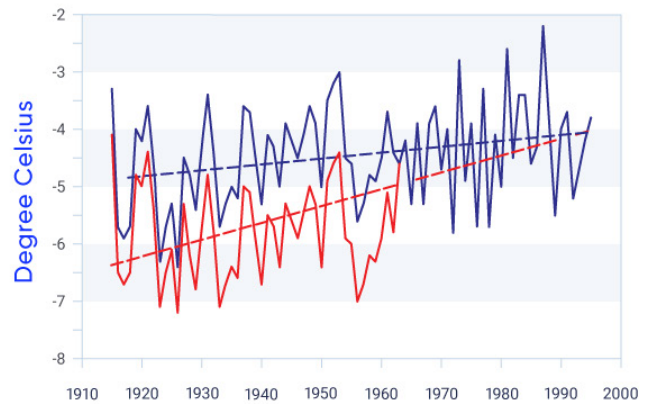
a) Amos, Quebec site before 1963**b) Amos, Quebec site after 1963****c) Difference between Amos, QC and reference station****d) Temperature prior to and after adjustment**

Figure 4.2: How artifacts in instrument data can affect temperature change estimates

Figure caption: Photos of the observing site Amos, Quebec, taken by inspectors showing the site before 1963 (a) and after 1963 (b). (c) Time series of the difference in the annual mean of the daily minimum temperatures between Amos and a reference station shows a decreasing step in 1927 and an increasing step in 1963, (d) The original (red line) and adjusted (blue line) time series of the annual mean of the daily minimum temperatures. The red dashed line shows an increasing trend of 2.4°C for 1915–1995 in the original series, while the blue dashed line shows an increasing trend of 0.8°C for 1915–1995 in the homogenized data.

FIGURE SOURCE: CLIMATE RESEARCH DIVISION, ENVIRONMENT AND CLIMATE CHANGE CANADA.

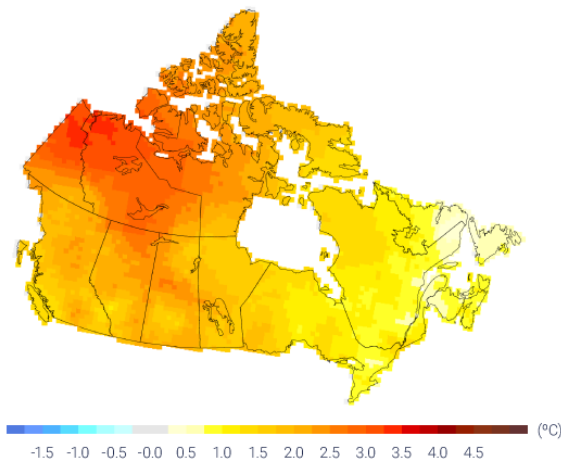
4.2.1: Mean temperature

4.2.1.1: Observed changes

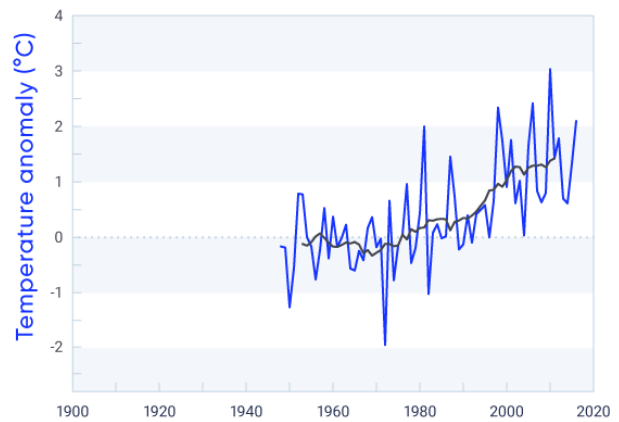
The annual average temperature in Canada increased by 1.7°C (*likely* range 1.1°C –2.3°C¹⁷) between 1948 and 2016 (updated from Vincent et al., 2015; Figure 4.3 and Table 4.1), roughly twice the increase observed for the Earth as a whole (0.8°C for 1948–2016 according to the global mean surface temperature dataset produced by the Met Office Hadley Centre and the Climatic Research Unit at the University of East Anglia, UK, HadCRUT4 [Osborn and Jones, 2014]). Warming was not uniform across seasons, with considerably more warming in winter than in summer. The mean temperature increased by 3.3°C in winter, 1.7°C in spring, 1.5°C in summer, and 1.7°C in autumn between 1948 and 2016 (see Figure 4.4 and Table 4.1). The changes in temperatures are significant at the 5% level (i.e., there is only a 5% possibility that such changes are due to chance). As well, warming was unevenly distributed across the country. The largest increases in the annual mean temperature were in the northwest, where it increased by more than 3°C in some areas. Annual mean temperature over northern Canada increased by 2.3°C (*likely* range 1.7 °C–3.0°C) from 1948 to 2016, or roughly three times the global mean warming rate. Warming was much weaker in the southeast of Canada, where average temperature increased by less than 1°C in some maritime areas. Winter warming was predominant in northern British Columbia and Alberta, Yukon, Northwest Territories, and western Nunavut, ranging from 4°C to 6°C over the 1948–2016 period. Spring had a similar warming pattern, but with smaller magnitude. Summer warming was much weaker than that in winter and spring, but the magnitude of the warming was generally more uniform across the country than during other seasons. During autumn, most of the warming was observed in the northeast regions of Canada (mainly in northern Northwest Territories, Nunavut, and northern Quebec). In addition to higher temperatures, the reduction in snow cover (see Chapter 5) and earlier snowmelt (see Chapter 6) also indicate Canada has warmed.

17 The 95% uncertainty range of the trend estimate based on the annual temperature is 1.1 °C–2.3°C. Here and elsewhere, in this chapter, computed 90% and 95% uncertainty ranges are referred to as the likely range (nominally representing 66% likelihood). This is done to account for other sources of uncertainty, such as data quantity and spatial/temporal coverage.

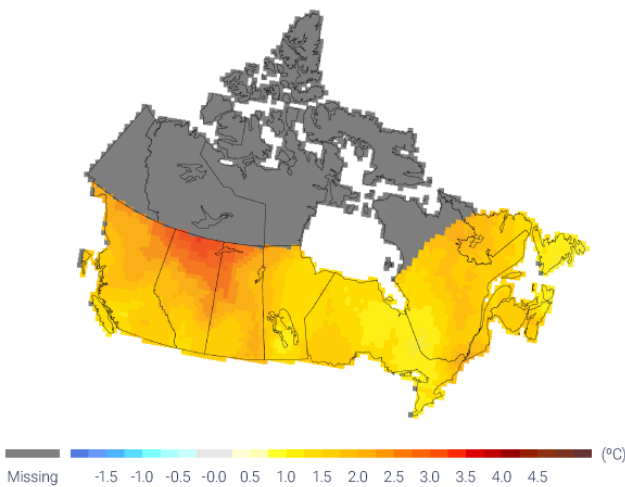
a) 1948–2016



b) 1948–2016



c) 1900–2016



d) 1900–2016

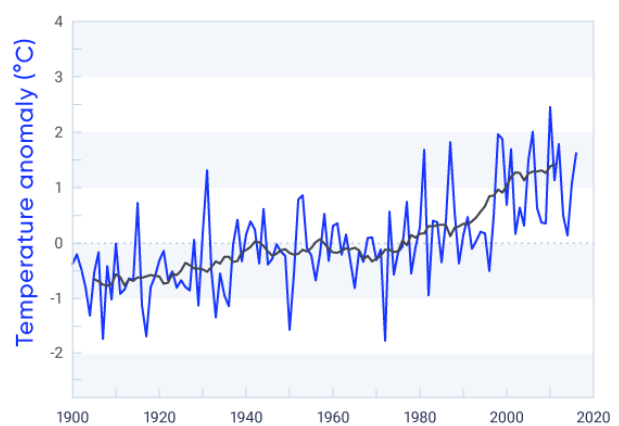


Figure 4.3: Trends in annual temperatures across Canada

Figure caption: Observed changes (°C) in annual temperature between (a) 1948 and 2016 and (c) 1900 and 2016. Changes are computed based on linear trends over the respective periods. Annual temperature anomalies (departures from baseline means) are expressed relative to the mean for the period 1961–1990 (b) for Canada as a whole and (d) for southern Canada (south of 60° north latitude); the black lines are 11-year running means. Estimates are derived from the gridded station data. There are insufficient data in northern Canada to confidently calculate warming trends from 1900 to 2016.

FIGURE SOURCE: UPDATED FROM FIGURE 2 OF VINCENT ET AL., 2015.

Table 4.1: Observed changes in annual and seasonal mean temperature between 1948 and 2016 for six regions and for all Canadian land area^a

REGION	CHANGE IN TEMPERATURE, °C				
	Annual	Winter	Spring	Summer	Autumn
British Columbia	1.9	3.7	1.9	1.4	0.7
Prairies	1.9	3.1	2.0	1.8	1.1
Ontario	1.3	2.0	1.5	1.1	1.0
Quebec	1.1	1.4	0.7	1.5	1.5
Atlantic	0.7	0.5	0.8	1.3	1.1
Northern Canada	2.3	4.3	2.0	1.6	2.3
Canada	1.7	3.3	1.7	1.5	1.7

^a Changes are represented by linear trends over the period. Estimates are derived from the gridded station data. There is a lack of data for northern Canada (see Figure 4.1).

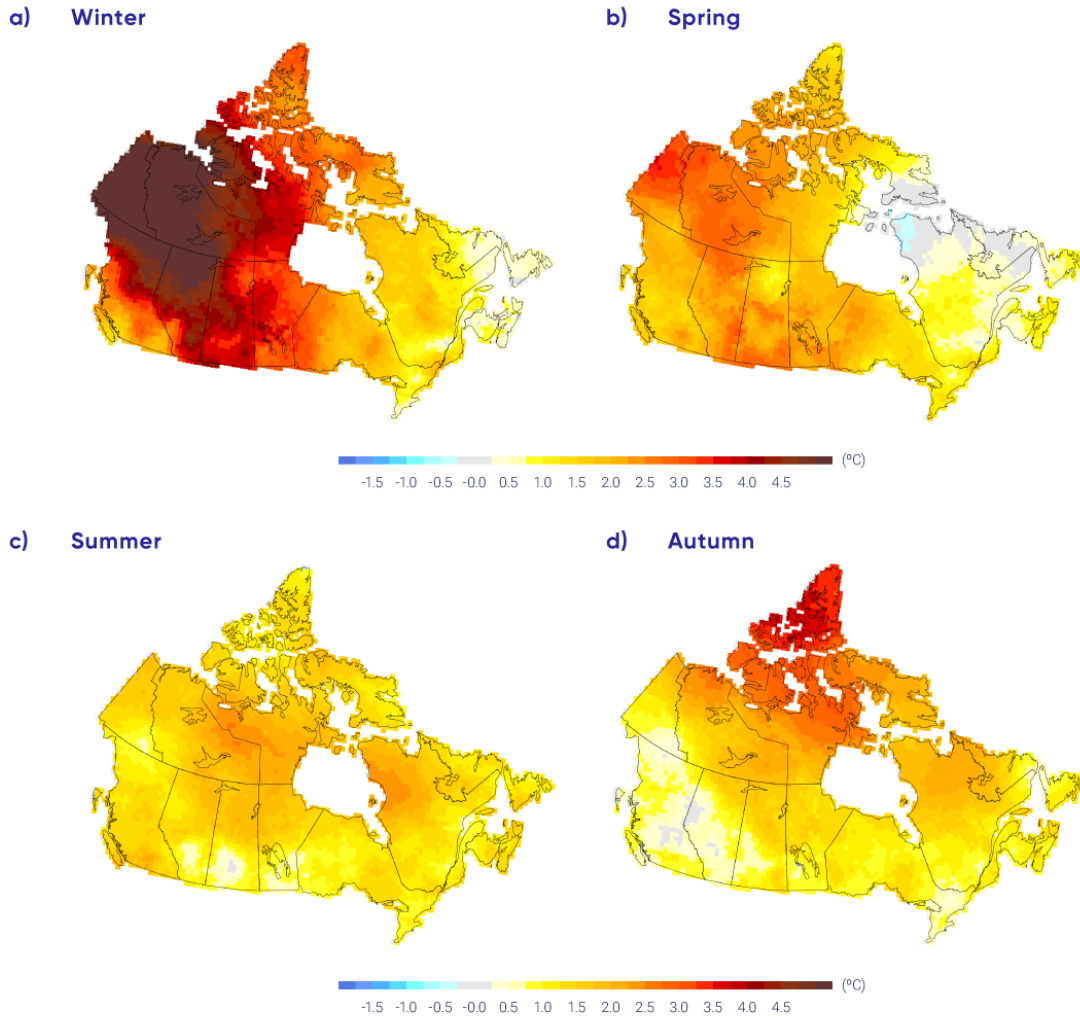


Figure 4.4: Trends in seasonal temperatures across Canada

Figure caption: Observed changes (°C) in seasonal mean temperatures between 1948 and 2016 for the four seasons. Estimates are derived based on linear trends in the gridded station data.

FIGURE SOURCE: UPDATED FROM FIGURE 3 OF VINCENT ET AL., 2015.

In southern Canada, annual mean temperature increased by 1.9°C between 1900 and 2016 (updated from Vincent et al., 2015). This warming is significant at the 5% level. This temperature did not rise steadily over time. Temperature increased until about the 1940s, decreased slightly until 1970, and then increased rapidly through 2016. This long-term behaviour of temperature is consistent with that observed globally (see Chapter 2, Section 2.2.1; Hartmann et al., 2013), but the magnitude of warming in Canada is larger. Mean temperature in southern Canada increased by 2.8°C in winter, 2.2°C in spring, 1.7°C in summer, and 1.6°C in autumn during the same period.

4.2.1.2: Causes of observed changes

It is *extremely likely* that human activities have caused more than half of the observed increase in global mean surface temperature from 1951 to 2010 (Bindoff et al., 2013). This causal effect was established through detection and attribution analysis, comparing the observed changes with the natural internal climate variability and with the expected climate responses to human activities (see Chapter 2, Section 2.3.4). Changes in the climate become detectable if they are large when compared with natural internal climate variability, and the change is attributed to human activity if it is (1) consistent with the expected “fingerprint” of human-caused change, as simulated by climate models (see Chapter 3); and (2) inconsistent with other plausible causes. For Canada and the Arctic, where natural internal variability of temperature is high, attribution of observed warming is more difficult than it is on a global scale. Nevertheless, evidence of anthropogenic influence on Canadian temperature has emerged (Gillett et al., 2004; Zhang et al., 2006; Wan et al., 2018), with a detectable contribution to warming in annual and seasonal temperatures and in extreme temperatures.

Two modes of natural internal climate variability that affect temperatures in Canada are the Pacific Decadal Oscillation (PDO) and the North Atlantic Oscillation (NAO) (see Chapter 2, Box 2.5). About 0.5°C of the observed warming of 1.7°C over the 1948–2012 period can be explained by a linear relationship between the PDO and the NAO. Assuming this is completely due to natural climate variability, roughly 1.1°C (*likely* range 0.6°C–1.5°C) of the observed 1.7°C increase in annual mean temperature in Canada from 1948–2012 can be attributed to human influence (see Figure 4.5; Wan et al., 2018). There is a 33% probability that anthropogenic influence increased Canadian temperature by at least 0.9°C. It is *likely* that more than half of the observed warming in Canada is due to human influence. The effects of natural internal climate variability on Canadian temperature trends differ in different parts of Canada, enhancing the warming trend in the western Canada and reducing the warming trend in eastern Canada over the past half of the 20th century (Vincent et al., 2015). The detection of anthropogenic influence on Canadian temperature is also corroborated by other independent evidence, including the attribution of Arctic temperature change to the influence of GHGs and aerosols (Najafi et al., 2015). The reduction in spring snow pack and the ensuing reduction in summer streamflow in British Columbia have been attributed to anthropogenic climate change (Najafi et al. 2017a, 2017b; see Chapter 6, Section 6.2.1). Anthropogenic warming has also increased fire risk in Alberta (Kirchmeier-Young et al., 2017a; see Section 4.4.1.2).

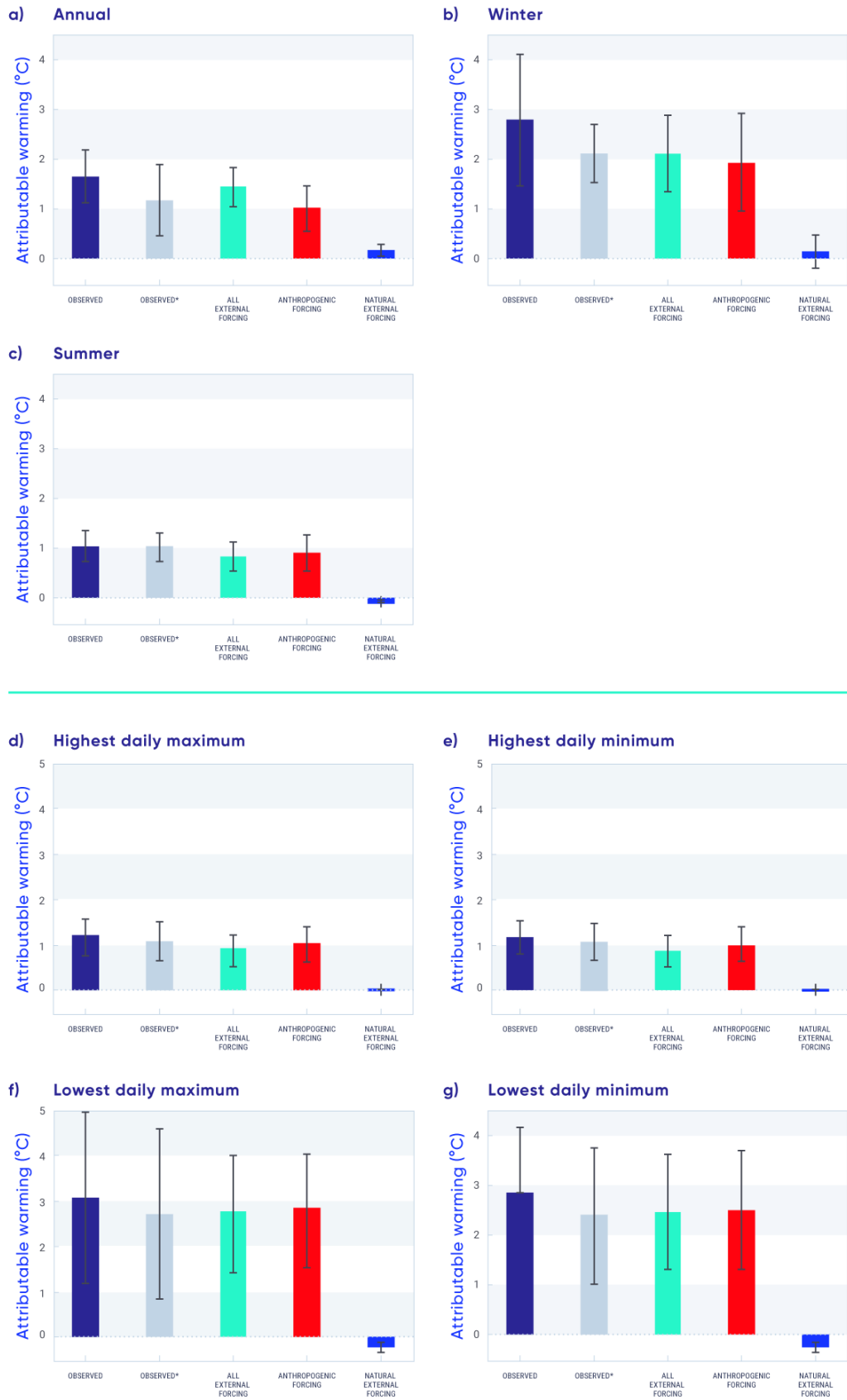


Figure 4.5: Attribution of causes to temperature change in Canada, 1948–2012

Figure caption: Changes in the observations (Observed, navy) and in the observed data removing the effects of the Pacific Decadal Oscillation and the North Atlantic Oscillation (Observed*, grey), along with the estimated contribution of all external forcing, anthropogenic forcing, and natural external forcing (effects of solar and volcanic activities) to observed changes in mean (a, b, c) and extreme (d, e, f, g) temperatures for Canada as a whole over the 1948–2012 period. The top panels show the estimations of attributable warming for (a) annual, (b) winter, and (c) summer mean temperatures. The bottom panels show estimates of attributable warming for extreme temperatures, including (d) annual highest daily maximum temperature, (e) annual highest daily minimum temperature, (f) annual lowest daily maximum temperature, and (g) annual lowest daily minimum temperature. The thin black bars indicate the 5%–95% uncertainty range.

FIGURE SOURCE: ADAPTED FROM FIGURE 7 OF WAN ET AL., 2018

4.2.1.3: Projected changes and uncertainties

Earth system models or global climate models provide projections of future climate change based on a range of future scenarios incorporating GHGs, aerosols, and land-use change (see Chapter 3, Section 3.3.1). The fifth phase of the Coupled Model Intercomparison Project (CMIP5, see Chapter 3, Box 3.1) was an internationally coordinated effort that produced a multi-model ensemble of climate projections. Results from this ensemble specific to Canada have been generated using output from 29 CMIP5 models, based on three scenarios: a low emission scenario (RCP2.6), a medium emission scenario (RCP4.5), and a high emission scenario (RCP8.5). Results for a fourth scenario that was part of the CMIP5 protocol (RCP6.0) are also available, but from fewer models. These multi-model results are described by Environment and Climate Change Canada (ECCC, 2016) and are available for download from the [Canadian Climate Data and Scenarios website](http://climate-scenarios.canada.ca/?page=download-intro) (<<http://climate-scenarios.canada.ca/?page=download-intro>>).

In the following, multi-model climate change projections for 2031–2050 and 2081–2100 (relative to a 1986–2005 reference period) are shown for Canada for a low emission scenario (RCP2.6) and a high emission scenario (RCP8.5), spanning the range of available scenarios. The low emission scenario assumes rapid and deep emission reductions and near-zero emissions this century, whereas the high emission scenario assumes continued growth in emissions this century. The two time periods were chosen to provide information for the near term (2031–2050), when differences in emission scenarios are modest, and for the late century (2081–2100), when climatic responses to the low and high emission scenarios will have diverged considerably. This latter difference illustrates the long-term climate benefit associated with aggressive mitigation efforts. The multi-model median change is shown in map form, along with time series of the average from individual models, which is computed for all Canadian land area. The box and whisker symbols at the right side of the time series provide an indication of the spread across models for 2081–2100. Values for different regions in Canada are provided in Table 4.2.

Table 4.2: Projected change in annual mean surface air temperature for six regions and for all Canadian land area, relative to 1986–2005^a

REGION ^b	SCENARIO; PERIOD; MEDIAN TEMPERATURE (25TH, 75TH PERCENTILE), °C			
	RCP2.6		RCP8.5	
	2031–2050	2081–2100	2031–2050	2081–2100
British Columbia	1.3 (0.8, 1.9)	1.6 (1.1, 2.1)	1.9 (1.4, 2.5)	5.2 (4.3, 6.2)
Prairies	1.5 (1.1, 2.1)	1.9 (1.2, 2.2)	2.3 (1.7, 3.0)	6.5 (5.2, 7.0)
Ontario	1.5 (1.1, 2.1)	1.7 (1.0, 2.1)	2.3 (1.7, 2.9)	6.3 (5.3, 6.9)
Quebec	1.5 (1.0, 2.1)	1.7 (1.0, 2.2)	2.3 (1.7, 2.9)	6.3 (5.3, 6.9)
Atlantic	1.3 (0.9, 1.8)	1.5 (0.9, 2.0)	1.9 (1.5, 2.4)	5.2 (4.5, 6.1)
North	1.8 (1.2, 2.5)	2.1 (1.3, 2.5)	2.7 (2.0, 3.5)	7.8 (6.2, 8.4)
Canada	1.5 (1.0, 2.1)	1.8 (1.1, 2.5)	2.3 (1.7, 2.9)	6.3 (5.6, 7.7)

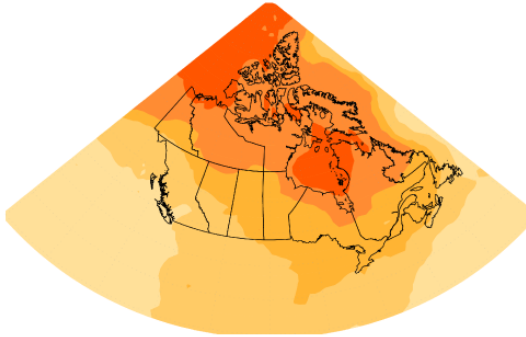
^a The median or 50th percentile value is based on the CMIP5 multi-model ensemble. The 25th percentile value indicates that 25% of the CMIP5 model projections have a change smaller than this value. The 75th percentile value indicates 25% of CMIP5 model projections have a change larger than this value.

^b The linear warming trend from 1948 (start date for climate trend analysis for all of Canada based on historical observations) to 1996 (mid-point of 1986–2005) is calculated to be 1.2°C. ^c Regions are defined by political boundaries; “North” includes the three territories (see Figure 1.1).

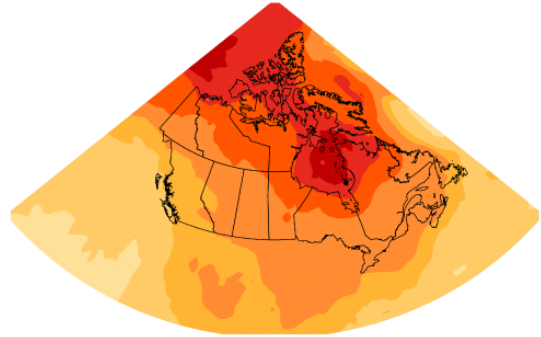
Projected temperature changes for winter (December–February average), summer (June–August average), and annual mean are shown in Figures 4.6, 4.7, and 4.8, respectively. Enhanced warming at higher latitudes is evident in the winter and annual mean. This is a robust feature of climate projections, both for Canada and the Earth, and is due to a combination of factors, including reductions in snow and ice (and thus a reduction in albedo) and increased heat transport from southern latitudes (see Chapter 3). This high-latitude amplification is not apparent in the summer maps because, over the Arctic Ocean, summer temperatures remain near 0°C – the melting temperature of snow and sea ice. In the near term (2031–2050), the differences in pattern and magnitude between the low emission scenario (RCP2.6) and the high emission scenario (RCP8.5) are modest (on the order of 0.5°C to 1°C). However, for the late century (2081–2100), the differences become very large. Under the high emission scenario, projected temperature increases are roughly 4°C higher, when averaged for Canada as a whole, than under the low emission scenario. The differences are even greater in northern Canada and the Arctic in winter. In southern Canada, projected winter temperature change is larger in the east than in the west, with British Columbia projected to warm slightly less than elsewhere in Canada. The projected summer change is more uniform across the country.

a) Temperature change RCP2.6 (2031–2050)

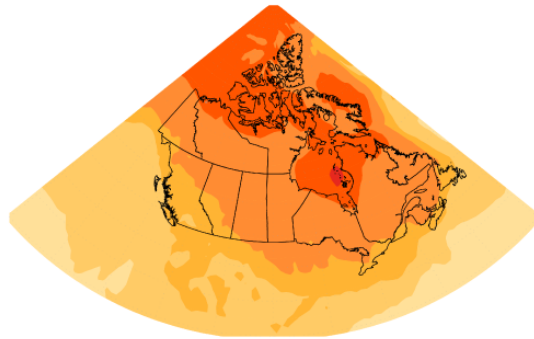
December–February

**b) Temperature change RCP8.5 (2031–2050)**

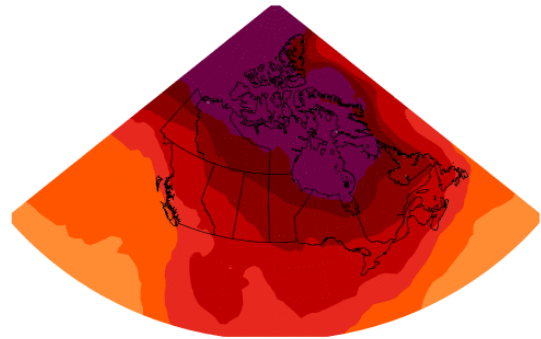
December–February

**c) Temperature change RCP2.6 (2081–2100)**

December–February

**d) Temperature change RCP8.5 (2081–2100)**

December–February



-2 -1.5 -1 -0.5 0 0.5 1 1.5 2 3 4 5 7 9 11 (°C)

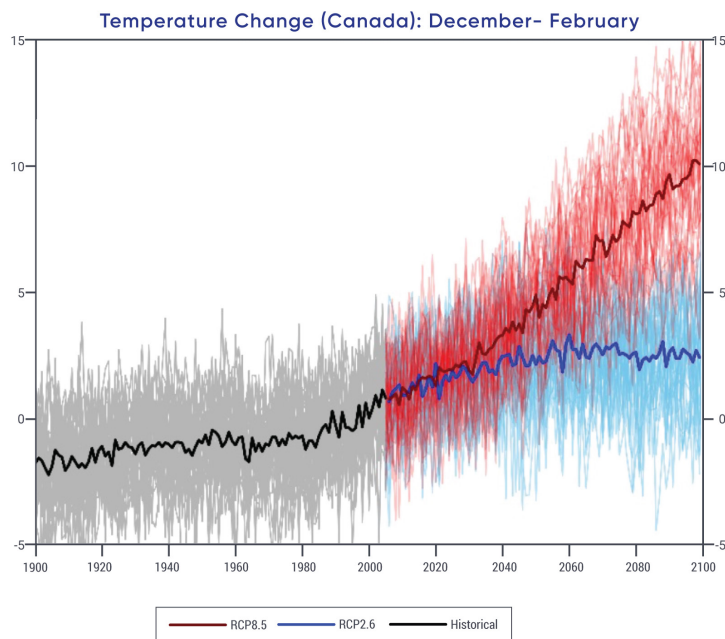


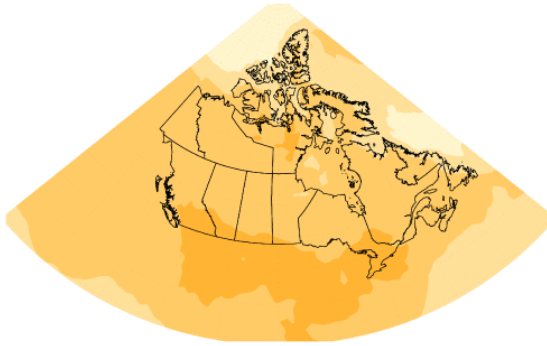
Figure 4.6: Projected temperature changes for winter season



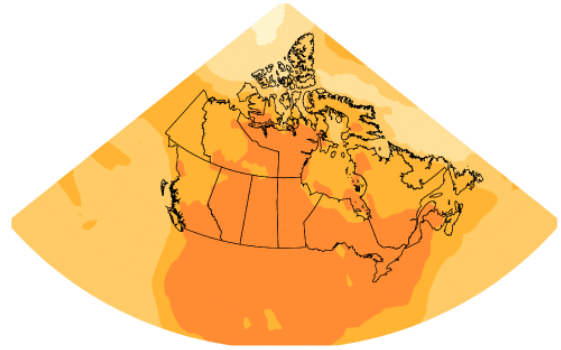
Figure caption: Maps and time series of projected temperature change (°C) for December, January, and February, as represented by the median of the CMIP5 multi-model ensemble. Changes are relative to the 1986–2005 period. The upper maps show temperature change for the 2031–2050 period and the lower maps, for the 2081–2100 period. The left-hand maps show changes resulting from the low emission scenario (RCP2.6), whereas the right-hand maps show changes from the high emission scenario (RCP8.5). The time series at the bottom of the figure shows the temperature change averaged for the Canadian land area over the 1900–2100 period. The thin lines show results from the individual CMIP5 models, and the heavy line is the multi-model mean. The spread among models, evident in the thin lines, is quantified by the box and whisker plots to the right of each panel. They show, for the 2081–2100 period, the 5th, 25th, 50th (median), 75th, and 95th percentile values.

FIGURE SOURCE: CLIMATE RESEARCH DIVISION, ENVIRONMENT AND CLIMATE CHANGE CANADA.

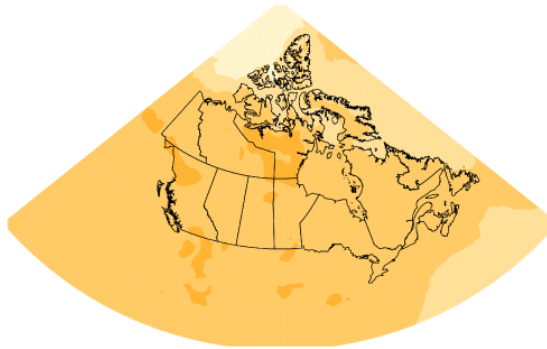
a) **Temperature change RCP2.6 (2031–2050)**
June–August



b) **Temperature change RCP8.5 (2031–2050)**
June–August



c) **Temperature change RCP2.6 (2081–2100)**
June–August



d) **Temperature change RCP8.5 (2081–2100)**
June–August

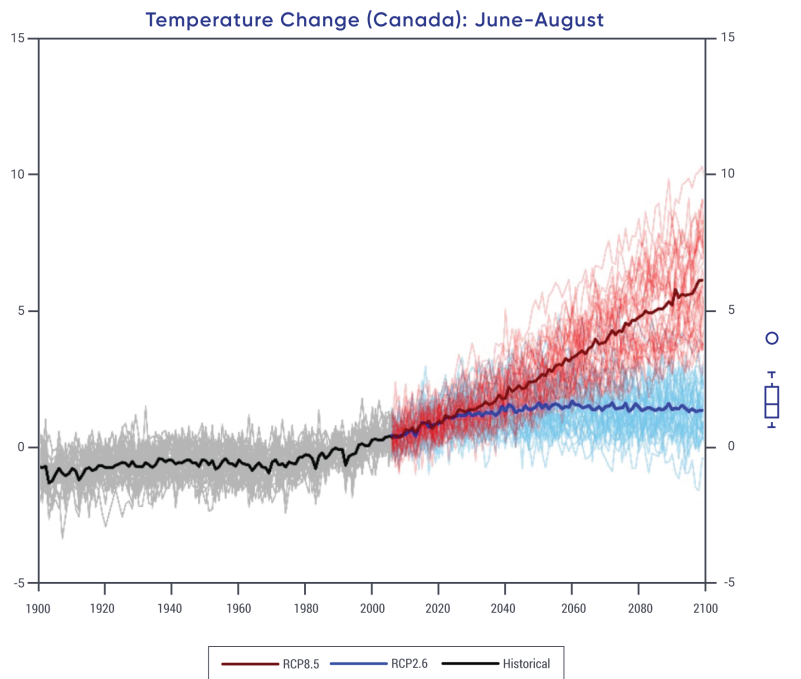
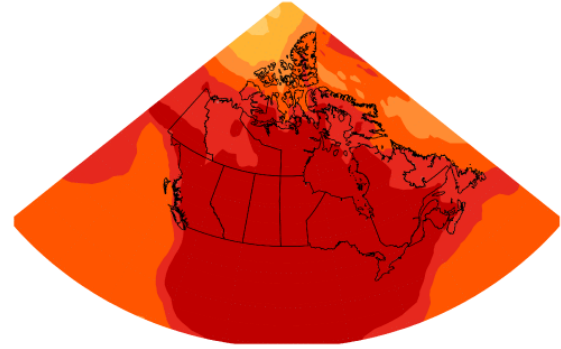


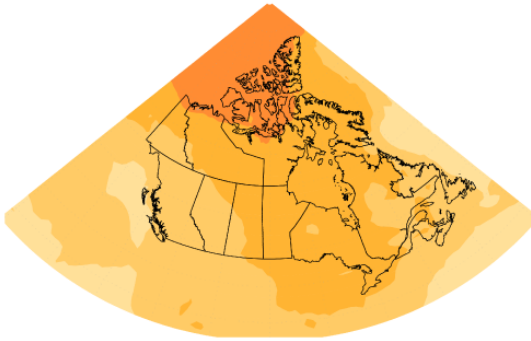
Figure 4.7: Projected temperature changes for summer season



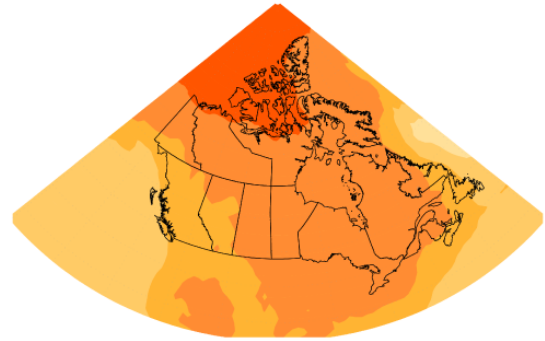
Figure caption: Maps and time series of projected temperature change (°C) for June, July, and August as represented by the median of the CMIP5 multi-model ensemble. Changes are relative to the 1986–2005 period. The upper maps show temperature change for the period 2031–2050 and the lower maps, for the 2081–2100 period. The left-hand maps show changes resulting from the low emission scenario (RCP2.6), whereas the right-hand maps show changes from the high emission scenario (RCP8.5). The time series at the bottom of the figure show the temperature change averaged for the Canadian land area and over the 1900–2100 period. The thin lines show results from the individual CMIP5 models, and the heavy line is the multi-model mean. The spread among models, evident in the thin lines, is quantified by the box and whisker plots to the right of each panel. They show, for the 2081–2100 period, the 5th, 25th, 50th (median), 75th, and 95th percentile values.

FIGURE SOURCE: CLIMATE RESEARCH DIVISION, ENVIRONMENT AND CLIMATE CHANGE CANADA.

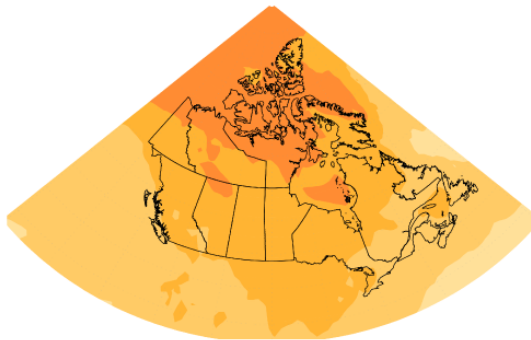
a) **Temperature change RCP2.6 (2031–2050)**
Annual



b) **Temperature change RCP8.5 (2031–2050)**
Annual



c) **Temperature change RCP2.6 (2081–2100)**
Annual



d) **Temperature change RCP8.5 (2081–2100)**
Annual

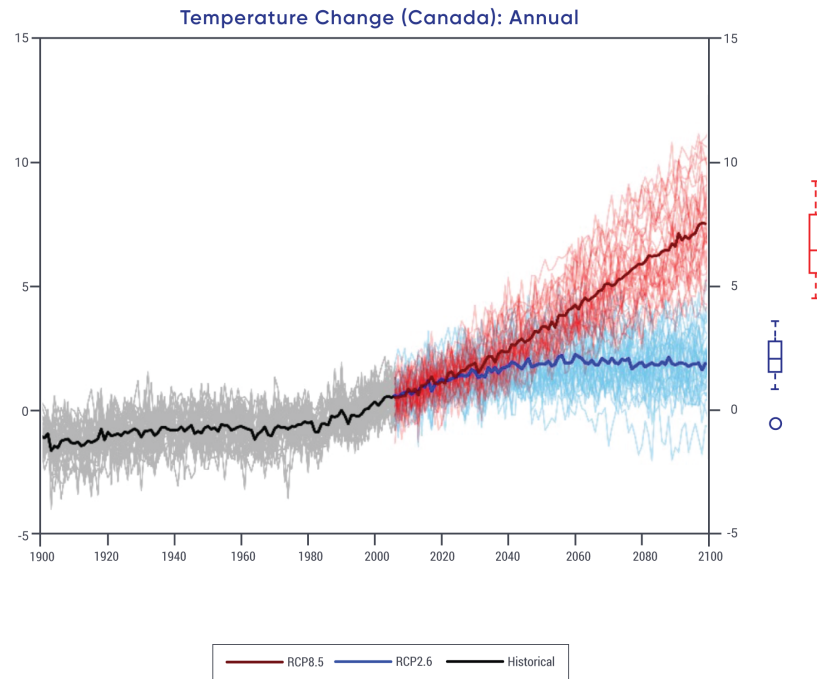
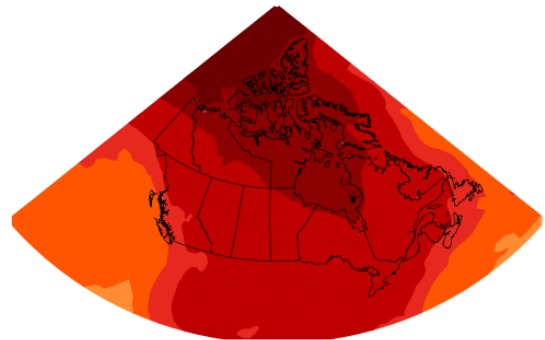


Figure 4.8: Projected annual temperature changes



Figure caption: Maps and time series of projected annual mean temperature change, (°C) as represented by the median of the fifth phase of the Coupled Model Intercomparison Project (CMIP5) multi-model ensemble. Changes are relative to the 1986–2005 period. The upper maps show temperature change for the 2031–2050 period and the lower maps, for the 2081–2100 period. The left-hand maps show changes resulting from the low emission scenario (RCP2.6), whereas the right-hand maps show changes from the high emission scenario (RCP8.5). The time series at the bottom of the figure shows the temperature change averaged for the Canadian land area and over the 1900–2100 period. The thin lines show results from the individual fifth phase of the Coupled Model Intercomparison Project (CMIP5) models, and the heavy line is the multi-model mean. The spread among models, evident in the thin lines, is quantified by the box and whisker plots to the right of each panel. They show, for the 2081–2100 period, the 5th, 25th, 50th (median), 75th, and 95th percentile values.

FIGURE SOURCE: CLIMATE RESEARCH DIVISION, ENVIRONMENT AND CLIMATE CHANGE CANADA.

The maps in Figures 4.6, 4.7, and 4.8 illustrate the median projection from the CMIP5 multi-model ensemble – some models project larger changes and some project smaller changes. The spread across models provides an indication of the projection uncertainty discussed in Chapter 3, Section 3.3.2. The spread among the CMIP5 ensemble is only an ad hoc measure of uncertainty. Actual uncertainty could be larger, because CMIP5 models may not represent the full spectrum of plausible representations of all relevant physical processes (Kirtman et al., 2013). The spread across models also includes natural, year-to-year variability, which continues in the future much as it has in the past. Even when averaged for a region as large as Canada, differences in projected temperature among models are on the order of a couple of degrees. Under a low emission scenario (RCP2.6), annual mean warming in Canada stabilizes at about 1.8°C above the 1986–2005 reference period after about 2050, whereas, under a high emission scenario (RCP8.5), annual warming continues throughout the 21st century and beyond, reaching about 6.3°C above the reference period by 2100. Additional values for Canada as a whole and for various regions are presented in Table 4.2.

Temperature change is one of the key indicators of a changing climate, and many other climate variables are directly or indirectly tied to temperature. The changes in mean temperature are the projected response to emissions of GHGs and aerosols from human activities, and natural internal climate variability will continue to be superimposed on these forced changes. Natural internal climate variability is simulated by the climate models used to make projections of future climate change, and this is evident in the year-to-year variability in the Canada-average temperature time series in Figures 4.6, 4.7, and 4.8 (the individual thin lines). Indeed, this year-to-year variability looks much like what has been observed in the past (see Figure 4.2). In contrast, the underlying forced response (approximated by the multi-model average – the thick line in the figures) is a slowly, monotonically changing value that closely tracks the cumulative emissions of GHGs since the pre-industrial era (see Chapter 3, Section 3.4.1). In assessing the impacts of a warming climate, this combination of slow forced change and natural internal variability is important to keep in mind – the future will continue to have extreme warm and cold periods superimposed on a slow warming forced by human activities.

Because the components of the global climate system are closely interconnected, temperature change in a particular region, such as Canada, is closely related to the change in global mean. This is illustrated in the left panel of Figure 4.9, which shows Canadian mean temperature change versus global mean temperature change. As noted previously, Canadian mean temperature is projected to increase at roughly double the global mean rate, regardless of the forcing scenario. That is, the relationship between Canadian and global temperature change remains constant, as shown by the fact that the results from the different scenarios are all aligned. This connection between global mean and Canadian mean temperature change provides a way of estimating the implications of global change for Canada under alternative forcing scenarios. In other words, impacts estimated under one forcing scenario can be scaled to approximate impacts under another forcing scenario, since the ratio of Canadian to global temperature change is roughly constant. Of course, this assumes that impacts scale directly with temperature (which may not always be the case).

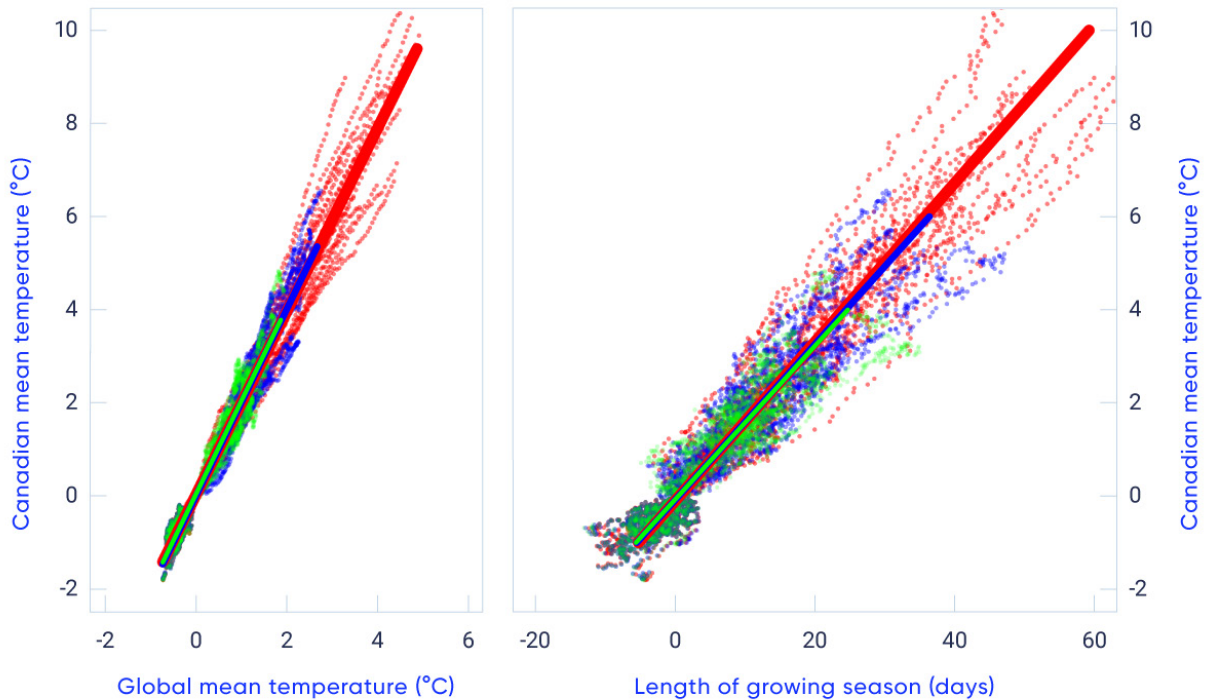


Figure 4.9: Connections between global mean and Canadian mean temperature change, and changes in length of the growing season

Figure caption: The left-hand panel shows Canadian mean temperature change plotted against global mean temperature change (°C for 20-year averages relative to 1986–2005) from fifth phase of the Coupled Model Intercomparison Project (CMIP5) model simulations for three different forcing scenarios (green: RCP2.6; blue: RCP4.5; red: RCP8.5). Heavy lines are least-squares linear fits, whereas thinner dashed lines are individual model results. The right-hand panel shows the changing length of the growing season (in days, see Chapter 1, Section 1.2) for warm-season crops in the Canadian Prairies, as a function of changes in Canadian mean temperature.

FIGURE SOURCE: ADAPTED FROM LI ET AL., 2018.

The IPCC Fifth Assessment concluded that “Global mean temperatures will continue to rise over the 21st century if GHG emissions continue unabated” (Collins et al., 2013, p. 1031). Because of the connection between global mean and Canadian mean temperature changes, it is *virtually certain* that temperature will also continue to increase in Canada as long as GHG emissions continue.

4.2.2: Temperature extremes and other indices

This subsection describes changes in temperature extremes and other indices relevant to impact assessments. All are derived from daily temperature data. Some indices, such as the annual highest and lowest day or night temperatures, represent temperature extremes and have widespread applications, such as in building design. Others are important for specific users. For example, degree days are a commonly used indicator of building cooling or heating demand, and of the amount of heat available for crop growth. Heating degree days (the annual sum of daily mean temperature below 18°C) or cooling degree days (the annual sum of daily mean temperature above 18°C) are used for energy utility planning, while growing degree days (the sum of daily mean temperature above 5°C in a growing season) is an important index for agriculture. Some indices, such as the number of days when daily maximum temperature is above 30°C or when daily minimum temperature is above 22°C, have important health implications (Casati et al., 2013). Observed changes in temperature indices and extremes indicate that warm events are becoming more intense and more frequent, while cold events are becoming less intense and less frequent. These have important implications; for example, extreme winter cold days are important in limiting the occurrence of some forest pests (Goodsman et al., 2018).

4.2.2.1: Observed changes

The annual highest daily maximum temperature, averaged across the country, increased by 0.61°C between 1948 and 2016 (updated from Wan et al., 2018). The largest increases were in northern Canada, while decreases were observed in the southern Prairies (see Figure 4.10a). The highest daily maximum temperature that occurs once in 20 years, on average, also increased (Wang et al., 2014). The annual lowest daily minimum temperature, averaged across the country, increased by 3.3°C between 1948 and 2016, with the strongest warming in the west (see Figure 4.10b) (updated from Wan et al., 2018). The lowest daily minimum temperature that occurs once in 20 years, on average, increased more strongly (Wang et al., 2014). Overall, extreme cold temperatures increased much more rapidly than the extreme warm temperatures, consistent with greater warming in winter than in summer, as well as greater warming in night temperatures than in day temperatures.

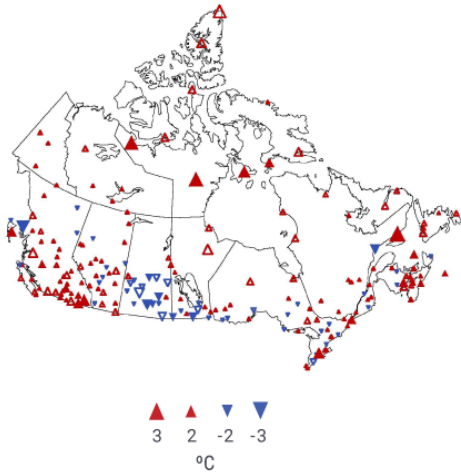
Indices of high temperature, such as hot days and hot nights, are particularly relevant to public health. Hot days, defined as days with maximum temperature above 30°C, are rarely observed in the regions north of 60° north latitude. In southern Canada, the number of hot days annually increased by about 1 to 3 days at a few stations over the 1948–2016 period (see Figure 4.10c; also see Vincent et al., 2018). Most locations in Canada are not warm enough to have hot nights, defined as nights with daily minimum temperature above 22°C, and the number of hot nights has significantly increased only at a few stations in southern Ontario and Quebec.

Warming in winter and spring has resulted in a significant decrease in the number of frost days (days with daily minimum temperature of 0°C or lower) and ice days (days with daily maximum temperature of 0°C or

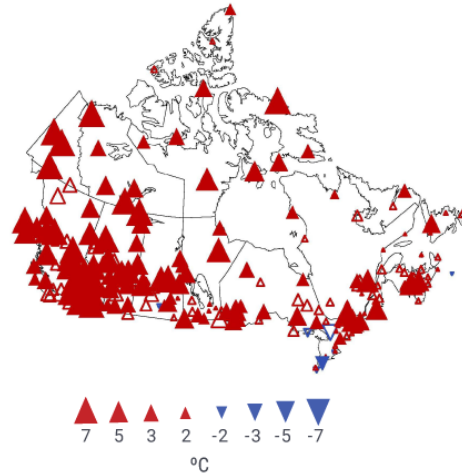


lower), as well as shortened winter seasons (Vincent et al., 2018). Averaged for the country as a whole, frost days have decreased by more than 15 and ice days by more than 10 days from 1948 to 2016. These changes are consistent across the country. As a result, the frost-free season has been extended by 20 days, starting about 10 days earlier and ending about 10 days later. Heating degree days have decreased while cooling degree-days have increased (see Figure 4.10e and f). The length of growing seasons (see Figure 4.10d) and the number of growing degree days have also increased. The growing season, which starts when there are six consecutive days with daily mean temperature above 5°C in spring or summer and ends when this condition fails to be met late in the year, started earlier and ended later, resulting in an increase in growing season length of about 15 days between 1948 and 2016. With the longer growing season, the number of growing degree days increased.

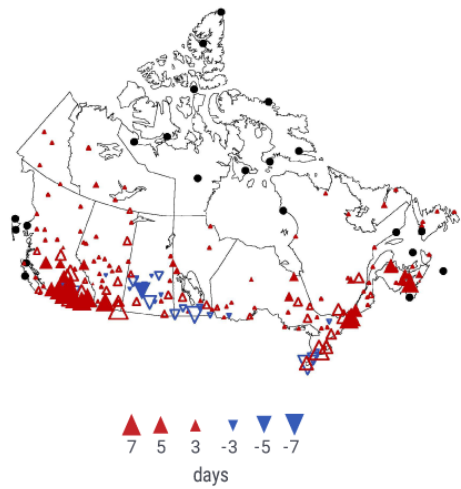
a) Highest daily maximum (°C)



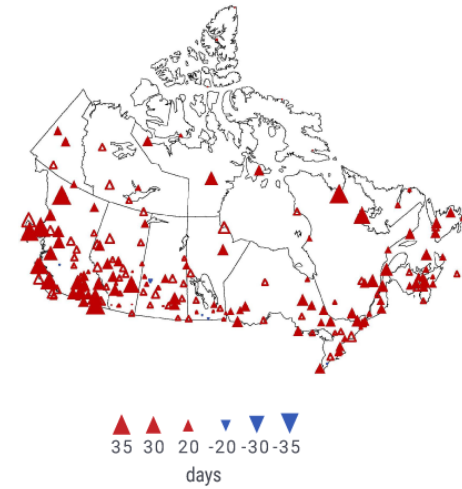
b) Lowest daily minimum (°C)



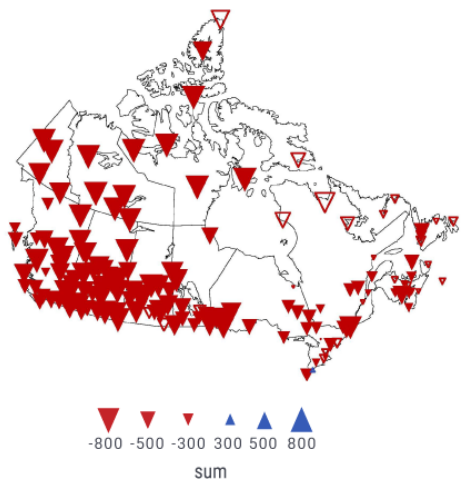
c) Number of hot days (days)



d) Length of growing season (days)



e) Heating degree days (°C-day)



f) Cooling degree days (°C-day)

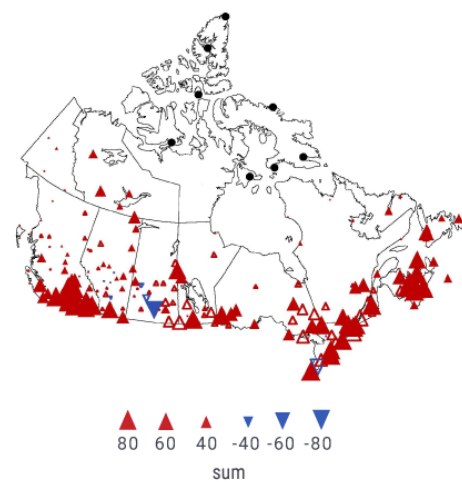


Figure 4.10: Changes in selected temperature indicators, 1948–2016

Figure caption: Observed changes in: (a) annual highest daily maximum temperature, (b) annual lowest daily minimum temperature, (c) annual number of hot days (when daily maximum temperature is above 30°C), (d) length of growing season, and (e) heating and (f) cooling degree days. Changes are computed based on linear trends over the 1948–2016 period. Filled triangles indicate trends significant at the 5% level. The black dots on (c) and (f) mark stations where hot days or daily mean temperature above 18°C do not normally occur. The legend may not include all sizes shown in the figure.

FIGURE SOURCE: ADAPTED FROM VINCENT ET AL., 2018.

4.2.2.2: Causes of observed changes

It is *very likely* that anthropogenic forcing has contributed to the observed changes in the frequency and intensity of daily temperature extremes on the global scale since the mid-20th century (Bindoff et al., 2013; see also Chapter 2, Section 2.3.4). Several detection studies have shown that the annual lowest daily minimum temperature (Zwiers et al., 2011; Min et al., 2013; Kim et al., 2015) and the annual highest daily maximum temperatures (Wang et al., 2017) have been influenced by human activity in three subregions of North America. In Canada, an increase of 3.2°C in the annual lowest daily minimum temperature was observed from 1948 to 2012 (Wan et al., 2018). Only a small fraction (about 0.5°C) of this increase can be related to natural internal climate variability, and anthropogenic influence may have contributed as much as 2.8°C (*likely* range 1.5° to 4.2°C) to the warming (see Figure 4.5). In addition, much of the observed warming seen in the annual highest daily maximum temperature may also be attributable to anthropogenic influence. Overall, most of the observed increase in the coldest (*likely*) and warmest (*high confidence*) daily temperatures of the year in Canada from 1948 to 2012 can be attributed to anthropogenic influence.

While there is a lack of studies directly attributing observed changes in other temperature indices, there is *high confidence* that substantial parts of the observed changes in most of these temperature indices are also due to anthropogenic influence. It is more difficult to detect anthropogenic influence in values such as annual lowest daily minimum temperature, which are sampled once a year, than in other temperature indices that integrate information from many data samples in a year. These indices are less affected by natural internal variability, while nevertheless retaining the climate responses to external forcing.

4.2.2.3: Projected changes and uncertainties

The models used to make projections of future climate are discussed in Chapter 3, Section 3.3. When using climate model projections for impact studies, it is often important to consider that the model simulated



current climate may differ from observed climate — a reflection of model biases (Flato et al. 2013). Many temperature indices are connected to absolute thresholds (like the freezing temperature), and, so, mean biases can substantially alter their usefulness. As a result, where absolute values are important, some form of bias correction is needed. This is a method of correcting the model output to remove, to the extent possible, the influence of model biases. The assessments of projected changes in temperature indices discussed in this subsection are, unless otherwise stated, based on statistically downscaled and bias-corrected data (Li et al., 2018; Murdock et al., 2014; Werner and Cannon, 2016; see Chapter 3, Section 3.5).

Daily extreme temperatures, hot and cold, are projected to increase substantially (see Figure 4.11). Annual highest daily maximum temperature is projected to track the projected changes in summer mean temperature, but at a slightly higher rate (the largest difference between the two is less than 0.5°C, appearing in 2081–2100 under a high emission scenario [RCP8.5]). Annual lowest daily minimum temperature is projected to warm faster than winter mean temperature over most of Canada, increasing the extreme minimum temperature in southern Canada by about 3°C by the end of the century under a high emission scenario (RCP8.5). Table 4.3 summarizes projected changes in Canada. For example, averaged over the country, the annual highest daily maximum temperatures are projected to increase by 1.4°C over the 2031–2050 period under a low emission scenario (RCP2.6), and by 2°C for the same period under a high emission scenario (RCP8.5) compared with the current climate (1986–2005). The corresponding projected increase in 2081–2100 under the low emission scenario (RCP2.6) is 1.5°C, only slightly higher than the increases in 2031–2050. A much larger increase, of about 6°C, is expected in 2081–2100 under the high emission scenario (RCP8.5).

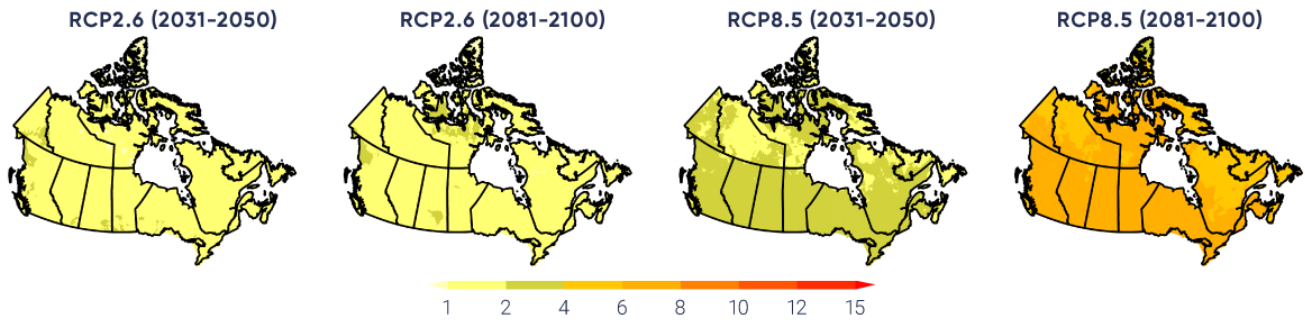
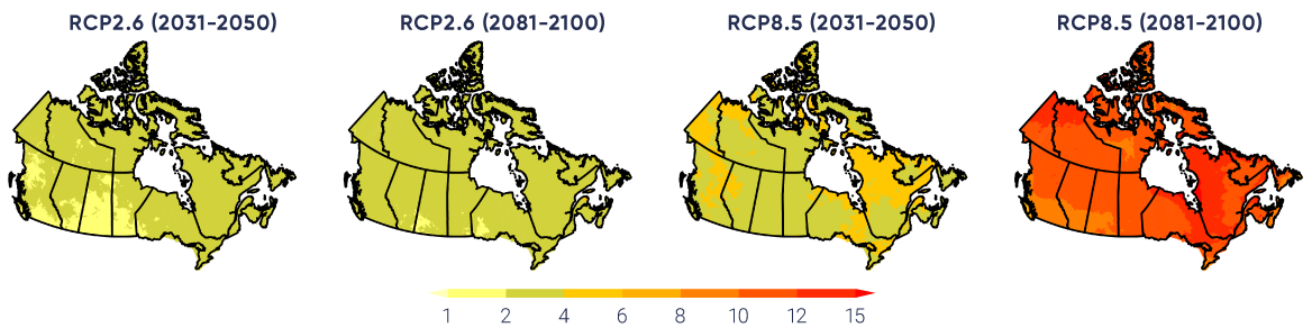
a) Annual highest daily maximum temperature (°C)**b) Annual lowest daily minimum temperature (°C)**

Figure 4.11: Future projections for selected temperature indices (extremes)

Figure caption: Multi-model median projected changes in (a) annual highest daily maximum temperature, (b) annual lowest daily minimum temperature. All maps are based on statistically downscaled and bias-corrected temperature data from simulations by 24 Earth system models. The two left-hand panel show projections for 2031–2050 and 2081–2100 under a low emission scenario (RCP2.6), while the two right-hand panels show projections for 2031–2050 and 2081–2100 under a high emission scenario (RCP8.5).

FIGURE SOURCE: ADAPTED FROM LI ET AL., 2018.

Table 4.3: Multi-model changes in indicators of temperature^a

REGION ^b	SCENARIO; PERIOD; MEDIAN (25%, 75% PERCENTILE)			
	RCP2.6		RCP8.5	
	2031–2050	2081–2100	2031–2050	2081–2100
Annual highest daily maximum temperature, °C				
British Columbia	1.7 (0.9, 2.4)	1.7 (1.2, 2.4)	2.3 (1.6, 3.2)	6.7 (4.9, 7.9)
Prairies	1.6 (0.9, 2.3)	1.6 (1.1, 2.4)	2.5 (1.8, 3.1)	6.9 (5.2, 8.2)
Ontario	1.6 (1.0, 2.4)	1.5 (0.8, 2.2)	2.5 (1.9, 3.0)	6.6 (5.2, 7.7)
Quebec	1.4 (0.8, 2.2)	1.3 (0.7, 2.0)	2.1 (1.5, 2.7)	5.9 (4.7, 7.1)
Atlantic	1.4 (0.9, 1.9)	1.2 (0.6, 1.9)	1.9 (1.4, 2.4)	5.5 (4.6, 6.5)
North	1.3 (0.6, 2.2)	1.5 (0.7, 2.2)	1.8 (0.9, 2.7)	5.7 (3.6, 7.3)
Canada	1.4 (0.7, 2.3)	1.5 (0.8, 2.2)	2.0 (1.2, 2.8)	6.1 (4.2, 7.5)
Annual highest daily minimum temperature, °C				
British Columbia	2.1 (1.1, 3.7)	2.7 (1.4, 4.2)	3.7 (2.4, 5.3)	10.1 (8.5, 11.7)
Prairies	2.1 (1.3, 3.3)	2.5 (1.6, 3.8)	3.5 (2.5, 4.9)	10.5 (9.3, 12.8)
Ontario	2.6 (1.9, 3.5)	2.7 (2.0, 3.8)	3.9 (2.9, 4.7)	11.7 (10, 13.8)
Quebec	2.8 (1.9, 3.9)	3.2 (2.0, 4.4)	4.2 (3.2, 5.3)	12.6 (10.7, 15.7)
Atlantic	2.8 (1.8, 3.8)	3.0 (1.8, 4.5)	3.8 (2.8, 4.9)	11.2 (9.6, 13.6)
North	2.6 (1.8, 3.4)	2.9 (1.9, 4.0)	3.9 (3.0, 4.8)	11.1 (9.4, 14.0)
Canada	2.5 (1.7, 3.5)	2.8 (1.8, 4.1)	3.8 (2.9, 4.9)	11.2 (9.5, 13.8)
Annual number of hot days, days				
British Columbia	1.6 (0.7, 2.5)	1.5 (0.8, 2.5)	2.5 (1.7, 3.6)	16.0 (9.0, 20.0)
Prairies	4.5 (2.5, 6.7)	4.6 (2.6, 6.8)	7.2 (5.2, 9.4)	34.3 (22.8, 40.1)
Ontario	5.4 (3.6, 7.1)	4.7 (2.8, 6.8)	8.8 (6.8, 10.8)	38.0 (28.1, 44.5)
Quebec	1.7 (1.0, 2.3)	1.4 (0.8, 2.1)	2.7 (1.9, 3.4)	14.5 (10.1, 17.3)
Atlantic	1.4 (0.9, 2.0)	1.2 (0.6, 1.8)	2.1 (1.5, 2.8)	12.1 (9.3, 16.7)
North	0.3 (0.1, 0.5)	0.3 (0.1, 0.5)	0.5 (0.3, 0.7)	3.5 (2.0, 5.1)
Canada	1.6 (0.9, 2.3)	1.5 (0.9, 2.3)	2.6 (1.8, 3.3)	13.2 (8.8, 16.2)
Length of growing season for warm-season crops, days				
British Columbia	17.6 (12, 23.5)	22 (14.3, 28.5)	23.3 (17.7, 29.3)	61.1 (48.1, 70.5)
Prairies	11.5 (6.4, 16.0)	13.5 (9.1, 18.3)	15.5 (11.0, 20.5)	43.6 (35.6, 50.8)
Ontario	11.8 (6.9, 17.5)	13.0 (8.0, 19.1)	17.0 (11.8, 22.8)	44.4 (36.9, 53.7)
Quebec	13.6 (8.7, 18.7)	14.0 (7.7, 20.2)	19.3 (13.2, 24.8)	50.1 (40.2, 62.1)
Atlantic	13.7 (8.6, 18.2)	14.3 (8.9, 19.6)	18.6 (13.7, 25.2)	51.1 (42.5, 63.8)
North	8.8 (4.7, 13.4)	10.2 (5.0, 15.3)	12.9 (7.3, 18.4)	37.8 (25.5, 49.9)
Canada	10.8 (6.3, 15.6)	12.4 (7.0, 17.7)	15.3 (9.9, 20.9)	42.8 (31.9, 53.8)

Table 4.3: Multi-model changes in indicators of temperature^a

Cooling degree days, °C-days				
British Columbia	16 (9, 22)	16 (10, 25)	26 (19, 34)	168 (97, 211)
Prairies	52 (32, 74)	55 (32, 79)	85 (66, 108)	386 (260, 461)
Ontario	67 (44, 90)	58 (44, 89)	108 (88, 125)	408 (306, 491)
Quebec	25 (18, 37)	23 (16, 32)	42 (33, 49)	183 (136, 236)
Atlantic	28 (19, 40)	29 (18, 37)	42 (33, 54)	187 (150, 268)
North	6 (4, 10)	7 (4, 10)	10 (7, 13)	58 (34, 83)
Canada	21 (14, 30)	21 (14, 31)	35 (27, 43)	160 (109, 204)
Heating degree days, °C-days				
British Columbia	-497 (-651, -408)	-651 (-829, -502)	-731 (-907, -585)	-1873 (-2115, -1621)
Prairies	-545 (-654, -435)	-648 (-809, -508)	-781 (-957, -635)	-2036 (-2262, -1779)
Ontario	-550 (-681, -448)	-607 (-752, -448)	-770 (-948, -655)	-1990 (-2337, -1749)
Quebec	-596 (-796, -477)	-646 (-913, -480)	-869 (-1061, -690)	-2257 (-2759, -1916)
Atlantic	-524 (-679, -418)	-573 (-839, -428)	-730 (-897, -592)	-1895 (-2372, -1662)
North	-744 (-977, -593)	-884 (-1174, -563)	-1057 (-1352, -877)	-2880 (-3568, -2447)
Canada	-656 (-850, -525)	-772 (-1020, -527)	-936 (-1178, -770)	-2503 (-3033, -2142)

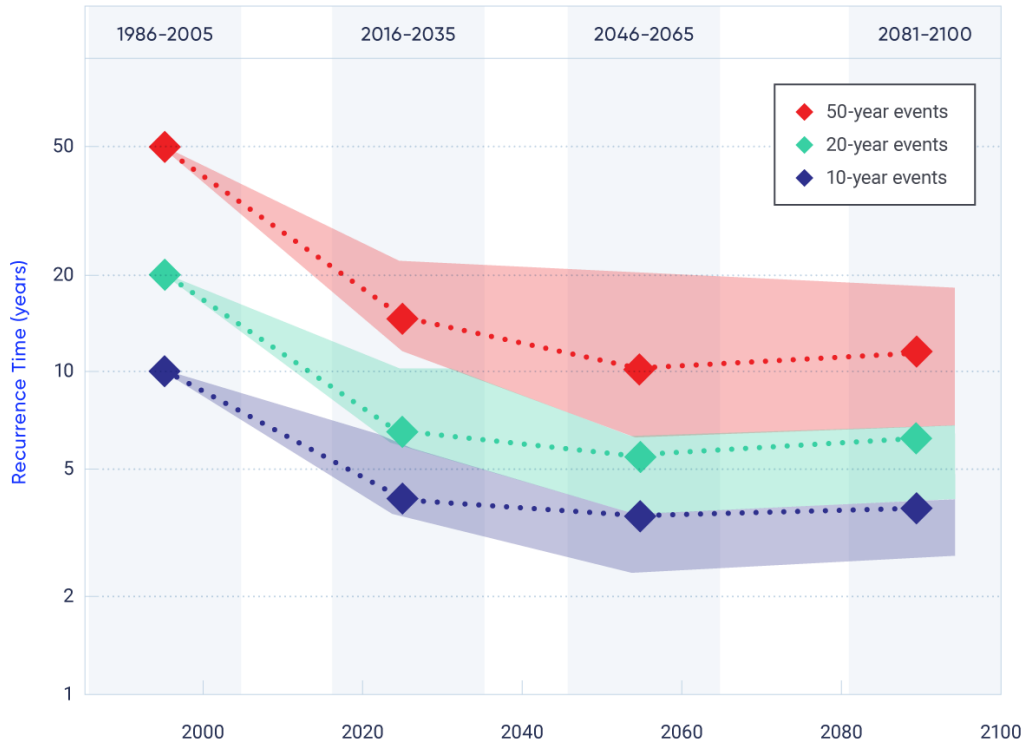
^a Based on statistically downscaled temperature from simulations by 24 Earth system models (adopted from Li et al., 2018).

^b Regions are defined by political boundaries; "North" includes the three territories (see Figure 1.1).

In addition to changes in magnitude, the frequency of certain temperature extremes is also expected to change. Extreme hot temperatures are expected to become more frequent, while extreme cold temperatures less frequent. For example, under a high emission scenario (RCP8.5), the annual highest daily temperature that would currently be attained once every 10 years, on average, will become a once in two-year event by 2050 – a five-fold increase in frequency. The annual highest daily temperature that occurs once every 50 years in the current climate is projected to become a once in five-year event by 2050 – a 10-fold increase in frequency (see Figure 4.12). These projected changes indicate not only more frequent hot temperature extremes, but also relatively larger increases in frequency for more rare events (e.g., 10-year extreme versus 50-year extreme; see also Kharin et al., 2018).



a) Annual maximum temperature RCP2.6



b) Annual maximum temperature RCP8.5

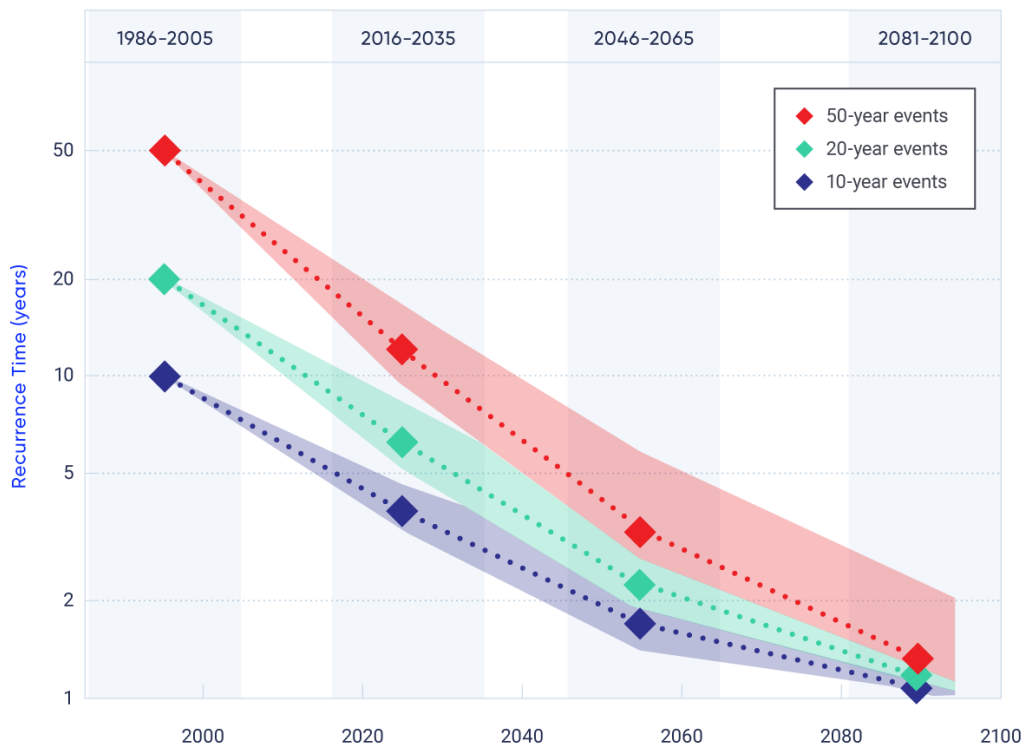


Figure 4.12: Projected changes in recurrence time for extreme temperatures

Figure caption: Projected changes in recurrence time (in years) for annual highest temperatures that occurred, on average, once in 10, 20, and 50 years in the late-20th century across Canada, as simulated by Earth system models contributing to fifth phase of the Coupled Model Intercomparison Project (CMIP5) under a low emission scenario RCP2.6 (upper) and a high emission scenario RCP8.5 (lower). The shading represents the range between the 25th and 75th percentiles

FIGURE SOURCE: VALUES ARE COMPUTED BASED ON KHARIN ET AL., 2013, ADAPTED FROM ECCCL, 2016.

The projected increase in the number of hot days is substantial. In regions that currently experience hot days, the increase may be more than 50 days by the late century under RCP8.5 (see Figure 4.13a). Areas with hot days will progressively expand northward, depending on the level of global warming. The number of frost days and ice days is projected to decrease, with projections ranging from about 10 fewer days in 2031–2050 under the low emission scenario (RCP2.6) to more than 40 fewer days in 2081–2100 under the high emission scenario (RCP8.5) (see Table 4.3) The length of the growing season (see Figure 4.13b) and the number of cooling degree days (see Figure 4.13c) are projected to increase, while heating degree days (see Figure 4.13d) are projected to decrease (see Table 4.3).

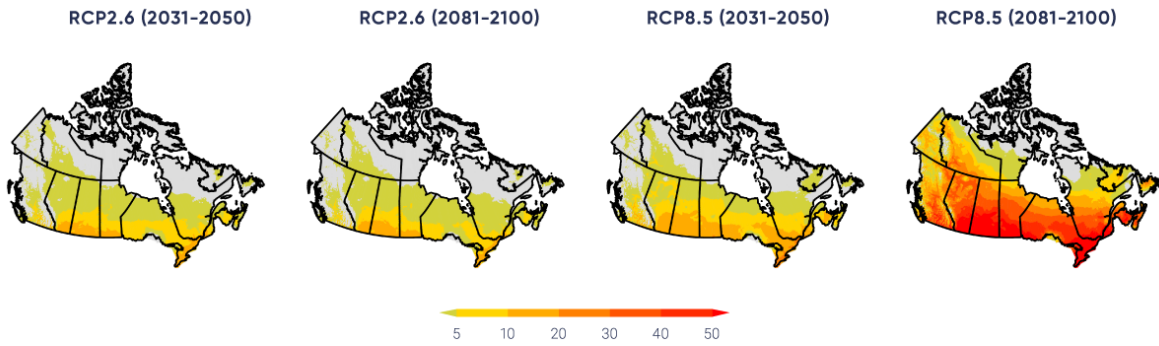
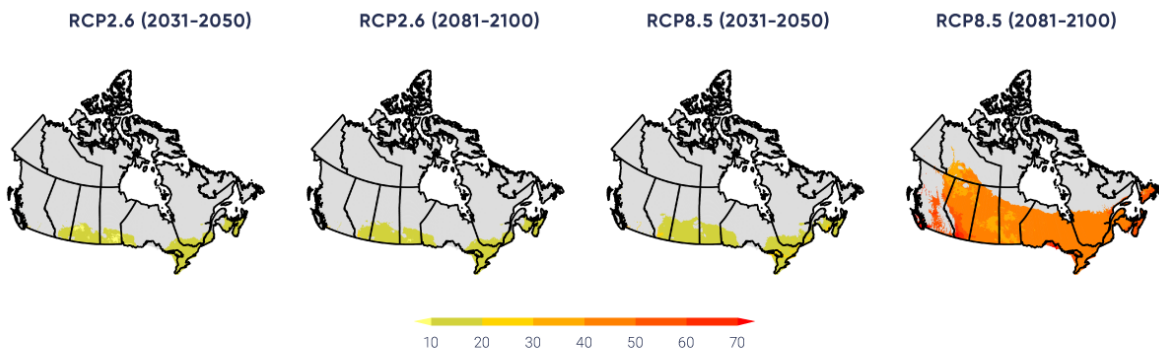
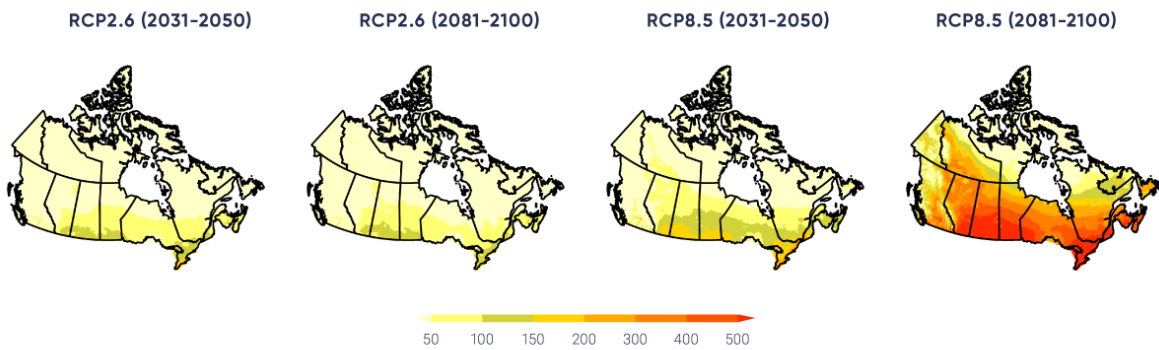
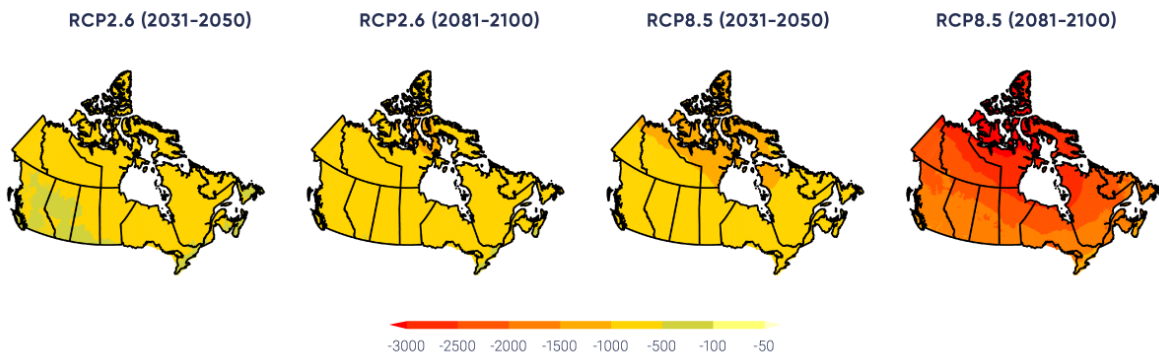
a) Annual number of hot days (days) when daily maximum temperature is above 30°C (TX30)**b) Length of growing season for warm season crops (days) (GSL)****c) Cooling-degree days (°C-days) (CDD)****d) Heating degree days (°C-days) (HDD)**

Figure 4.13: Future projections for selected temperature indices (degree days)

Figure caption: Multi-model median projected changes in (a) annual number of hot days (days) when daily maximum temperature is above 30°C (TX30), (b) length of growing season for warm-season crops (days) (GSL), (c) cooling degree days (°C-days) (CDD), (d) heating degree days (°C-days) (HDD). All maps are based on statistically downscaled temperature from simulations by 24 Earth system models. The two left-hand panels show projections for 2031–2050 and 2081–2100 under a low emission scenario (RCP2.6), while two right-hand panels display projections for 2031–2050 and 2081–2100 under a high emissions scenario (RCP8.5), respectively. Areas with less than one hot day per year on average are marked with grey in panel (a), while areas without sufficient cumulative heat during the growing season to support growing warm season crops such as corn or soybean are marked with grey in panel (b)

FIGURE SOURCE: ADAPTED FROM LI ET AL., 2018.

Changes in temperature indices and extremes are closely related to changes in mean temperature. The linear relationship between the change in growing season length and Canadian mean temperature (the right side of Figure 4.9; Li et al., 2018) is one example of how impacts (in this case related to agricultural productivity or forest growth) can be related to temperature change, regardless of the specific pathway of future GHG emissions. Such relationships not only assist impact assessments, but also assist plain-language communication regarding global mitigation efforts and their effect on regional climate impacts. A second example is freezing degree days, a measure of winter severity (e.g., Assel, 1980), which is the annual sum of degrees below freezing for each day, expressed in units of °C-d. A reduction of several hundred °C-d is projected across southern Canada in the late century, with changes of 1000°C-d or more projected for the North (see Figure 4.14). For context, the historical value of freezing degree days at Whitehorse is roughly 1800°C-d, at Edmonton, roughly 1400°C-d, and at Toronto, roughly 375°C-d (based on 1981–2010 data <http://climate.weather.gc.ca/climate_normals/index_e.html>).

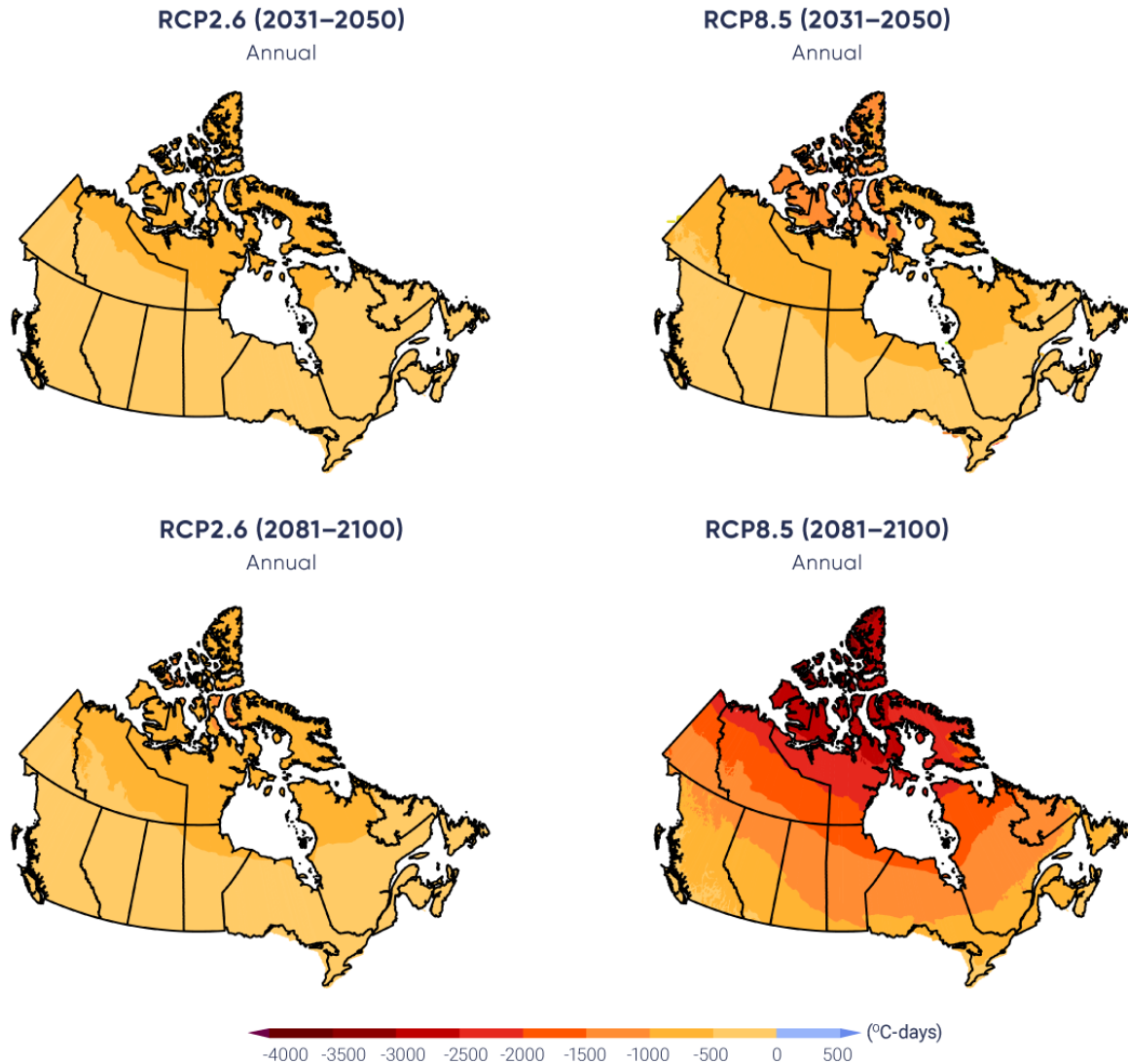


Figure 4.14: Future projections for freezing degree days

Figure caption: Projected change in freezing degree days ($^{\circ}\text{C-d}$) for the period 2031–2050 (upper panels) and 2081–2100 (lower panels) relative to 1986–2005 average, computed from statistically downscaled daily temperatures based on simulations by 24 models of Fifth phase of the Coupled Model Intercomparison Project (CMIP5) models (Li et al., 2018). The left-hand panels show results for a low emission scenario (RCP2.6) and the right-hand panels show results for a high emission scenario (RCP8.5).

FIGURE SOURCE: LI ET AL., 2018.

For temperature indices and extremes, projections by different models for the near term (2031–2050) under a high emission scenario (RCP8.5) agree on the direction (increasing or decreasing) of changes for almost all

regions. The model projections for the late century (2081–2100) also agree on the direction of changes for all temperature indices and extremes for every region under a high emission scenario (RCP8.5). This indicates the robustness of projected changes in temperature indices for the future.

It is *virtually certain* that, in most places in the world, there will be more hot and fewer cold temperature extremes as global mean temperatures increase (Collins et al. 2013). This will also be the case for Canada.

Section summary

In summary, it is *virtually certain* that the Canadian climate has warmed and that it will warm further in the future, as additional emissions of GHGs are unavoidable. To date, warming has been stronger in winter than in other seasons. Widespread changes in temperature indices and extremes associated with warming have been observed. Both human activities and natural variation of the climate have contributed to this warming, with human factors being dominant. The magnitude of future warming will be determined by the extent of future GHG mitigation. Temperature indices and extremes will continue to change as Canada continues to warm, affecting Canada's natural, social, and economic systems. Substantial changes are projected in temperature extremes. There will be more hot and fewer cold temperature extremes. The increase in Canadian mean temperature is about twice the rate of global mean temperature. This is the case in the historical record and also applies to future change, regardless of the emissions pathway that the Earth will follow. As changes in temperature indices and extremes are closely tied to changes in mean temperature, changes in Canadian climate and their resulting impacts are closely linked to changes in global mean temperature and, ultimately, future emissions of GHGs.

4.3: Precipitation

Key Message

There is *medium confidence* that annual mean precipitation has increased, on average, in Canada, with larger percentage increases in northern Canada. Such increases are consistent with model simulations of anthropogenic climate change.

Key Message

Annual and winter precipitation is projected to increase everywhere in Canada over the 21st century, with larger percentage changes in northern Canada. Summer precipitation is projected to decrease over southern Canada under a high emission scenario towards the end of the 21st century, but only small changes are projected under a low emission scenario.

Key Message

For Canada as a whole, observational evidence of changes in extreme precipitation amounts, accumulated over periods of a day or less, is lacking. However, in the future, daily extreme precipitation is projected to increase (*high confidence*).

Precipitation, as the ultimate source of water for our lands, lakes, and rivers, plays an important role in human society and in shaping and sustaining ecosystems. Human society and natural systems have evolved and adapted to variable precipitation in the past. However, shifts in precipitation beyond its historical range of variability could have profound impacts.

The amount of precipitation varies widely across Canada. The Pacific Coastal and Rocky Mountain ranges of western Canada block much of the moisture brought by westerly winds from the Pacific. As a result, some locations on the west coast receive an average of 3000 mm of precipitation or more in a year. In contrast, the annual mean precipitation can be as low as 300 mm in parts of the Prairies. Because warm air can hold more moisture, the amount of precipitation decreases from south to north, with annual precipitation of only about 200 mm in the far north (Environment Canada, 1995).

Precipitation records for some locations in Canada extend back for more than a century. While the Meteorological Service of Canada has many observational stations at any given time, including more than 2500 stations currently active, only a few hundred stations have continuous long-term records. As with temperature observations, there have been significant changes in observing instruments and/or procedures, including many manned stations having been replaced by automated observing systems. Integrating the data from the manned and automatic observations into one continuous series is challenging, as it requires the accumulation of sufficient data from the new systems to fully understand their characteristics (Milewska and Hogg, 2002). Precipitation measurements have additional challenges when compared with temperature measurements, as they are affected by weather conditions at the time of observation. This is because thermometers are placed in well-protected screens, while precipitation gauges are in the open air. In general, precipitation gauges catch only a portion of precipitation if it is windy, and they become less efficient as wind speed increases (Mekis and Vincent, 2011; Milewska et al., 2018). Additionally, a small amount of precipitation is lost due to evaporation and wetting of the inside of the gauge. Precipitation in the form of snowfall is particularly difficult to observe. A gauge can catch only a small fraction of total snowfall; drifting snow makes it even more complicated to measure snowfall amount. The introduction, over time, of new precipitation gauges has unintentionally introduced data inhomogeneity into the records. The effect of weather conditions and the use of different gauges on observational data need to be carefully adjusted for, to reflect the actual amount of precipitation at a particular site.

Monitoring precipitation over a region is challenging because a gauge measurement is a point observation and thus may not represent precipitation conditions over a large area. As precipitation is sporadic in time and space, point observations of precipitation amount in a day can represent only a very small area surrounding the observational site. However, station observations of precipitation amounts accumulated over longer time

periods (a month or a year) can represent larger areas. For example, total precipitation for a season may be interpolated for a location without observations with reasonable accuracy, if the location is within 20 to 120 km from the observational sites, depending on the season (Milewska and Hogg, 2001). Factors such as topography, season, and dominant weather systems all affect the spatial representativeness of point observations of precipitation.

In general, there is insufficient station density in Canada to compute national average precipitation with desirable accuracy; thus, there is *low confidence* in quantifying regional or national total amounts of precipitation. This is because the distance between observational stations with long-term records (see Figure 4.1) is generally greater than 120 km and because there is a large variation in precipitation over space. In northern Canada, the distance between stations is often more than 1000 km. Locally normalized precipitation (the amount of precipitation divided by its long-term mean) has been used in the past as one alternative. This measure is less variable over space than precipitation amount. As a result, its value at a point location can represent the average over a larger area. Stations with long-term records can provide regional averages for normalized precipitation across southern Canada with reasonable accuracy, although this is not the case for northern Canada (Milewska and Hogg, 2001). As a result, much of the assessment of national or regional changes in precipitation is based on locally normalized precipitation, expressed as a percentage. While this makes it possible to compute some form of national and regional averages, such averages should not be interpreted as normalized spatial averages of precipitation. This is because the local normalization factor is not constant in space.

4.3.1: Mean precipitation

4.3.1.1: Observed changes

Averaged over the country, normalized precipitation has increased by about 20% from 1948 to 2012 (Vincent et al., 2015; Figure 4.15 and Table 4.4). The percentage increase was larger in northern Canada – including Yukon, Northwest Territories, Nunavut, and northern Quebec – than in southern Canada. Nonetheless, significant increases were experienced in parts of southern Canada, including eastern Manitoba, western and southern Ontario, and Atlantic Canada. As mean precipitation is typically higher in southern Canada, the absolute amount of precipitation increase is higher in the south, even though the increase in normalized precipitation is smaller in the region. The regional average of normalized precipitation based on the few available long-term data from stations in northern Canada shows an increase of about 30% from 1948 to 2012 (Vincent et al., 2015); confidence in the regional average is *low*, however. As trends from individual locations in northern Canada are all increasing, there is a *medium confidence* that annual mean precipitation has increased in this region. Taken together, there is *medium confidence* that annual precipitation has increased for Canada as a whole. Additionally, the percentage increase in normalized precipitation is larger than what might be expected from the warming-induced increase in water-holding capacity of the atmosphere, leading to doubt over the magnitude of historical trends. There is *low confidence* in the estimate of the magnitude of the trend.

Precipitation has increased in every season in northern Canada. In southern Canada, precipitation has also increased in most seasons but the increase is generally not statistically significant. However, a statistically significant decrease in winter precipitation has been observed in British Columbia, Alberta, and Saskatchewan (Vincent et al., 2015; Figure 4.16 and Table 4.4).

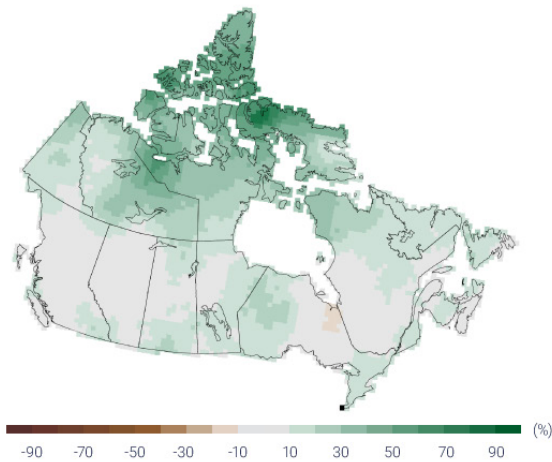
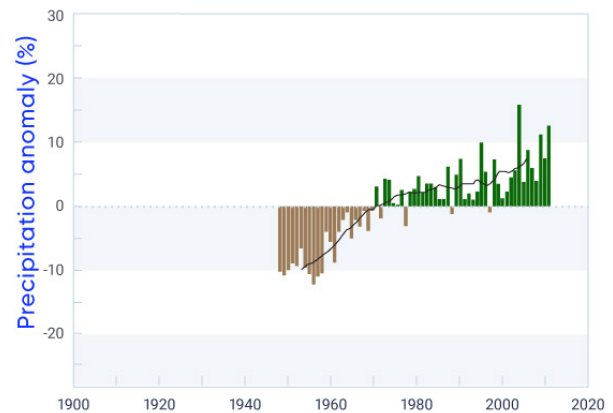
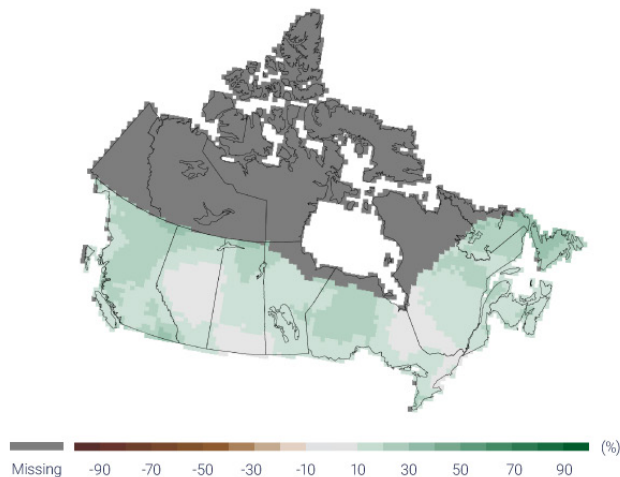
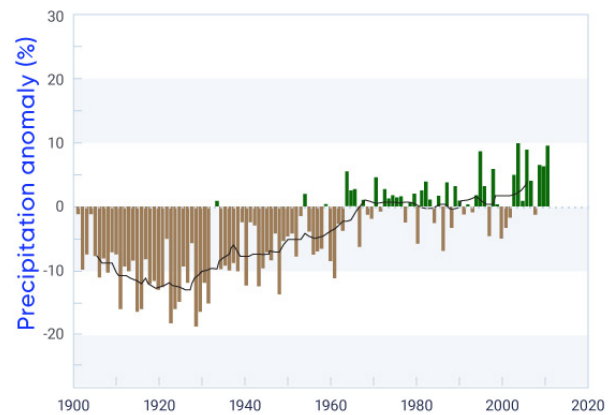
a) 1948–2012**b) 1948–2012****c) 1900–2012****d) 1900–2012**

Figure 4.15: Changes in annual precipitation, 1948–2012 and 1900–2012

Figure caption: Observed changes in locally normalized annual precipitation (%) between (a) 1948 and 2012 and (c) 1900 and 2012; changes are computed based on linear trends over the respective periods. Average of normalized precipitation relative to the 1961–1990 mean (b) across Canada and (d) in southern Canada (south of 60° north latitude); the black lines are 11-year running mean. Estimates are derived from the gridded station data. There is a lack of data in northern Canada (see Figure 4.1).

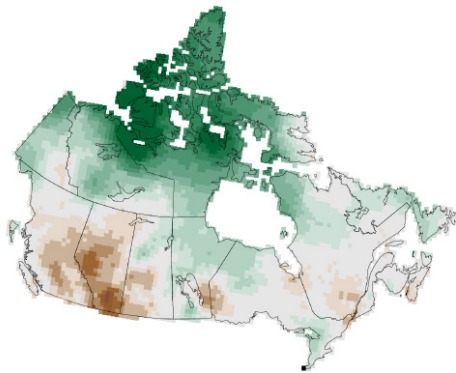
FIGURE SOURCE: UPDATED FROM FIGURE 4 OF VINCENT ET AL., 2015.

Table 4.4: Observed changes in normalized annual and seasonal precipitation between 1948 and 2012 for six regions and for all Canadian land area^a

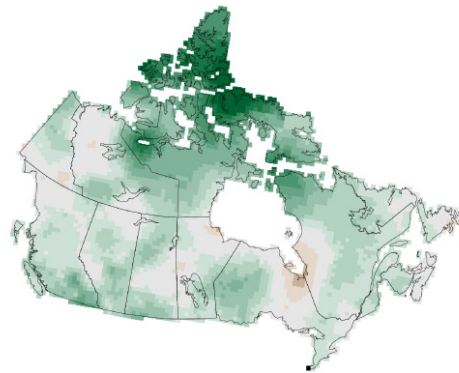
REGION	CHANGE IN PRECIPITATION, %				
	Annual	Winter	Spring	Summer	Autumn
British Columbia	5.0	-9.0	18.2	7.9	11.5
Prairies	7.0	-5.9	13.6	8.4	5.8
Ontario	9.7	5.2	12.5	8.6	17.8
Quebec	10.5	5.3	20.9	6.6	20.0
Atlantic	11.3	5.1	5.7	11.2	18.2
Northern Canada	32.5	54.0	42.2	18.1	32.1
Canada	18.3	20.1	25.3	12.7	19.0

^a Changes are represented by linear trends over the period. Estimates are derived from the gridded station data. There is a lack of data for northern Canada (see Figure 4.1 for the location of stations), which reduces confidence in the estimate.

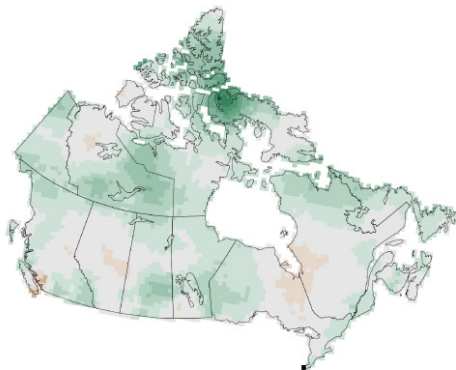
a) Winter



b) Spring



c) Summer



d) Autumn

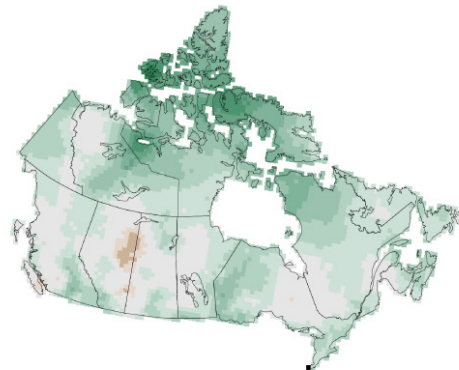


Figure 4.16: Changes in seasonal precipitation, 1948–2012

Figure caption: Observed changes in normalized seasonal precipitation (%) between 1948 and 2012 for the four seasons. Changes are computed based on linear trends over the respective periods. Estimates are derived from the gridded station data. There is a lack of data in northern Canada (see Figure 4.1).

FIGURE SOURCE: FIGURE 5 OF VINCENT ET AL., 2015.

For long-term observed trends, at the century scale, changes in precipitation can be assessed only for southern Canada, due to the lack of data for northern Canada. An increase was observed over all regions of southern Canada since 1900 and is statistically significant at that spatial scale at the 5% level. Warming has resulted in the proportion of the amount of precipitation falling as snow (i.e., the ratio of snowfall to total precipitation) steadily and significantly decreasing over southern Canada, especially during spring and autumn (Vincent et al., 2015). This is also the case for the Arctic region. There is a pronounced decline in summer snowfall over the Arctic Ocean and the Canadian Arctic Archipelago, and this decline is almost entirely caused by snowfall being replaced by rain (Screen and Simmonds, 2012). Such a change in the form of precipitation, from snow to rain, has profound impacts in other components of the physical environment, such as river flow, with the spring freshet becoming significantly earlier (Vincent et al., 2015; see Chapter 6, Section 6.2).

4.3.1.2: Causes of observed changes

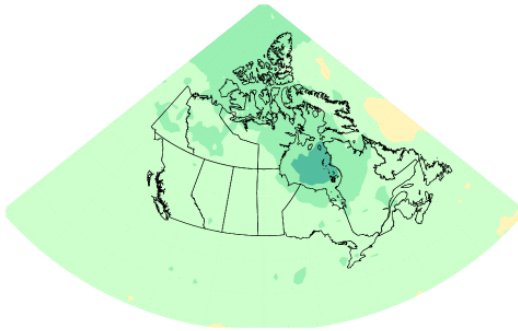
There is *medium confidence* that there is a human-caused contribution to observed global-scale changes in precipitation over land since 1950 (Bindoff et al., 2013). Much of the evidence of human influence on global-scale precipitation results from precipitation increases in the northern mid- to high latitudes (Min et al., 2008; Marvel and Bonfils, 2013; Wan et al., 2014). This pattern of increase is clear in climate model simulations with historical forcing (e.g., Min et al., 2008) and in future projections (Collins et al., 2013). Observed precipitation in northern high latitudes, including Canada, has increased and can be attributed – at least in part – to external forcing (Min et al., 2008; Wan et al., 2014). Atmospheric moisture increases with warming in both observations and model simulations. Natural internal climate variability from decade to decade contributes little to the observed changes (Vincent et al., 2015). This evidence, when combined, leads us to conclude that there is *medium confidence* that the observed increase in Canadian precipitation is at least partly due to human influence.

4.3.1.3: Projected changes and uncertainties

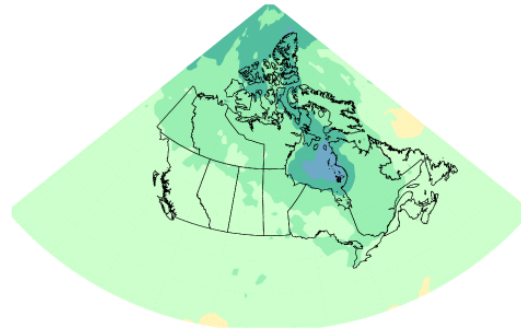
Multi-model projections of percentage changes (relative to 1986–2005) in winter, summer, and annual precipitation in Canada are shown in Figures 4.17, 4.18, and 4.19. The figures include maps of change for the low emission scenario (RCP2.6) and high emission scenario (RCP8.5) for the near term (2031–2050) and late century (2081–2100), and a national average time series of the normalized local changes for Canada as a whole for the period 1900–2100. Unlike for temperature, which is projected to increase everywhere in every season, precipitation has patterns of increase and decrease. In the near term, a small (generally less than 10%) increase in precipitation is projected in all seasons, with slightly larger values in northeastern Canada. In the late century (2081–2100), under the high emission scenario, the changes are much larger, with extensive areas of increased precipitation in northern Canada (more than 30% of the annual mean in the high Arctic). Since annual mean precipitation is low in the Arctic, even modest changes in absolute amount translate into a large percentage change. In contrast, large areas of southern Canada are projected to see a reduction in precipitation in summer under the high emission scenario (RCP8.5); for example, a median reduction of more than 30% is projected for southwestern British Columbia (see Figure 4.18). The projected decrease in summer precipitation (also projected in other parts of the world) is a consequence of overall surface drying and changes in atmospheric circulation (Collins et al., 2013).

As was the case for temperature, the national average time series for precipitation in the lower panels of the three figures show relatively small differences between the low emission scenario (RCP2.6) and high emission scenario (RCP8.5) in the near term (2031–2050). The winter season precipitation changes projected under the two scenarios diverge somewhat by the late century, while the summertime changes are near zero over the entire century, regardless of emission scenario. This small change in national average of locally normalized precipitation hides the fact that summertime precipitation changes are projected to be large (and hence impactful) in many areas of Canada. The large percent increases in northern Canada are generally offset by the large percent decreases in southern Canada, so that the average of percent changes for Canada as a whole in the time series plots shows little overall change in summer precipitation. As mean precipitation is much larger in southern Canada than in northern Canada, the absolute amount of precipitation decrease in the southern Canada is larger than the absolute value of precipitation increase in northern Canada. Regional differences are clearly important for impact studies, and quantitative information at the regional level is provided in Table 4.5. In general, changes in precipitation exhibit more temporal and regional variation than changes in temperature, and, so, projection results for precipitation have less confidence than projection results for temperature.

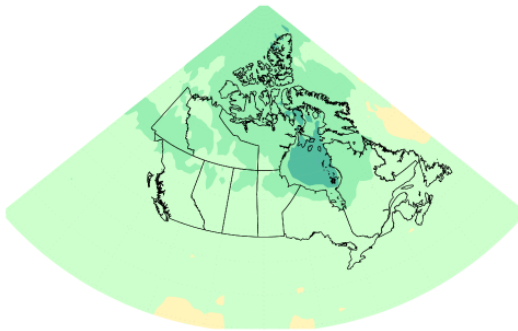
Precipitation change RCP2.6 (2031–2050)
December–February



Precipitation change RCP8.5 (2031–2050)
December–February



Precipitation change RCP2.6 (2081–2100)
December–February



Precipitation change RCP8.5 (2081–2100)
December–February

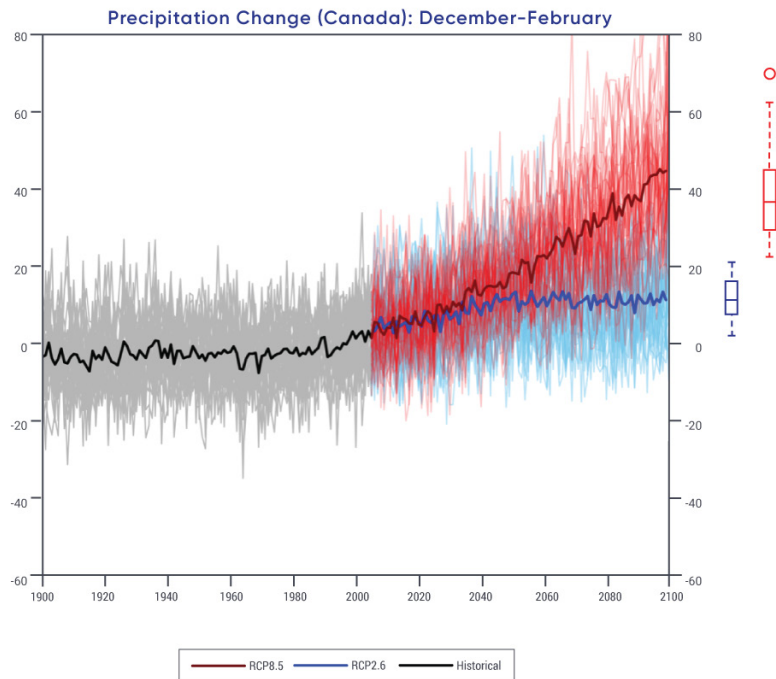
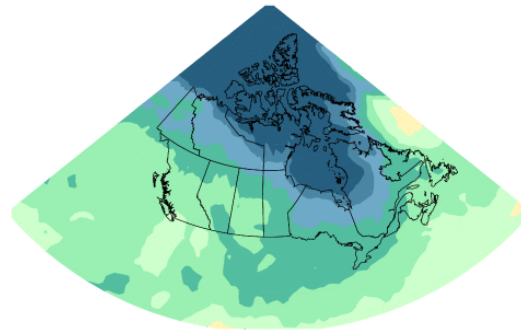


Figure 4.17: Projected precipitation changes for winter season



Figure caption: Maps and time series of projected precipitation change (%) for December, January, and February, as represented by the median of the fifth phase of the Coupled Model Intercomparison Project (CMIP5) multi-model ensemble. Changes are relative to the 1986–2005 period. The upper maps show precipitation change for the 2031–2050 period and the lower maps, for the 2081–2100 period. The left-hand maps show changes resulting from the low emission scenario (RCP2.6), whereas the right-hand maps show changes from the high emission scenario (RCP8.5). The time series at the bottom of the figure shows the change averaged over Canadian land area and spans the 1900–2100 period. The thin lines show results from the individual CMIP5 models, and the heavy line is the multi-model mean. The spread among models, evident in the thin lines, is quantified by the box-and-whisker plots to the right of each panel. They show, for the 2081–2100 period, the 5th, 25th, 50th (median), 75th, and 95th percentile values.

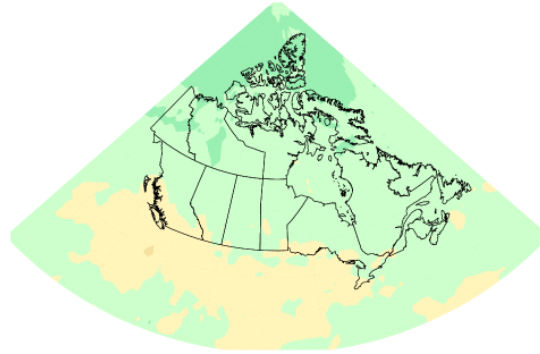
FIGURE SOURCE: CLIMATE RESEARCH DIVISION, ENVIRONMENT AND CLIMATE CHANGE CANADA.

Precipitation change RCP2.6 (2031–2050)

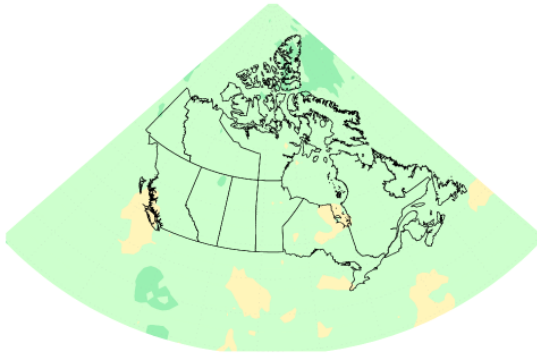
June–August

**Precipitation change RCP8.5 (2031–2050)**

June–August

**Precipitation change RCP2.6 (2081–2100)**

June–August

**Precipitation change RCP8.5 (2081–2100)**

June–August

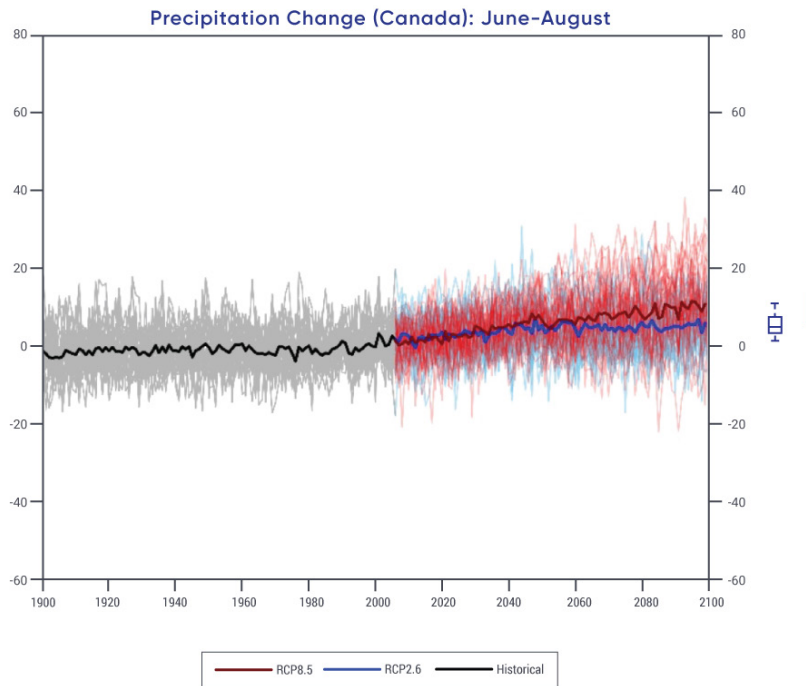
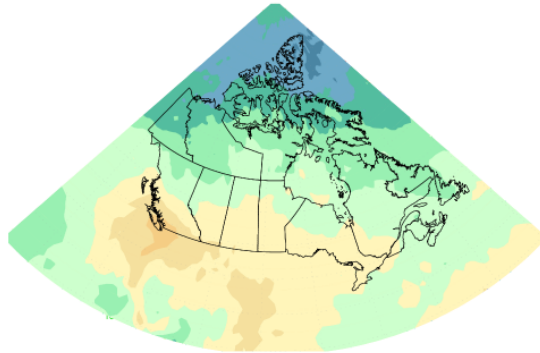


Figure 4.18: Projected precipitation changes for summer season

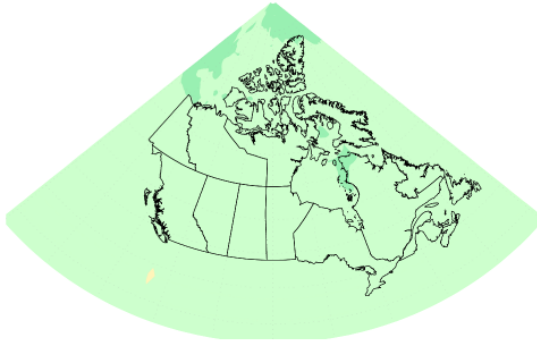


Figure caption: Maps and time series of projected precipitation change (%) for June, July, and August, as represented by the median of the fifth phase of the Coupled Model Intercomparison Project (CMIP5) multi-model ensemble. Changes are relative to the 1986–2005 period. The upper maps show precipitation change for the 2031–2050 period and the lower maps, for the 2081–2100 period. The left-hand maps show changes resulting from the low emission scenario (RCP2.6), whereas the right-hand maps show changes from the high emission scenario (RCP8.5). The time series at the bottom of the figure shows the change averaged over Canadian land area and over the 1900–2100 period. The thin lines show results from the individual CMIP5 models, and the heavy line is the multi-model mean. The spread among models, evident in the thin lines, is quantified by the box-and-whisker plots to the right of each panel. They show, for the 2081–2100 period, the 5th, 25th, 50th (median), 75th, and 95th percentile values.

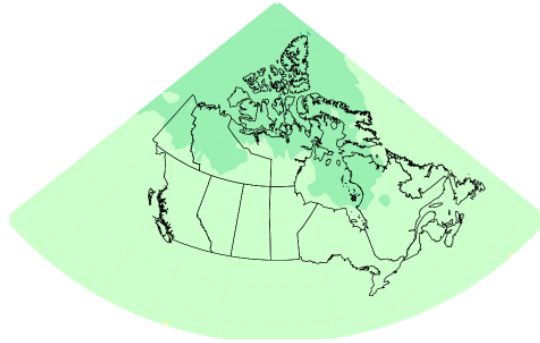
FIGURE SOURCE: CLIMATE RESEARCH DIVISION, ENVIRONMENT AND CLIMATE CHANGE CANADA.

Precipitation change RCP2.6 (2031–2050)

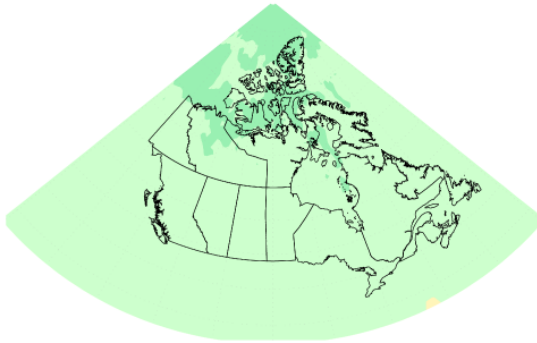
Annual

**Precipitation change RCP8.5 (2031–2050)**

Annual

**Precipitation change RCP2.6 (2081–2100)**

Annual

**Precipitation change RCP8.5 (2081–2100)**

Annual

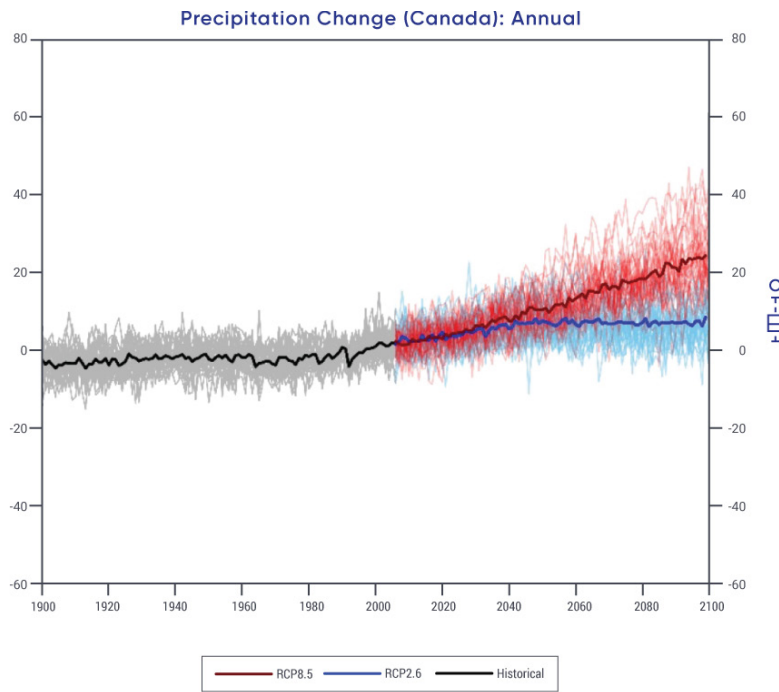
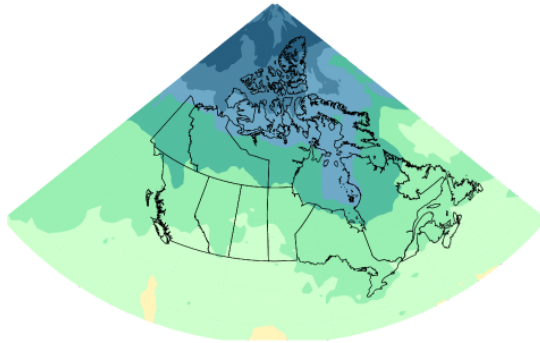


Figure 4.19: Projected annual precipitation changes



Figure caption: Maps and time series of projected annual mean precipitation change (%) as represented by the median of the fifth phase of the Coupled Model Intercomparison Project (CMIP5) multi-model ensemble. Changes are relative to the 1986–2005 period. The upper maps show precipitation change for the 2031–2050 period and the lower maps, for the 2081–2100 period. The left-hand maps show changes resulting from the low emission scenario (RCP2.6), whereas the right-hand maps show changes from the high emission scenario (RCP8.5). The time series at the bottom of the figure shows the change averaged over Canadian land area and over the 1900–2100 period. The thin lines show results from the individual CMIP5 models, and the heavy line is the multi-model mean. The spread among models, evident in the thin lines, is quantified by the box-and-whisker plots to the right of each panel. They show, for the 2081–2100 period, the 5th, 25th, 50th (median), 75th, and 95th percentile values.

FIGURE SOURCE: CLIMATE RESEARCH DIVISION, ENVIRONMENT AND CLIMATE CHANGE CANADA.

Table 4.5: Projected percentage change in annual mean precipitation for six regions and for all Canadian land area relative to 1986–2005^a

REGION ^b	SCENARIO; PERIOD; MEDIAN (25TH, 75TH PERCENTILE), %			
	RCP2.6		RCP8.5	
	2031–2050	2081–2100	2031–2050	2081–2100
British Columbia	4.3 (-0.4, 9.8)	5.8 (0.4, 11.9)	5.7 (0.0, 11.4)	13.8 (5.7, 22.4)
Prairies	5.0 (-0.7, 10.8)	5.9 (-0.2, 12.1)	6.5 (0.4, 13.1)	15.3 (6.3, 24.9)
Ontario	5.5 (0.4, 11.1)	5.3 (-0.1, 10.8)	6.6 (1.8, 12.4)	17.3 (8.5, 26.1)
Quebec	7.1 (2.0, 12.2)	7.2 (2.2, 13.0)	9.4 (4.5, 14.7)	22.5 (14.8, 32.0)
Atlantic	3.8 (-0.8, 9.1)	4.7 (0.3, 9.0)	5.0 (0.6, 9.9)	12.0 (5.7, 19.3)
North	8.2 (2.1, 14.6)	9.4 (2.8, 16.7)	11.3 (5.4, 18.1)	33.3 (22.1, 46.4)
Canada	5.5 (0.2, 11.2)	6.8 (0.4, 14.4)	7.3 (2.0, 13.2)	24.2 (13.7, 36.2)

^a The median or 50th percentile value is based on the CMIP5 multi-model ensemble. The 25th percentile value indicates that 25% of the CMIP5 model projections have a change smaller than this value. The 75th percentile value indicates 25% of CMIP5 model projections have a change larger than this value.

^b Regions are defined by political boundaries; "North" includes the three territories (see Figure 1.1).

As the climate warms, particularly in northern Canada, there will inevitably be an increased likelihood of precipitation falling as rain rather than snow. This is consistent with the observed changes in the snowfall fraction noted earlier. Although there has not been a systematic analysis for Canada, one analysis projected a decrease in the fraction of precipitation falling as snow, especially in the autumn and spring, for southern Alaska and eastern Quebec (Krasting et al., 2013). In addition, regional climate model projections show a general increase in rain-on-snow events over the coming century (Jeong and Sushama, 2017).

These results for changes in mean precipitation are consistent with the IPCC Fifth Assessment, in that the high latitudes are projected to experience a large increase in annual mean precipitation by the late of this century under the high emission (RCP8.5) scenario. The projected increase in annual mean precipitation in the high latitudes is a common feature of generations of climate models. It can be explained by the expected warming-induced large increase in atmospheric water vapour (Collins et al. 2013). Over the historical period, an increase in annual total precipitation in the high latitudes has been detected and can be attributed to human influence (Min et al., 2008; Wan et al., 2014). There is **high confidence** in the projected increase in annual mean precipitation. Confidence in projected changes in seasonal mean precipitation is lower. It should be noted that models generally project less summertime precipitation for southern Canada under a high emission scenario.

4.3.2: Extreme precipitation

Mean precipitation over a day or less can cause localized damage to infrastructure, such as roads and buildings, while heavy multi-day episodes of precipitation can produce flooding over a large region. This section assesses only changes in short-duration (a day or less) extreme precipitation, for which there is relatively more data and research than for longer-duration extremes.

4.3.2.1: Observed changes

There do not appear to be detectable trends in short-duration extreme precipitation in Canada for the country as a whole based on available station data. More stations have experienced an increase than a decrease in the highest amount of one-day rainfall each year, but the direction of trends is rather random over space. Some stations show significant trends, but the number of sites that had significant trends is not more than what one would expect from chance (Shephard et al., 2014; Mekis et al., 2015; Vincent et al., 2018). This seems to be inconsistent with global results (Westra et al., 2013) and the results for the contiguous region of the United States (Barbero et al., 2017). The number of days with heavy rainfall¹⁸ has increased by only 2 to 3 days since 1948 at a few locations in southern British Columbia, Ontario, Quebec, and the Atlantic provinces (Vincent et al., 2018). The number of days with one hour total rainfall greater than 10 mm, with 24-hour total rainfall greater than 25 mm, or with 48-hour total rainfall greater than 50 mm also did not show any consistent change across the country (Mekis et al., 2015). Days with heavy snowfall¹⁹ have decreased by a few days at numerous locations in western Canada (British Columbia to Manitoba), while they have increased at several locations in the North (Yukon, Northwest Territories, and western Nunavut). The highest one-day snowfall amount has decreased by several millimetres (snow water equivalent) at several locations in the southern region of British Columbia and Alberta (Mekis et al., 2015; Vincent et al., 2018).

The lack of a detectable change in extreme precipitation in Canada is not necessarily evidence of a lack of change. On one hand, this is inconsistent with the observed increase in mean precipitation. As the variance of precipitation is proportional to the mean, and as there is a significant increase in mean precipitation, one would expect to see an increase in extreme precipitation. On the other hand, the expected change in response to warming may be small when compared with natural internal variability. Warming has resulted in an increase in atmospheric moisture, which is expected to lead to an increase in extreme precipitation if other conditions, such as atmospheric circulation, do not change. On the global scale, observations indicate an increase in extreme precipitation associated with warming. Moreover, the increase can be attributed to human influence (Min et al., 2011; Zhang et al., 2013). The median increase in extreme precipitation is about 7% per 1°C increase in global mean temperature, consistent with the increase in the water-holding capacity of the atmosphere due to warming (Westra et al., 2013). Compared with the natural internal variability of precipitation,

18 Heavy rainfall is defined as rainfall greater than the annual 90th percentile from all rainfall events greater than 1 mm per day.

19 Heavy snowfall is defined as snowfall greater than the annual 90th percentile from all events greater than 1 mm per day.

this amount of increase would be too small to be detectable at individual locations. Only about 8.5% of all stations over global land areas with more than 30 years of data show an increase in extreme precipitation at the 5% significance level, which is slightly higher than the rate of stations showing an increase (5%) that could be expected from chance (Westra et al., 2013). The detection of the increasing intensity of extreme precipitation over lands on Earth is possible because of the vast amount of data available. On the regional scale, there is much less information, which is the case for Canada, where long-term observations are very limited, and detection becomes more difficult.

4.3.2.2: Projected changes and uncertainties

In the future, extreme precipitation is projected to increase in Canada. Averaged for Canada, extreme precipitation with a return period²⁰ of 20 years in the late century climate is projected to become a once in about 10-year event in 2031–2050 under a high emission scenario (RCP8.5) (see Figure 4.20). Beyond mid-century, these changes are projected to stabilize under the low emission scenario (RCP2.6), but to continue under the high emission scenarios (RCP8.5). An extreme event that currently occurs once in 20 years is projected to become about a once in five-year event by late century under the high emission scenario (RCP8.5). In other words, extreme precipitation of a given magnitude is projected to become more frequent. Moreover, the relative change in event frequency is larger for more extreme and rarer events. For example, an event that currently occurs once in 50 years is projected to occur once in 10 years by late 21st century under a high emission scenario (RCP8.5). The amount of precipitation with a certain recurrence interval is projected to increase. The amount of 24-hour extreme precipitation that occurs once in 20 years on average is projected to increase by about 5% under a low emission scenario (RCP2.6) and by 12% under a high emission scenario (RCP8.5) by 2031–2050, and to increase as much as 25% by 2081–2100 under a high emission scenario (RCP8.5). Differences in the projected percentage changes in annual maximum 24-hour precipitation among regions of Canada for the same emission scenario and time period are notably small. The median value for every region is in general within the range of 25th to 75th percentiles of other regions, except under the high emission scenario toward the late century (see Table 4.6).

20 A return period describes how common an event is. For example, a 20-year return period means the event has a 1 in 20 probability of occurring each year. Thus, a 20-year event would be expected to occur every 20 years, on average.

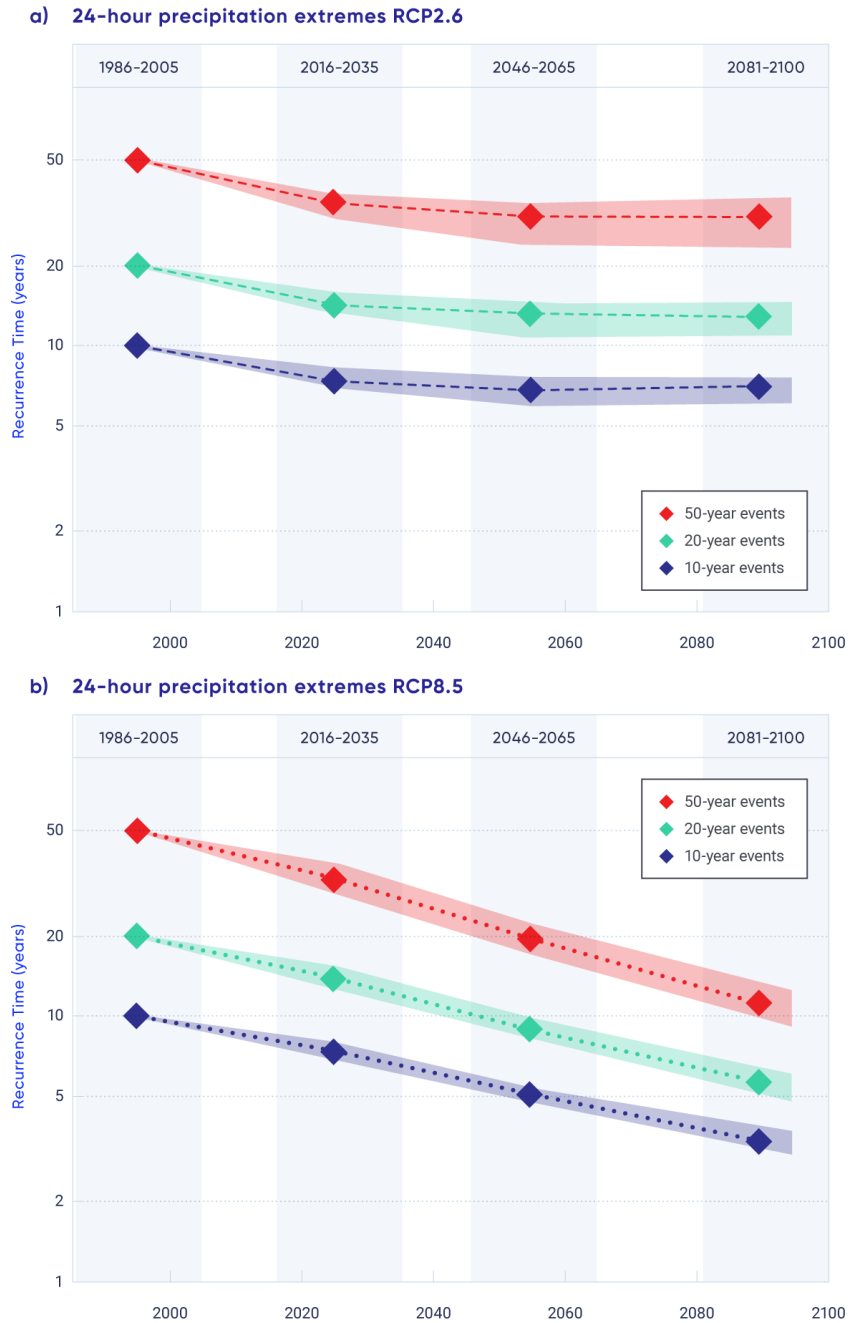


Figure 4.20: Projected changes in recurrence time for extreme precipitation

Figure caption: Projected changes in recurrence time for annual maximum 24-hour precipitation that occurs, on average, once in 10, 20, and 50 years in the late century across Canada, as simulated by Earth system models contributing to the fifth phase of the Coupled Model Intercomparison Project (CMIP5) under a low emission scenario (RCP2.6; upper) and a high emission scenario (RCP8.5; lower). The projections are at global climate model resolution, and the processes that produce 24-hour extreme precipitation at local scale are not well represented. Therefore, projections should be interpreted with caution. The shading represents the range between the 25th and 75th percentiles.

FIGURE SOURCE: VALUES ARE COMPUTED BASED ON KHARIN ET AL., 2013, ADAPTED FROM ECCC, 2016.

Table 4.6: Projected changes in annual maximum 24-hour precipitation that occur, on average, once in 10, 20, and 50 years, as simulated by Earth system models contributing to the fifth phase of the Coupled Model Intercomparison Project (CMIP5)^a

REGION ^b	SCENARIO; PERIOD; MEDIAN (25TH, 75TH PERCENTILE), %			
	RCP2.6		RCP8.5	
	2031–2050	2081–2100	2031–2050	2081–2100
	10-year return value			
British Columbia	5.9 (3.8, 9.3)	8.0 (4.5, 13.3)	9.8 (7.4, 12.7)	26.1 (20.4, 31.3)
Prairies	5.5 (2.3, 9.2)	5.1 (2.2, 8.9)	7.8 (4.5, 10.1)	17.5 (12.6, 23.8)
Ontario	6.0 (1.4, 8.4)	5.3 (2.1, 10.9)	8.5 (3.6, 11.4)	20.5 (15.4, 26.7)
Quebec	6.8 (2.7, 10.6)	7.2 (4.6, 10.2)	10.0 (6.2, 15.6)	26.0 (17.8, 30.2)
Atlantic	6.8 (3.4, 10.2)	8.5 (6.1, 11.1)	13.5 (7.8, 18.2)	30.2 (22.9, 38.3)
North	7.1 (4.1, 8.7)	7.8 (4.7, 10.8)	10.8 (8.2, 13.5)	29.8 (23.2, 36.2)
Canada	6.1 (4.0, 8.5)	6.7 (4.1, 9.5)	8.4 (6.9, 11.4)	22.9 (18.8, 26.9)
	20-year return value			
British Columbia	6.3 (3.6, 9.9)	6.7 (4.1, 14.1)	9.8 (7.4, 13.6)	25.8 (21.8, 30.8)
Prairies	5.6 (2.6, 10.2)	6.0 (2.6, 10.3)	8.8 (4.7, 10.8)	19.1 (14.1, 25.3)
Ontario	5.7 (0.8, 7.8)	5.1 (2.3, 10.7)	8.2 (2.4, 12.2)	20.1 (16.1, 25.6)
Quebec	6.0 (2.2, 10.8)	8.6 (3.8, 9.9)	10.2 (5.1, 15.8)	25.8 (18.3, 32.0)
Atlantic	7.9 (3.6, 11.9)	9.5 (6.7, 11.8)	13.7 (7.9, 19.2)	30.9 (24.1, 39.1)
North	6.8 (3.6, 9.4)	7.4 (3.1, 11.4)	10.7 (7.9, 13.3)	30.0 (22.9, 35.1)
Canada	6.1 (3.7, 8.7)	6.9 (4.5, 10.0)	8.8 (6.6, 11.6)	24.2 (19.2, 27.8)
	50-year return value			
British Columbia	7.0 (3.0, 10.5)	9.2 (5.1, 16.0)	10.1 (7.5, 15.5)	28.7 (21.9, 33.5)
Prairies	6.1 (2.3, 10.5)	6.5 (2.0, 11.3)	10.0 (6.2, 12.1)	21.3 (14.8, 26.8)
Ontario	4.9 (0.9, 8.4)	7.6 (0.8, 11.0)	8.5 (2.8, 13.0)	20.1 (13.3, 28.0)
Quebec	6.3 (0.9, 9.9)	7.7 (3.3, 11.9)	10.8 (4.7, 17.1)	26.5 (17.9, 33.8)
Atlantic	7.7 (3.5, 12.8)	9.2 (6.6, 14.3)	14.3 (7.9, 21.2)	32.4 (24.9, 42.6)
North	4.9 (2.4, 9.0)	6.4 (1.7, 10.2)	10.8 (7.8, 13.0)	30.1 (24.9, 33.8)
Canada	6.2 (3.8, 9.2)	7.4 (5.0, 10.4)	9.2 (7.0, 11.9)	24.7 (19.6, 29.7)

^a The median or 50th percentile value is based on the CMIP5 multi-model ensemble. The 25th percentile value indicates that 25% of the CMIP5 model projections have a change smaller than this value. The 75th percentile value indicates 25% of CMIP5 model projections have a change larger than this value.

^b Regions are defined by political boundaries; "North" includes the three territories (see Figure 1.1).

While results from global climate model projections (such as those above) are useful for impact assessment and adaptation planning, there is an important caveat, especially for extreme precipitation. It is difficult to interpret these projections at local scales. The spatial resolution of global climate models is coarse (typically 100–250 km). The precipitation extremes in a model therefore represent averages over an area of several thousand square kilometres, and so convey different information than may be required for practical applications. More importantly, climate models may not include all of the physical processes that produce local intense rainstorms. This affects the confidence we can have in statistical downscaling products that transform precipitation from coarse resolution models to smaller areas. While regional climate models may operate at much smaller scales, conventional regional climate models, which are used to conduct most of the dynamical downscaling, do not accurately simulate important processes such as convection. These limitations must be kept in mind when using projections for the purpose of regional and local adaptation; in particular, the projected values given by these global or regional climate models should not be interpreted literally as the measured amount of precipitation at a point location.

Estimating changes in short-duration extreme precipitation at a point location is complex because of the lack of observations in many places and the discontinuous nature of precipitation at small scales. Projection of such extreme precipitation is also difficult because of the shortage of simulations by models with a very high resolution that resolve the physical processes that produce those extreme events (Zhang et al., 2017). Nevertheless, multiple lines of evidence support *high confidence* in projecting an increase in extreme precipitation globally. These lines of evidence include attribution of an observed increase in high-latitude total precipitation to human influence, consistency in projected future increases in extreme precipitation by multiple models, and the physical understanding that warming would result in an increase in atmospheric moisture. It is *likely* that extreme precipitation will increase in Canada in the future, although the magnitude of the increase is much more uncertain.

Box 4.2: The impact of combined changes in temperature and precipitation on observed and projected changes in fire weather

Changes in temperature and in precipitation each have impacts across many sectors. However, combined changes in temperature and precipitation can have additional impacts, and some sectors rely on information regarding concurrent changes in these two variables. An example is fire weather. Changing precipitation and temperature (along with changing wind) alter the risk of extreme wildfires that can result from hot, dry, and windy conditions. Understanding changes in both temperature and precipitation lends insight into changes in wildfire risk and how it might evolve in the future.

The Canadian Forest Fire Weather Index (FWI) System is a collection of indices that use weather variables, including temperature and precipitation, to characterize fire risk. It includes an index, labelled FWI, that synthesizes information from the collection of indices to quantify day-to-day changes in the risk of a spreading fire. A threshold of this index is often used to define days conducive to fire spread (Wang et al., 2015; Jain et

al., 2017). In addition, three of the most commonly used indices are moisture codes, describing the dryness of different categories of fuels (Wotton, 2009). All of the FWI indices represent factors affecting fire potential, with larger values indicating greater fire potential, although the occurrence of a large wildfire also depends on ignition sources, fuel characteristics, and fire management actions.

A few studies have looked at trends in these indices across Canada. Large year-to-year variability in the FWI indices hinders detection of trends (Amiro et al., 2004; Girardin et al. 2004). Trends may sometimes be discerned from a very long record of data, as is the case with increases in the Drought Code²¹ in northern Canada and decreases in the Drought Code in western Canada and parts of eastern Canada during the 20th century (Girardin and Wotton, 2009). Another study found that the mean number of fire spread days across Canada increased over 1979 to 2002, although the trends varied regionally, and only some were significant (Jain et al., 2017). Despite inconsistent trends in the FWI indices, there has been a significant increase in annual area burned across Canada (Podur et al., 2002; Gillett et al., 2004).

Higher temperatures in the future will contribute to increased values of the FWI indices and, therefore, increased fire risk. The increase in precipitation that would be required to offset warming for most of the FWI indices exceeds both projected and reasonable precipitation changes (Flannigan et al. 2016). Increases in extreme values of the Duff Moisture Code²² are projected across most of the forested ecozones of Canada by 2090 (Wotton et al., 2010). Increases in fire spread days and extreme values of the FWI are projected, with the largest changes in the western Prairies (Wang et al., 2015). Several other studies also project increases in the FWI indices and the length of the fire season in Canada in the future (Flannigan et al., 2009; de Groot et al., 2013; Flannigan et al., 2013; Kochtubajda et al., 2006). Although the magnitude of projected changes varied among these studies, most project increases in the FWI indices that correspond to higher fire risk.

Section summary

In summary, there is *medium confidence* that annual mean precipitation has increased, on average, in Canada, with larger percentage increases in northern Canada. There is *low confidence* in the magnitude of the increase because of poor spatial coverage of long-term, observational records. Such increases are consistent with model simulated precipitation response to anthropogenic climate change. Annual and winter precipitation is projected to increase everywhere in Canada over the 21st century, with larger percentage changes in northern Canada. Summer precipitation is projected to decrease over southern Canada under a high emission scenario toward the end of the 21st century, but only small changes are projected under a low emission scenario. For Canada as a whole, there is a lack of observational evidence of changes in daily and short-duration

21 The Drought Code describes dryness in the deepest forest floor layers and in large debris; precipitation influences the amount of moisture in this layer and temperature controls the rate at which the layer dries (Wotton et al., 2009).

22 The Duff Moisture Code describes dryness in the upper layer of forest floor debris; precipitation provides moisture and both temperature and relative humidity control the rate at which the layer dries (Wotton et al., 2009).

extreme precipitation. This is not unexpected, as extreme precipitation response to anthropogenic climate change during the historical period would have been small relative to its natural variability and as such, difficult to detect. However, in the future, daily extreme precipitation is projected to increase (*high confidence*).

4.4: Attribution of extreme events

Key Message

Anthropogenic climate change has increased the likelihood of some types of extreme events, such as the 2016 Fort McMurray wildfire (*medium confidence*) and the extreme precipitation that produced the 2013 southern Alberta flood (*low confidence*).

There has been an increase in costly extreme weather and climate events worldwide (WMO, 2014) and across Canada (Kovacs and Thistlethwaite, 2014; OAGC, 2016; OPBO, 2016). Much of this rise is due to greater exposure to the effects of such extreme events, as Canada's population and the value of its supporting infrastructure have both increased considerably. Changes in the intensity and frequency of damaging extreme weather and climate events due to climate change (IPCC, 2013) may also be playing a role. These extreme weather/climate events attract attention because they are rare and often have notable impacts on our society and economy.

It is generally not feasible to answer the question, Did human-induced climate change cause a particular weather or climate event? Often, that event could have occurred in the absence of human effects. Instead, recent research has focused on whether human activity has influenced the probability of particular weather or climate events or, in some cases, the strength or intensity of the events. As the climate changes, largely due to anthropogenic influences, the likelihood of a particular class of events – all events as extreme as or more extreme than the one defined in the study – also changes (NASEM, 2016). In this sense, an extreme event may be attributable to causes external to the natural climate system. Thus, a new branch of climate science, called event attribution, has emerged that evaluates how the probability or intensity of an extreme event, or more generally, a class of extreme events, has changed as a result of increases in atmospheric GHGs from human activity.

A growing number of extreme events in Canada and worldwide are being examined in this way (e.g., Herring et al., 2017; NASEM 2016). Several of these event attribution analyses are relevant to Canadians (see Table 4.7). Two examples are highlighted in this section, including a description of methods of analysis in Box 4.3.

Table 4.7: Event attribution analyses relevant to Canada

EVENT	REFERENCE	BRIEF OVERVIEW OF CONCLUSIONS
Drought		
2015 drought in western Canada	Szeto et al., 2016 ^a	Anthropogenic climate change increased likelihood of extremely warm spring but no contribution to the observed weather pattern was detected.
Flooding		
2014 flooding in south-east Prairies	Szeto et al., 2015 ^a	Anthropogenic influence may have increased rainfall, but landscape modification played a key role in increased runoff.
2013 Alberta floods	Teufel et al., 2017 ^b	Increased likelihood of extreme rainfall in this region due to the anthropogenic component; no anthropogenic influence detected for runoff.
Cold extremes		
Cold February 2015 in North America	Bellprat et al., 2016	Determined event was mainly due to natural variability, although there might have been some contribution from decreased Arctic sea ice and increased sea surface temperatures.
Extreme cold winter of 2013/2014 in North America	Yu and Zhang, 2015	Suggest warming trend made event less extreme than it might have been.
Extreme cold winter of 2013/2014	Wolter et al., 2015 ^a	Extreme cold events have become much less likely due to the long-term, anthropogenic warming trend.
Warm extremes		
November/December 2016 extreme warm Arctic temperatures	Kam et al., 2017 ^a	Extremely warm Arctic temperatures most likely would not have occurred without the anthropogenic contribution.
2014 extreme warm temperatures in eastern Pacific and western Atlantic	Kam et al., 2015 ^a	Extreme warm temperatures over the eastern Pacific and western Atlantic considerably more likely with the anthropogenic component.

Table 4.7: Event attribution analyses relevant to Canada

Arctic sea ice ^a		
2012 record minimum sea ice extent	Kirchmeier-Young et al., 2017 ^b	Record minimum in summer Arctic sea ice extent would not have occurred without the anthropogenic contribution.
March 2015 record low sea ice extent	Fučkar et al., 2016 ^a	The observed sea ice extent would not have occurred without the underlying climate change influence.
2012 record minimum sea ice extent	Zhang and Knutson, 2013	Record minimum in summer Arctic sea ice extent <i>extremely unlikely</i> to be due to internal variability.
Wildfires		
2016 Fort McMurray wildfire	Kirchmeier-Young et al., 2017 ^{a,b}	Anthropogenic contribution increased likelihood of extreme wildfire risk and the length of fire seasons.
2016 Fort McMurray wildfire	Tett et al., 2017 ^a	Anthropogenic contribution increased likelihood of extreme vapour pressure deficits, which increase fire risk.
2015 Alaska wildfire season	Partain et al., 2016 ^a	Anthropogenic contribution increased likelihood of extreme wildfire risk.

a Included in the annual Bulletin of the American Meteorological Society special reports on event attribution.

b Discussed in more detail in this section.

c Discussed in more detail in Chapter 5.

Box 4.3: Methods for event attribution

Event attribution is used to quantify how human-influenced climate change affects the occurrence of a particular type (or class) of extreme event. Its goals are similar to those of the detection and attribution process described in Chapter 2 (see Section 2.3.4), but it focuses on individual events. Event attribution analyses (NASEM, 2016) compare the likelihood of a particular class of events (e.g., all events as extreme, or more extreme, than the event defined in the study) between a factual world, which includes the human component, and a counter-factual world that comprises only natural factors – that is, the “climate that might have been” in the absence of the human component.

To demonstrate, Figure 4.21 shows distributions of possible values of a climate variable for the world without the human contribution in blue, and for a scenario like the one we have experienced with the human contri-

bution in red. The shaded regions represent the probability that a particular extreme event (an outcome as extreme, or more so, than the one indicated by the vertical bar) will occur in each scenario. The probability of the event increases when the human contribution is included — from 1 in 60 to 1 in 5. The ratio of the probability with the human contribution to the probability without the human contribution is referred to as a “risk ratio.” Although this event could occur in the absence of human influence, it is 12 times as likely (risk ratio of 12) when the human component is included.

The conclusions of an event attribution analysis often depend on how the question is posed. This includes the choices made when defining events and designing the analysis approach. For example, the change in probability between the two scenarios in Figure 4.21 depends on the placement of the vertical bar, or the lower bound on the magnitude that defines the chosen event. Changes in the probabilities of temperature and precipitation extremes depend on the probability of the events in the current climate, with larger risk ratios corresponding to more extreme (rarer) events (Kharin et al., 2018). The uncertainty in the risk ratio (i.e., the event attribution result) becomes larger for rarer events, as it is more difficult to estimate the probabilities of these very rare events. The choice of the variable and/or region to determine the distributions also has an impact on the results.

Two types of questions have been asked in event attribution analyses: How has the probability of the extreme event (frequency) changed, and how has the intensity of the event (magnitude) changed? As an example, event attribution for a flood-producing heavy rainfall event may try to answer, “Has human-induced climate change made this type of heavy rainfall event occur more often?” (frequency) or “Has human-induced climate change increased the amount of rainfall in these types of storms?” (magnitude). The human influence could have a different impact on the frequency than on the magnitude of a particular event. It is thus important to understand the characteristics of the event being assessed and to interpret the results of an event attribution analysis in context.

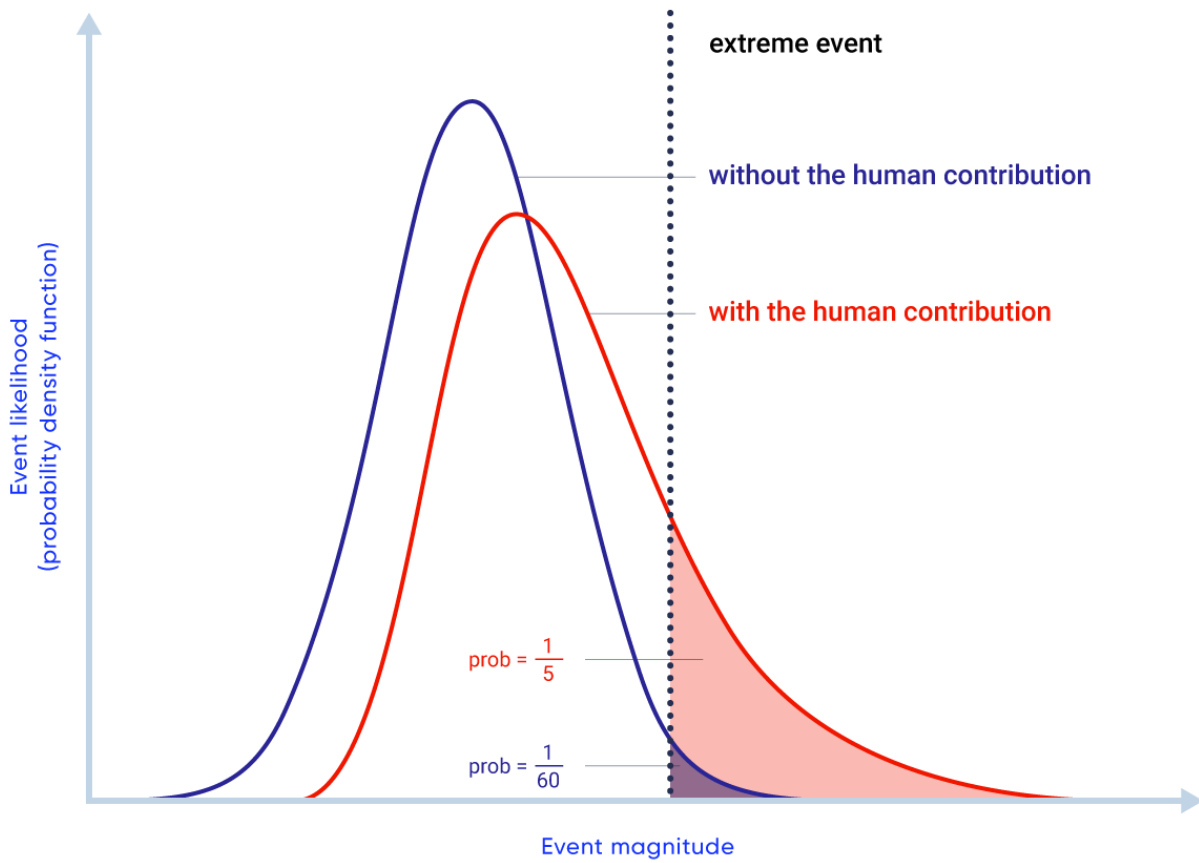


Figure 4.21: Hypothetical illustration of event attribution

Figure caption: The blue distribution represents the possible values of a climate variable in a world without a human influence. The red distribution represents the possible values of the same variable in a world with the human contribution. The shaded areas indicate the probability of experiencing an extreme event (defined by the dashed vertical bar) in each scenario.

FIGURE SOURCE: PRODUCED FOR THIS REPORT BY THE PACIFIC CLIMATE IMPACTS CONSORTIUM (PCIC).

4.4.1: Attribution of two recent events

4.4.1.1: 2013 Southern Alberta flood

In June 2013, an extreme flood event in southern Alberta became Canada's costliest natural disaster to that date, with significant damage to property and infrastructure throughout the region, including in the City of Calgary. The flood displaced almost 100,000 people and resulted in \$6 billion in damage, including \$2 billion in insured losses (ECCC, 2017).

A storm producing heavy rainfall over the region triggered the flooding event in the Bow River basin, but a combination of both meteorological and hydrological factors led to the extreme flooding. A recent study (Teufel et al., 2017) assessed the contributions of several of these factors, including anthropogenic GHG emissions.

The study used the Canadian Regional Climate Model (CRCM5) to run large ensembles of high-resolution simulations for North America. To assess the contribution of human climate change, simulations of the model were run using present-day levels of GHGs and also using pre-industrial levels to represent the time before humans had a discernable impact on the climate.

To estimate the probability of the event, return periods were calculated for three-day rainfall totals during May and June exceeding the observed amount. The return period for the observed event in the present-day climate in the Bow River was estimated to be about 60 years. Using climate projections, the return period is estimated to be reduced to about 20 years by the late 21st century (under both an intermediate emission scenario [RCP4.5] and a high emission scenario [RCP8.5]), implying that the type of extreme rainfall that led to the southern Alberta flooding event will become much more common in the future.

Estimated return periods were compared between the present-day and pre-industrial climates, in order to determine the human contribution (see Figure 4.22). Including human GHG emissions resulted in shorter return periods (the event is more likely) for three-day maximum precipitation over the entire southern Alberta region than for pre-industrial levels (see Figure 4.22a). Weather and climate variability tends to be larger for smaller regions, resulting in a smaller ratio between the anthropogenic influence and natural internal variability. Therefore, the anthropogenic influence on the rainfall events over the smaller Bow River basin region was less pronounced (see Figure 4.22b). There is no discernable difference for maximum three-day surface runoff, and thus no anthropogenic influence is detected for this variable (see Figure 4.22c). The authors acknowledge the uncertainties in modelling complex surface hydrological processes and suggest that any increase in rainfall could be offset by decreases in snowpack or frozen ground conditions.

In summary, human influence was detected for the flood-producing rainfall, particularly over the larger region, but human influence could not be detected for the flood itself. A flood event is the result of many factors in addition to the amount of rainfall, including the ground conditions, characteristics of the snowpack, and size and orientation of the storm. As a result, two events with the same rainfall amounts do not necessarily produce floods of the same magnitude. The complex hydrological processes that occur after the rainfall reaches the ground add additional uncertainty which decreases the ability to detect human influence.

Increased GHG emissions, largely due to human activities, result in increased temperatures. Increased temperatures allow more moisture to be available in the atmosphere for precipitation, leading to increased intensity of extreme rainfall events. The 2013 southern Alberta flood was the result of a combination of many factors, and this study demonstrated that human-induced emission of GHGs had increased the likelihood of an extreme amount of precipitation in southern Alberta, at least as large as the amount observed during this event.

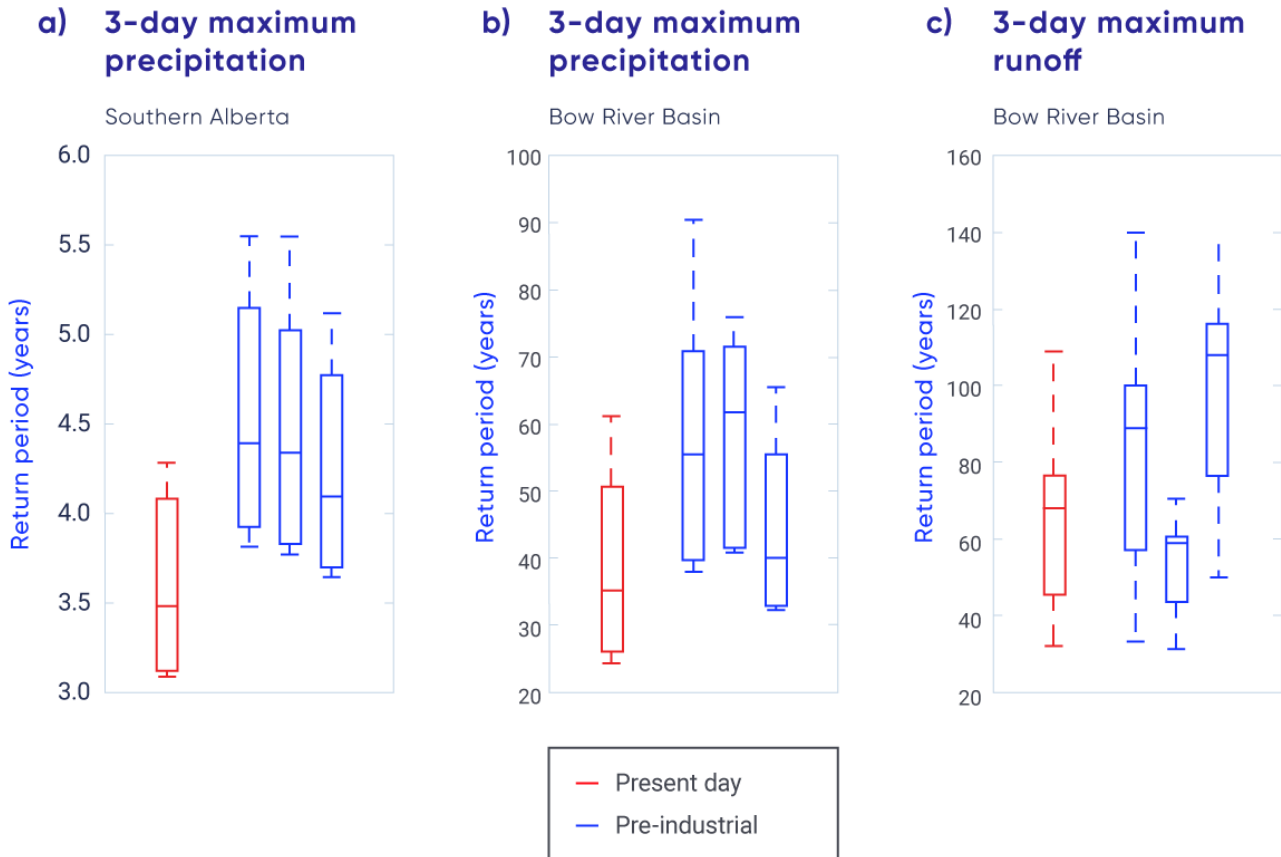


Figure 4.22: Precipitation and runoff that led to the 2013 southern Alberta flood

Figure caption: Return periods for the observed three-day maximum precipitation (a, b) and three-day maximum runoff (c) that led to the 2013 southern Alberta extreme flooding event. Present-day return periods are shown in red, and return periods from three pre-industrial simulations are shown in blue. Analysis is for the larger southern Alberta region (a) and the smaller Bow River basin (b, c). The box plots show the spread in the return periods across different estimates of the observed values from the reference simulations. The box boundaries indicate the range from the 25th to 75th percentiles, the middle line indicates the 50th percentile, and the whiskers extend to 1.5 times the width of the box or the most extreme value.

FIGURE SOURCE: ADAPTED FROM TEUFEL ET AL., 2017.

4.4.1.2: 2016 Fort McMurray wildfire

In early May 2016, a large wildfire burned almost 600,000 ha (a land area covering 6000 square kilometres) in northern Alberta. This fire resulted in the evacuation of all of the residents of Fort McMurray (over 80,000 people) and halted production in the oil sands (Government of Alberta, 2016). Insured losses are estimated at \$3.5 billion (IBC, 2016). The total cost of the event is still being determined, but it is expected to be considerably higher.

The fire ignited near the Horse River amid very dry fuel conditions. High winds a few days later resulted in rapid spread and fire growth. A study has used event attribution to assess the influence of human-induced climate change on several measures of wildfire risk (see Box 4.2), albeit not extreme fire itself, in this region (Kirchmeier-Young et al., 2017a).

Like the previous example, the study used large ensembles of model simulations, in this case employing the Canadian Earth System Model (CanESM2). To assess human influence, the model was run with only natural forcings (solar and volcanic effects) and also with a combination of natural and anthropogenic forcings. The anthropogenic component includes GHG emissions, aerosols, atmospheric ozone changes, and land-use change.

Fire weather (see Box 4.2), fire behaviour, and fire season measures were calculated to characterize fire risk from climate model output. To quantify the anthropogenic contribution, a risk ratio (NASEM, 2016) was calculated as the ratio of two probabilities: one for the event's occurrence when the human component is included, and one for the occurrence of the same event with only natural factors. The risk ratio can be interpreted as how many times as likely the event is as a result of anthropogenic factors. For example, a risk ratio of 1 implies no change in the probability of occurrence, and a risk ratio of 2 implies the event is twice as likely, or that there has been a 100% increase in the probability of the event compared with the unperturbed climate.

Results of the analysis show that three of the fire risk indices – extreme values of the Fire Weather Index (FWI; see Box 4.2), high number of spread days, and long fire seasons – all show risk ratio values greater than 1 (see Figure 4.23), indicating extreme values of each measure of wildfire risk are more likely when anthropogenic warming is included. Risk ratios vary among the different fire risk indices analyzed. However, extreme values of all measures describing wildfire risk are more likely with anthropogenic forcing.

Increasing temperatures, like those observed across Canada (see Section 4.2), will lead to drier fuels, and thus increased fire potential, as well as longer fire seasons. It would require increases in precipitation well beyond what is expected with climate change to offset increasing temperatures in terms of the FWI indices (Flannigan et al., 2016). The study demonstrated that the extreme Alberta wildfire of 2016 occurred in a world where anthropogenic warming has increased fire risk, fire spread potential, and the length of fire seasons across parts of Alberta and Saskatchewan.

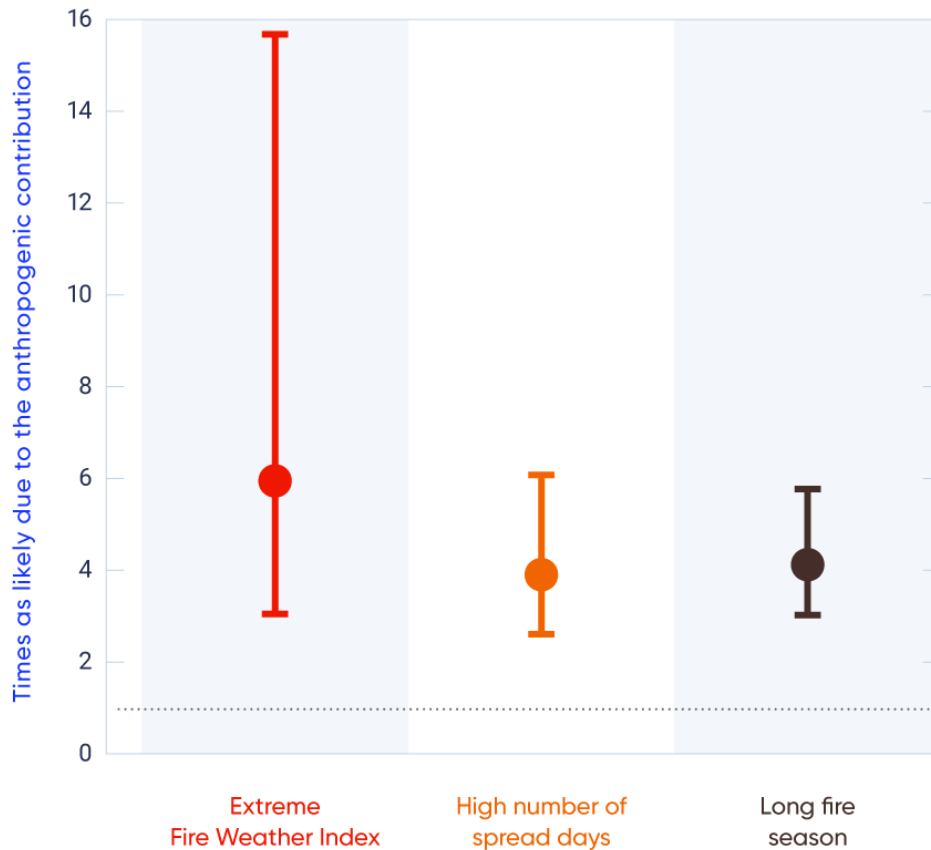


Figure 4.23: Risk ratios for three measures of extreme wildfire risk

Figure caption: Risk ratios for three measures of extreme wildfire risk in the Southern Prairies Homogeneous Fire Regime zone (Boulanger et al., 2014), showing the increase in likelihood due to the anthropogenic contribution. A risk ratio greater than 1 (dashed line) indicates the extreme event is more likely when the human contribution is included. The three measures used to characterize extreme wildfire risk in this region are fire weather (extreme Fire Weather Index), fire behaviour (high number of fire spread days), and fire season (long fire seasons). The error bars represent the 5–95% uncertainty range.

FIGURE SOURCE: ADAPTED FROM KIRCHMEIER-YOUNG ET AL., 2017A.





Section summary

In summary, a new field of event attribution has emerged, which aims to assess the role of human-induced climate change in extreme events. Some recent extreme events across Canada have been analyzed in this way, including the southern Alberta flood in 2013 and the Fort McMurray wildfire of 2016. For the first event, GHG emissions from human activity increased the likelihood of extreme, flood-producing rainfall, but the confidence in this attribution is low because of the difficulties in modelling precipitation extremes, which exhibit large variability at small scales, such as for this event. For the second event, there is *medium confidence* that human-induced climate change increased the likelihood of the extreme wildfire risk associated with the 2016 Fort McMurray wildfire. The assessment of *medium confidence* balances *high confidence* in human influence on the increase in temperature, which affects fire risk strongly, with many other factors contributing to this event that are more difficult to represent in a climate model.

References

Amiro, B.D., Logan, K.A., Wotton, B.M., Flannigan, M.D., Todd, J.B., Stocks, B.J., and Martell, D.L. (2004): Fire weather index system components for large fires in the Canadian boreal forest. *International Journal of Wildland Fire*, v. 13, p. 391–400, doi:10.1071/WF03066.

Assel, R.A. (1980): Maximum freezing degree-days as a winter verity index for the Great Lakes, 1897–1977; *Monthly Weather Review*, v. 108, p. 1440–1445, doi:10.1175/1520-0493(1980)108%3C1440:MFDDAA%3E2.0.CO;2

Barbero, R., Fowler, H.J., Lenerink, G., Blenkinsop, S. (2017): Is the intensification of precipitation extremes with global warming better detected at hourly than daily resolutions? *Geophysical Research Letters*; doi:10.1002/2016GL071917

Bellprat, O., Massonnet, F., García-Serrano, J., Fučkar, N.S., Guemas, V. and Doblas-Reyes, F.J. (2016): The role of Arctic sea ice and sea surface temperatures on the cold 2015 February over North America; in *Explaining Extreme Events of 2015 from a Climate Perspective*; *Bulletin of the American Meteorological Society*, v. 97, p. S36–S41. doi:10.1175/BAMS-D-16-0159.1

Bindoff, N.L., Stott, P.A., AchutaRao, K.M., Allen, M.R., Gillett, N., Gutzler, D., Hansingo, K., Hegerl, G., Hu, Y., Jain, S., Mokhov, I.I., Overland, J., Perlwitz, J., Sebbari R. and Zhang, X. (2013): Detection and attribution of climate change: from global to regional; in *Climate Change 2013: The Physical Science Basis*; Contribution of Working Group I to the Fifth Assessment Report of the Intergovernmental Panel on Climate Change, (ed.) T.F. Stocker, D. Qin, G.-K. Plattner, M. Tignor, S.K. Allen, J. Boschung, A. Nauels, Y. Xia, V. Bex and P.M. Midgley; Cambridge University Press, Cambridge, United Kingdom and New York, NY, p. 867–952, <https://www.ipcc.ch/site/assets/uploads/2018/02/WG1AR5_Chapter10_FINAL.pdf>

Boulanger, Y., Gauthier, S., and Burton, P.J. (2014): A refinement of models projecting future Canadian fire regimes using homogeneous fire regime zones; *Canadian Journal of Forest Research*, v. 44, p. 365–376, doi:10.1139/cjfr-2013-0372.

Casati, B., Yagouti, A. and Chaumont, D. (2013): Regional climate projections of extreme heat events in nine pilot Canadian communities for public health planning; *Journal of Applied Meteorology and Climatology*, v. 52, p. 2669–2698. doi:10.1175/JAMC-D-12-0341.1

Collins, M., Knutti, R., Arblaster, J., Dufresne, J.-L., Fichet, T., Friedlingstein, P., Gao, X., Gutowski, W.J., Johns, T., Krinner, G., Shongwe, M., Tebaldi, C., Weaver, A.J. and Wehner, M. (2013): Long-term climate change: projections, commitments and irreversibility; in *Climate Change 2013: The Physical Science Basis*; Contribution of Working Group I to the Fifth Assessment Report of the Intergovernmental Panel on Climate Change, (ed.) T.F. Stocker, D. Qin, G.-K. Plattner, M. Tignor, S.K. Allen, J. Boschung, A. Nauels, Y. Xia, V. Bex and P.M. Midgley; Cambridge University Press, Cambridge, United Kingdom and New York, NY, USA; p. 1029–1136, <https://www.ipcc.ch/site/assets/uploads/2018/02/WG1AR5_Chapter12_FINAL.pdf>



de Groot, W.J., Flannigan, M.D. and Cantin, A.S. (2013): Climate change impacts on future boreal fire regimes. *Forest Ecology and Management*, v. 294, p. 35–44. doi:10.1016/j.foreco.2012.09.027.

DeBeer, C.M., Wheeler, H.S., Carey, S.K. and Chun, K.P. (2016): Recent climatic, cryospheric, and hydrological changes over the interior of western Canada: a review and synthesis; *Hydrology and Earth System Sciences*, v. 20, p. 1573–1598. doi: 10.5194/hess-20-1573-2016

ECCC [Environment and Climate Change Canada] (2016): Climate data and scenarios for Canada: Synthesis of recent observation and modelling results. Cat. No.: En84-132/2016E-PDF.

ECCC [Environment and Climate Change Canada] (2017): Canada's top ten weather stories of 2013; <<https://ec.gc.ca/meteo-weather/default.asp?lang=En&n=3318B51C-1>>

Environment Canada (1995): The State of Canada's Climate: Monitoring Variability and Change; A State of the Environment Report; SOE report no. 95-1, Catalogue no. En1-11/95-1E; Environment Canada, Ottawa, ON.

Flannigan, M., Cantin, A.S., de Groot, W.J., Wotton, M., Newbery, A., and Gowman, L.M. (2013): Global wildland fire season severity in the 21st century; *Forest Ecology and Management*, v. 294, p. 54–61. doi:10.1016/j.foreco.2012.10.022.

Flannigan, M.D., Krawchuk, M.A., de Groot, W.J., Wotton, B.M., and Gowman, L.M. (2009): Implications of changing climate for global wildland fire; *International Journal of Wildland Fire*, v. 18, p. 483–507. doi:10.1071/WF08187.

Flannigan, M.D., Wotton, B.M., Marshall, G.A., de Groot, W.J., Johnston, J., Jurko, N. and Cantin, A.S. (2016): Fuel moisture sensitivity to temperature and precipitation: climate change implications. *Climatic Change*, v. 134, p. 59–71. doi:10.1007/s10584-015-1521-0

Flato, G., Marotzke, J., Abiodun, B., Braconnot, P., Chou, S.C., Collins, W., Cox, P., Driouech, F., Emori, S., Eyring, V., Forest, C., Gleckler, P., Guilyardi, E., Jakob, C., Kattsov, V., Reason, C. and Rummukainen, M. (2013): Evaluation of climate models; in *Climate Change 2013: The Physical Science Basis; Contribution of Working Group I to the Fifth Assessment Report of the Intergovernmental Panel on Climate Change*, (ed.) T.F. Stocker, F. Qin, G.-K. Plattner, M. Tignor, S.K. Allen, J. Boschung, A. Nauels, Y. Xia, V. Bex, P.M. Midgley; Cambridge University Press, Cambridge, United Kingdom and New York, NY, USA, p. 741–866, <https://www.ipcc.ch/site/assets/uploads/2018/02/WG1AR5_Chapter09_FINAL.pdf>

Fučkar, N.S., Massonnet, F., Guemas, V., García-Serrano, J., Bellprat, O., Doblas-Reyes, F.J. and Acosta, M. (2016): Record low Northern Hemisphere sea ice extent in March 2015; in *Explaining Extreme Events of 2015 from a Climate Perspective; Bulletin of the American Meteorological Society*, v. 97, p. S136–S140. doi: 10.1175/BAMS-D-16-0153.1

Gillett, N.P., Weaver, A.J., Zwiers, F.W. and Flannigan, M.D. (2004): Detecting the effect of climate change on Canadian forest fires; *Geophysical Research Letters*, v. 31, 4 p. doi:10.1029/2004GL020876

Girardin, M.P., and Wotton, B.M. (2009): Summer moisture and wildfire risks across Canada. *Journal of Applied Meteorology and Climatology*. v. 48, p. 517–533, doi:10.1175/2008JAMC1996.1.



Girardin, M.-P., Tardif, J., Flannigan, M.D., Wotton, B.M., and Bergeron, Y. (2004): Trends and periodicities in the Canadian Drought Code and their relationships with atmospheric circulation for the southern Canadian boreal forest. *Canadian Journal of Forest Research*, v. 34, p. 103–119, doi:10.1139/X03-195.

Goodsman, D.W., Groszklos, G., Aukema, B.H., Whitehouse, C., Bleiker, K.P., McDowell, N.G., Middleton, R.S. and Xu, C. (2018): The effect of warmer winters on the demography of an outbreak insect is hidden by intraspecific competition; *Global Change Biology*, doi:10.1111/gcb.14284

Government of Alberta (2016): Final update 39: 2016 wild-fires; <<https://www.alberta.ca/release.cfm?xID=41701e7EC-BE35-AD48-5793-1642c499FF0DE4CF>>

Gullett, D.W. and Skinner, W.R. (1992): The state of Canada's climate: temperature change in Canada; A State of the Environment Report; SOE report no. 92-2, Cat. no. Enl-11/92-2E; Environment Canada, Ottawa, ON.

Hartmann, D.L., Klein Tank, A.M.G., Rusticucci, M., Alexander, L.V., Brönnimann, S., Charabi, Y., Dentener, F.J., Dlugokencky, E.J., Easterling, D.R., Kaplan, A., Soden, B.J., Thorne, P.W., Wild, M., and Zhai, P.M. (2013): Observations: Atmosphere and Surface; in *Climate Change 2013: The Physical Science Basis. Contribution of Working Group I to the Fifth Assessment Report of the Intergovernmental Panel on Climate Change*, (ed.) T.F. Stocker, D. Qin, G.-K. Plattner, M. Tignor, S.K. Allen, J. Boschung, A. Nauels, Y. Xia, V. Bex and P.M. Midgley; Cambridge University Press, Cambridge, United Kingdom and New York, NY, USA, pp. 159–254. doi:10.1017/CBO9781107415324.008

Herring, S.C., Christidis, N., Hoell, A., Kossin, J.P., Schreck III, C.J. and Stott, P.A. (2017): Explaining extreme events of 2016 from a climate perspective; *Bulletin of the American Meteorological Society*, v. 98, p. S1–S157.

Herring, S.C., Hoell, A., Hoerling, M.P., Kossin, J.P., Schreck III, C.J. and Stott, P.A. (2016): Explaining extreme events of 2015 from a climate perspective; *Bulletin of the American Meteorological Society*, v. 97, p. S1–S145.

IBC [Insurance Bureau of Canada] (2016): Northern Alberta wildfire costliest insured natural disaster in Canadian history – estimate of insured losses: \$3.58 billion; <<http://www.abc.ca/bc/resources/media-centre/media-releases/northern-alberta-wildfire-costliest-insured-natural-disaster-in-canadian-history>>.

IPCC [Intergovernmental Panel on Climate Change] (2013): Summary for policymakers; in *Climate Change 2013: The Physical Science Basis; Contribution of Working Group I to the Fifth Assessment Report of the Intergovernmental Panel on Climate Change*, (ed.) T.F. Stocker, D. Qin, G.-K. Plattner, M. Tignor, S. K. Allen, J. Boschung, A. Nauels, Y. Xia, V. Bex and P.M. Midgley; Cambridge University Press, Cambridge, United Kingdom and New York, NY, USA, p. 3–29. <https://www.ipcc.ch/site/assets/uploads/2018/02/WG1AR5_SPM_FINAL.pdf>.

Jain, P., Wang, X. and Flannigan, M.D. (2017): Trend analysis of fire season length and extreme fire weather in North America between 1979 and 2015; *International Journal of Wildland Fire*, v. 26, p. 1009–1020. doi:10.1071/WF17008

Jeong, D.I. and Sushama, L. (2017): Rain-on-snow events over North America based on two Canadian regional climate models; *Climate Dynamics*. doi:10.1007/s00382-017-3609-x

Kam, J., Knutson, T.R., Zeng, F. and Wittenberg, A.T. (2015): Record annual mean warmth over Europe, the northeast Pacific, and the north-west Atlantic during 2014: assessment of anthropogenic influence; in *Explaining Extreme Events of 2014 from a Climate Perspective*; *Bulletin of the American Meteorological Society*, v. 96, p. S61–S65. doi:10.1175/BAMS-D-15-00101.1

Kam, J., Knutson, T.R., Zeng, F. and Wittenberg, A.T. (2017): CMIP5 model-based assessment of anthropogenic influence on highly anomalous Arctic warmth during November–December 2016; in *Explaining extreme events of 2016 from a climate perspective*; *Bulletin of the American Meteorological Society*, v. 98, p. S34–S38. doi:10.1175/BAMS-D-17-0115.1

Kharin, V.V., Flato, G.M., Zhang, X., Gillett, N.P., Zwiers, F. and Anderson, K. (2018): Risks from climate extremes change differently from 1.5°C to 2.0°C depending on rarity; *Earth's Future*, v. 6, p. 704–715.

Kharin, V.V., Zwiers, F.W., Zhang, X. and Wehner, M. (2013): Changes in temperature and precipitation extremes in the CMIP5 ensemble; *Climatic Change*, v. 119, p. 345–357. doi:10.1007/s10584-013-0705-8

Kim, Y.-H., Min, S.-K., Zhang, X., Zwiers, F., Alexander, L.V., Donat, M.G. and Tung, Y.-S. (2015): Attribution of extreme temperature changes during 1951–2010; *Climate Dynamics*, v. 46, p. 1769–1782. doi: 10.1007/s00382-015-2674-2

Kirchmeier-Young, M.C., Zwiers, F.W., Gillett, N.P. and Cannon, A.J. (2017a): Attributing extreme fire risk in Western Canada to human emissions; *Climatic Change*, v. 144, p. 365–379. doi:10.1007/s10584-017-2030-0

Kirchmeier-Young, M.C., Zwiers, F.W. and Gillett, N.P. (2017b): Attribution of extreme events in Arctic sea ice extent; *Journal of Climate*, v. 30, p. 553–571. doi:10.1175/JCLI-D-16-0412.1

Kirtman, B., Power, S.B., Adedoyin, J.A., Boer, G.J., Bojariu, R., Camilloni, I., Doblas-Reyes, F.J., Fiore, A.M., Kimoto, M., Meehl, G.A., Prather, M., Sarr, A., Schär, C., Sutton, R., van Oldenborgh, G.J., Vecchi, G. and Wang, H.J. (2013): Near-term Climate Change: Projections and Predictability; in *Climate Change 2013: The Physical Science Basis. Contribution of Working Group I to the Fifth Assessment Report of the Intergovernmental Panel on Climate Change*, (ed.) T.F. Stocker, D. Qin, G.-K. Plattner, M. Tignor, S.K. Allen, J. Boschung, A. Nauels, Y. Xia, V. Bex and P.M. Midgley; Cambridge University Press, Cambridge, United Kingdom and New York, NY, USA.

Kochtubajda, B., Flannigan, M.D., Gyakum, J.R., Stewart, R.E., Logan, K.A., and Nguyen, T.-V. (2006): Lightning and fires in the Northwest Territories and responses to future climate change; *Arctic*, v. 59, p. 211–221.

Kovacs, P. and Thistlethwaite, J. (2014): Industry; in *Canada in a Changing Climate: Sector Perspectives on Impacts and Adaptation*, (ed.) F.J. Warren and D.S. Lemmen; Government of Canada, Ottawa, Ontario, p. 135–158.

Krasting, J.P., Broccoli, A.J., Dixon, K.W. and Lanzante, J.R. (2013): Future



changes in Northern Hemisphere snowfall; *Journal of Climate*, v. 26, p. 7813–7828. doi:10.1175/JCLI-D-12-00832.1

Li, G., Zhang, X., Cannon, A.J., Murdock, T., Sobie, S., Zwiers, F.W., Anderson, K. and Qian, B. (2018): Indices of Canada's future climate for general and agricultural adaptation applications; *Climatic Change*, v. 148, p. 249–263.

Marvel, K. and Bonfils, C. (2013): Identifying external influences on global precipitation; *Proceedings of the National Academy of Sciences*, v. 110. doi:10.1073/pnas.1314382110

Mekis, É. and Vincent, L.A. (2011): An overview of the second generation adjusted daily precipitation dataset for trend analysis in Canada; *Atmosphere-Ocean*, v. 49, p. 163–177. doi:10.1080/07055900.2011.583910

Mekis, E., Vincent, L.A., Shephard, M.W. and Zhang, X. (2015): Observed trends in severe weather conditions based on humidex, wind chill, and heavy rainfall events in Canada for 1953–2012; *Atmosphere-Ocean*, v. 53, p. 383–397. doi:10.1080/07055900.2015.1086970

Milewska, E., and Hogg, W.D. (2001): Spatial representativeness of a long-term climate network in Canada. *Atmosphere-Ocean*, v. 39, p. 145–161. doi:10.1080/07055900.2001.9649671

Milewska, E. and Hogg, W.D. (2002): Continuity of climatological observations with automation – temperature and precipitation amounts from AWOS (Automated Weather Observing System). *Atmosphere-Ocean*, v. 40, p. 333–359. doi:10.3137/ao.400304

Milewska, E.J. and Vincent, L.A. (2016): Preserving continuity of long-term daily maximum and minimum temperature observations with automation of reference climate stations using overlapping data and meteorological conditions; *Atmosphere-Ocean*, v. 54, p. 32–47. doi:10.1080/07055900.2015.1135784

Milewska, E.J., Vincent, L.A., Hartwell, M., Charlesworth, K. and Mekis, É. (2019): Adjusting precipitation amounts from Geonor and Pluvio automated weighing gauges to preserve continuity of observations in Canada. *Canadian Water Resources Journal*, doi:10.1080/07011784.2018.1530611.

Min, S.-K., Zhang, X. and Zwiers, F.W. (2008): Human-induced Arctic moistening; *Science*, v. 320, p. 518–520. doi:10.1126/science.1153468

Min, S.-K., Zhang, X., Zwiers, F.W. and Hegerl, G.C. (2011): Human contribution to more intense precipitation extremes; *Nature*, v. 470, p. 378–381. doi:10.1038/nature09763

Min, S.-K., Zhang, X., Zwiers, F., Shiogama, H., Tung, Y.-S. and Wehner, M. (2013): Multi-model detection and attribution of extreme temperature changes; *Journal of Climate*, v. 26, p. 7430–7451. doi: 10.1175/JCLI-D-12-00551.1

Murdock, T.Q., Cannon, A.J. and Sobie, S.R. (2014): Statistical downscaling of future climate projections for North America; Pacific Climate Impacts Consortium; Environment Canada, Victoria, British Columbia, <https://www.pacificclimate.org/sites/default/files/publications/PCIC_EC_downscaling_report_2014.pdf>



- Najafi, M.R., Zwiers, F.W. and Gillett, N.P. (2015): Attribution of Arctic temperature change to greenhouse-gas and aerosol influences; *Nature Climate Change*, v. 5, p. 246–249. doi:10.1038/nclimate2524
- Najafi, M.R., Zwiers, F. and Gillett, N. (2017a): Attribution of the observed spring snowpack decline in British Columbia to anthropogenic climate change; *Journal of Climate*, v. 30, p. 4113–4130.
- Najafi, M.R., Zwiers, F.W. and Gillett, N.P. (2017b): Attribution of observed streamflow changes in key British Columbia drainage basins; *Geophysical Research Letters*, v. 44, p. 11012–11020.
- NASEM [National Academies of Science, Engineering, and Medicine] (2016): Attribution of extreme weather events in the context of climate change; The National Academies Press, Washington, District of Columbia, USA. doi:10.17226/21852
- OAGC [Office of the Auditor General of Canada] (2016): Report 2: Mitigating the impacts of severe weather; Reports of the Commissioner of the Environment and Sustainable Development, <www.oag-bvg.gc.ca/internet/docs/parl_cesd_201605_02_e.pdf>.
- OPBO [Office of the Parliamentary Budget Officer] (2016): Estimate of the average annual cost for disaster financial assistance arrangements due to weather events; Ottawa, Canada. <https://www.pbo-dpb.gc.ca/web/default/files/Documents/Reports/2016/DFAA/DFAA_EN.pdf>.
- Osborn, T.J. and Jones, P.D. (2014): The CRUTEM4 land-surface air temperature data set: construction, previous versions and dissemination via Google Earth; *Earth System Science Data* v. 6, p. 61–68. doi:10.5194/essd-6-61-2014
- Partain, J.L., Alden, S., Bhatt, U.S., Bieniek, P.A., Brettschneider, B.R., Lader, R.T., Olsson, P.Q., Rupp, T.S., Strader, H., Thoman, R.L., Walsh, J., York, A.D. and Ziel, R.H. (2016): An assessment of the role of anthropogenic climate change in the Alaska fire season of 2015; in *Explaining Extreme Events of 2015 from a Climate Perspective*; *Bulletin of the American Meteorological Society*, v. 97, p. S14–S18. doi:10.1175/BAMS-D-16-0149.1
- Podur, J., Martell, D. L., and Knight, K. (2002): Statistical quality control analysis of forest fire activity in Canada; *Canadian Journal of Forest Research*, v. 32, p. 195–205. doi: 10.1139/X01-183
- Screen, J.A. and Simmonds, I. (2012): Declining summer snowfall in the Arctic: causes, impacts and feedbacks; *Climate Dynamics*, v. 38, p. 2243–2256.
- Shephard, M.W., Mekis, E., Morris, R.J., Feng, Y., Zhang, X., Kilcup, K. and Fleetwood, R. (2014): Trends in Canadian short-duration extreme rainfall: including an intensity-duration-frequency perspective; *Atmosphere-Ocean*, v. 52, p. 398–417.
- Szeto, K., Brimelow, J., Gysbers, P. and Stewart, R. (2015): The 2014 extreme flood on the southeastern Canadian Prairies; in *Explaining Extreme Events of 2014 from a Climate Perspective*; *Bulletin of the American Meteorological Society*, v. 96, p. S20–S24. doi:10.1175/BAMS-D-15-00110
- Szeto, K., Zhang, X., White, R.E. and Brimelow, J. (2016): The 2015 extreme drought in western Canada; in *Explaining Extreme Events of 2015*



from a Climate Perspective; *Bulletin of the American Meteorological Society*, v. 97, p. S42–S46. doi:10.1175/BAMS-D-16-0147.1

Tett, S.F.B., Falk, A., Rogers, M., Spuler, F., Turner, C., Wainwright, J., Dimdore-Miles, O., Knight, S., Freychet, N., Mineter, M.J. and Lehmann, C.E.R. (2017): Anthropogenic forcings and associated changes in fire risk in western North America and Australia during 2015/16; in *Explaining Extreme Events of 2016 from a Climate Perspective; Bulletin of the American Meteorological Society*, v. 98, p. S60–S64. doi:10.1175/BAMS-D-17-0096.1

Teufel, B., Diro, G.T., Whan, K., Milrad, S.M., Jeong, D.I., Ganji, A., Huziy, O., Winger, K., Gyakum, J.R., de Elia, R., Zwiers, F.W. and Sushama, L. (2017): Investigation of the 2013 Alberta flood from weather and climate perspectives; *Climate Dynamics*, v. 48, p. 2881–2899. doi:10.1007/s00382-016-3239-8

Vincent, L.A., Milewska, E.J., Wang, X.L. and Hartwell, M.M. (2017): Uncertainty in homogenized daily temperatures and derived indices of extremes illustrated using parallel observations in Canada; *International Journal of Climatology*, v. 38, p. 692–707. doi:10.1002/joc.5203

Vincent, L.A., Wang, X.L., Milewska, E.J., Wan, H., Yang, F. and Swail, V. (2012): A second generation of homogenized Canadian monthly surface air temperature for climate trend analysis; *Journal of Geophysical Research*, v. 117. doi:10.1029/2012JD017859

Vincent, L.A., Zhang, X., Bonsal, B.R. and Hogg, W.D. (2002): Homogenization of daily temperatures over Canada; *Journal of Climate*, v. 15, p. 1322–1334.

Vincent, L.A., Zhang, X., Brown, R.D., Feng, Y., Mekis, E., Milewska, E.J., Wan, H. and Wang, X.L. (2015): Observed trends in Canada's climate and influence of low-frequency variability modes; *Journal of Climate*, v. 28, p. 4545–4560. doi: <http://dx.doi.org/10.1175/JCLI-D-14-00697.1>

Vincent, L.A., Zhang, X., Mekis, E., Wan, H. and Bush, E.J. (2018): Monitoring changes in Canada's climate: Trends in temperature and precipitation indices based on daily monitoring data; *Atmosphere-Ocean*, doi: 10.1080/07055900.2018.1514579.

Wan, H., Zhang, X., Zwiers, F. and Min, S.-K. (2014): Attributing Northern high-latitude precipitation change over the period 1966–2005 to human influence; *Climate Dynamics*, v. 45, p. 1713–1726. doi:10.1007/s00383-014-2423-y

Wan, H., Zhang, X. and Zwiers, F.W. (2018): Human influence on Canadian temperatures; *Climate Dynamics*, v.52, p. 479-494.

Wang, X.L., Chen, H., Wu, Y., Feng, Y. and Pu, Q. (2010): New techniques for detection and adjustment of shifts in daily precipitation data series; *Journal of Applied Meteorology and Climatology*, v. 49, p. 2416–2436. doi:10.1175/2010JAMC2376.1

Wang, X.L., Feng, Y. and Vincent, L.A. (2014): Observed changes in one-in-20 year extremes of Canadian surface air temperatures; *Atmosphere-Ocean*, v. 52, p. 222–231. doi:10.1080/07055900.2013.818526



Wang, X., Thompson, D. K., Marshall, G. A., Tymstra, C., Carr, R., and Flannigan, M.D. (2015): Increasing frequency of extreme fire weather in Canada with climate change. *Climatic Change*, v. 130, p. 573–586. doi:10.1007/s10584-015-1375-5

Wang, X.L., Wen, Q.H. and Wu, Y. (2007): Penalized maximal t test for detecting undocumented mean change in climate data series; *Journal of Applied Meteorology and Climatology*, v. 46, p. 916–931. doi:10.1175/JAM2504.1

Wang, Z., Jiang, Y., Wan, H., Yan, J. and Zhang, X. (2017): Detection and attribution of changes in extreme temperatures at regional scale; *Journal of Climate*, v. 30, p. 7035–7047.

Werner, A.T. and Cannon, A.J. (2016): Hydrologic extremes – an intercomparison of multiple gridded statistical downscaling methods; *Hydrology and Earth System Sciences*, v. 20, p. 1483–1508. doi: 10.5191/hess-20-1483-2016

Westra, S., Alexander, L.V. and Zwiers, F.W. (2013): Global increasing trends in annual maximum daily precipitation; *Journal of Climate*, v. 26, p. 3904–3918. doi:10.1175/JCLI-D-12-00502.1

WMO [World Meteorological Organization] (2014): Atlas of mortality and economic losses from weather, climate and water extremes (1970–2012); WMO No. 1123.

Wolter, K., Hoerling, M., Eischeid, J.K., van Oldenborgh, G.J., Quan, X.-W., Walsh, J.E., Chase, T.N. and Dole, R.M. (2015): How unusual was the cold winter of 2013/14 in the upper Midwest; in *Explaining Extreme Events of 2014 from a Climate Perspective*; *Bulletin of the American Meteorological Society*, v. 96, p. S10–S14. doi:10.1175/BAMS-D-15-0126.1

Wotton, B.M. (2009): Interpreting and using outputs from the Canadian Forest Fire Danger Rating System in research applications; *Environmental and Ecological Statistics*, v. 16, p. 107–131. doi:10.1007/s10651-007-0084-2

Wotton, B.M., Nock, C.A. and Flannigan, M.D. (2010): Forest fire occurrence and climate change in Canada. *International Journal of Wildland Fire*; v. 19, p. 253–271. doi:10.1071/WF09002

Yu, B. and Zhang, X. (2015): A physical analysis of the severe 2013/2014 cold winter in North America; *Journal of Geophysical Research: Atmospheres*; v. 120, p. 10149–10165. doi:10.1002/2015JD02116

Zhang, R., and Knutson, T.R. (2013): The role of global climate change in the extreme low summer Arctic sea ice extent in 2012; in *Explaining Extreme Events of 2012 from a Climate Perspective*; *Bulletin of the American Meteorological Society*, v. 94, p. S23–S26.

Zhang, X., Wan, H., Zwiers, F.W., Hegerl, G.C. and Min, S.-K. (2013): Attributing intensification of precipitation extremes to human influence; *Geophysical Research Letters*, v. 40, p. 5252–5257. doi: 10.1002/grl.51010

Zhang, X., Zwiers, F.W., Li, G., Wan, H. and Cannon, A.J. (2017): Complexity in estimating past and future extreme short-duration rainfall; *Nature Geoscience*, v. 10. doi: 10.1038/ngeo2911



Zhang, X., Zwiers, F.W. and Stott, P. (2006): Multi-model multi-signal climate change detection at regional scale; *Journal of Climate*, v. 19, p. 4294–4307.

Zwiers, F.W., Zhang, X. and Feng, Y. (2011): Anthropogenic influence on long return period daily temperature extremes at regional scales; *Journal of Climate*, v. 24, p. 881–892. doi:10.1175/2010JCLI3908.1